

IL-36 GAMMA PROMOTES ANTI-TUMOR IMMUNITY THROUGH THERAPEUTIC
INDUCTION OF TUMOR-ASSOCIATED TERTIARY LYMPHOID STRUCTURES

by

Aliyah Miel Weinstein

B.A., Rutgers, the State University of New Jersey, 2012

Submitted to the Graduate Faculty of the
School of Medicine in partial fulfillment
of the requirements for the degree of
Doctor of Philosophy

University of Pittsburgh

2018

UNIVERSITY OF PITTSBURGH
SCHOOL OF MEDICINE

This dissertation was presented

by

Aliyah Miel Weinstein

It was defended on

March 16, 2018

and approved by

Lisa H. Butterfield, PhD, Professor, Department of Medicine

Binfeng Lu, PhD, Associate Professor, Department of Immunology

Adrian E. Morelli, MD, PhD, Associate Professor, Departments of Surgery and
Immunology

Donna Beer Stolz, PhD, Associate Professor, Department of Cell Biology

Dissertation Advisor: Walter J. Storkus, PhD, Professor, Department of Dermatology

Copyright © by Aliyah Miel Weinstein
2018

IL-36 GAMMA PROMOTES ANTI-TUMOR IMMUNITY THROUGH THERAPEUTIC INDUCTION OF TUMOR-ASSOCIATED TERTIARY LYMPHOID STRUCTURES

Aliyah Miel Weinstein, PhD

University of Pittsburgh, 2018

The last decade has advanced our understanding of the composition of the tumor-immune microenvironment and its role as a potential target for therapeutic intervention. Recently, tertiary lymphoid structures have been observed to develop in the tumor microenvironment and serve as a positive prognostic marker in many types of solid tumors. The major signals that control tertiary lymphoid organogenesis are the same as those that direct the development of secondary lymphoid organs. Tertiary lymphoid structures are classically characterized by high endothelial venules, which serve to recruit T cells, dendritic cells, and B cells to sites of persistent inflammation and locally prime T cells against tumor-derived antigens. Our group has long been interested in understanding whether tertiary lymphoid structures can be therapeutically induced to form within the tumor microenvironment and induce a protective anti-tumor immune response. In previous studies, we characterized dendritic cells engineered to overexpress the Type-1 transactivator *Tbet* (i.e. DC.Tbet) and showed that they are able to delay tumor progression following intratumoral injection in a murine model of sarcoma. In this work, I show that the effector molecule responsible for the therapeutic efficacy of DC.Tbet is IL-36 γ . Dendritic cells engineered to ectopically overexpress IL-36 γ and injected intratumorally into the murine MC38 model of colorectal carcinoma can direct the same magnitude of immune response as DC.Tbet therapy, even in the absence of Tbet expression by the injected cells. IL-36 γ drives intratumoral expression of lymphotoxins and chemokines that direct tertiary lymphoid organogenesis, and promotes an intratumoral Type-1 immune response in conjunction with delayed tumor progression. Finally, I evaluated the expression pattern of IL-36 γ in human colorectal

cancer. I show that within the immune compartment, expression of IL-36 γ by M1 macrophages is positively correlated with a high CD4+ central memory T cell infiltrate into those tumors; and that IL-36 γ expression on the tumor vasculature is associated with an increased density of B cells within tumor-associated tertiary lymphoid structures. Together, these data support IL-36 γ as a novel mediator of anti-tumor immunity and its further investigation as a therapeutic agent to enhance protective Type-1 immune responses in the tumor microenvironment.

TABLE OF CONTENTS

| | |
|--|----------|
| PREFACE | xvi |
| ABBREVIATIONS | xviii |
| 1.0 INTRODUCTION..... | 1 |
| 1.1 IMMUNE RESPONSES IN THE TUMOR MICROENVIRONMENT | 1 |
| 1.1.2 Tbet has a multitude of roles in the immune response, including the promotion of Type-1 immunity | 2 |
| 1.1.3 DCs in cancer | 4 |
| 1.1.3.1 Endogenous DCs | 4 |
| 1.1.3.2 DC-based immunotherapies | 5 |
| 1.1.3.3 Perspectives on DC-based Immunotherapy | 6 |
| 1.2 THERAPEUTIC LYMPHOID ORGANOGENESIS IN THE TUMOR MICROENVIROMENT | 6 |
| 1.2.1 Abstract..... | 7 |
| 1.2.2 Introduction | 8 |
| 1.2.3 Development of TLS in Chronically-Diseased Tissues | 8 |
| 1.2.3.1 TLS: Organizational structure | 10 |
| 1.2.4 TLS in cancer: Clinical Correlates of Disease Progression and Response to Treatment | 11 |
| 1.2.5 Cues for TLS Development..... | 17 |

| | |
|--|-----------|
| 1.2.5.1 The requirement for lymphotoxin signaling in the evolution of TLS in the TME | 18 |
| 1.2.5.2 EnLIGHTening Protective Immunity in TLS | 21 |
| 1.2.5.3 The Importance of CCR7 Agonists for TLS Evolution in the TME | 25 |
| 1.2.5.4 The Importance of CXCR5 agonists in TLS evolution | 29 |
| 1.2.6 Therapeutic Manipulation of TLS in Cancer Patients: Establishing a Paradigm for Anti-Tumor Efficacy | 32 |
| 1.2.7 Conclusions and Future Directions for Clinical Translation..... | 32 |
| 1.3 BIOSYNTHESIS AND FUNCTIONAL SIGNIFICANCE OF PERIPHERAL NODE ADDRESSIN IN CANCER-ASSOCIATED TLS..... | 34 |
| 1.3.1 Abstract..... | 34 |
| 1.3.2 Pathways regulating PNAd expression | 35 |
| 1.3.2.1 Signaling through the lymphotoxin beta receptor is required for HEV differentiation | 36 |
| 1.3.2.2 Post-translational modifications are required for L-selectin recognition of PNAd..... | 37 |
| 1.3.2.2.1 Sulfation | 39 |
| 1.3.2.2.2 Glycosylation..... | 40 |
| 1.3.3 Markers of high endothelial venules | 40 |
| 1.3.4 Immune Cell Recruitment by HEV | 40 |
| 1.3.5 Tertiary Lymphoid Organs | 41 |
| 1.3.5.1 TLS in Cancer | 43 |
| 1.3.5.1.1 Lung Cancer..... | 44 |
| 1.3.5.1.2 Skin cancers..... | 45 |
| 1.3.5.1.3 Colon Cancer | 46 |
| 1.3.5.2 Therapeutic induction of TLS | 46 |
| 1.3.6 Future Perspectives..... | 46 |
| 1.4. THE IL-36 CYTOKINE SUBFAMILY IN IMMUNE-MEDIATED PATHOGENESIS | 47 |

| | |
|--|-----------|
| 1.4.1 The IL-36 cytokines share unique characteristics with other IL-1 family cytokines..... | 48 |
| 1.4.2. IL-36R signaling..... | 49 |
| 1.4.3 IL-36 as an Early Inflammatory Mediator of Lymphoid Organogenesis in Tissues, Including Cancer | 52 |
| 2.0. TBET AND IL-36 γ COOPERATE IN THERAPEUTIC DC-MEDIATED PROMOTION OF ECTOPIC LYMPHOID ORGANOGENESIS IN THE TME..... | 56 |
| 2.1 ABSTRACT | 57 |
| 2.2 INTRODUCTION | 58 |
| 2.3 RESULTS | 60 |
| 2.3.1 DC.Tbet overexpress pro-inflammatory gene products, including IL-36 γ | 60 |
| 2.3.2 i.t. delivery of DC.Tbet results in rapid infiltration of lymphocytes and development of TLS in vivo. | 62 |
| 2.3.3 Therapeutic anti-tumor efficacy of i.t. DC.Tbet is not dependent on host LTA. | 65 |
| 2.3.4 Ablation of IL-36R signaling abrogates the therapeutic anti-tumor efficacy of i.t. DC.Tbet..... | 67 |
| 2.3.5 DC engineered to secrete bioactive rIL-36 γ (DC.IL-36 γ) recapitulate the effects of i.t. DC.Tbet treatment in vivo. | 72 |
| 2.4 DISCUSSION..... | 77 |
| 2.5 MATERIALS AND METHODS | 82 |
| 2.5.1 Study design..... | 82 |
| 2.5.2 Mice..... | 83 |
| 2.5.3 Tumor cell lines and culture..... | 83 |
| 2.5.4 Recombinant adenoviruses (rAd). | 83 |
| 2.5.5 Generation of BM-derived DC and transduction with adenoviral vectors in vitro..... | 84 |

| | |
|---|-----------|
| 2.5.6 In vitro stimulation of DC..... | 85 |
| 2.5.7 ELISA. | 85 |
| 2.5.8 DC-Based Therapy. | 85 |
| 2.5.9 In vivo depletion of CD4 ⁺ or CD8 ⁺ T cells. | 86 |
| 2.5.10 Imaging of tumor tissues..... | 87 |
| 2.5.11 Flow cytometric analyses..... | 87 |
| 2.5.12 RNA purification and PCR analyses. | 88 |
| 2.5.13 Statistical analyses. | 89 |
| 2.6 ADDITIONAL SUPPORTING INFORMATION..... | 89 |
| 2.6.1 Materials and Methods | 89 |
| 2.6.2 Adaptive immune cells are required for TLS formation | 90 |
| 2.6.3 Immune cell trafficking via CD62L-PNAd interactions is required for the therapeutic efficacy of DC.IL-36 γ -based therapy | 91 |
| 2.6.4 Interpretation..... | 93 |
| 3.0 ASSOCIATION OF IL-36 GAMMA WITH TERTIARY LYMPHOID STRUCTURES AND INFLAMMATORY IMMUNE INFILTRATES IN HUMAN COLORECTAL CANCER | 96 |
| 3.1 ABSTRACT | 97 |
| 3.2 INTRODUCTION | 98 |
| 3.3 MATERIALS AND METHODS | 99 |
| 3.3.1 Public transcriptomic data sets | 99 |
| 3.3.2 Patient cohort..... | 100 |
| 3.3.3 IHC, immunofluorescence and image quantification..... | 100 |
| 3.3.4 Tumor processing, surface staining and cell sorting..... | 101 |

| | |
|--|------------|
| 3.3.5 Gene array analyses..... | 102 |
| 3.3.6 Statistical analyses | 102 |
| 3.4 RESULTS | 103 |
| 3.4.1 IL-36 γ is detected in the immune and vascular compartments in the TME .. | 103 |
| 3.4.2 IL-36 γ expression by macrophages is associated with markers of inflammation | 106 |
| 3.4.3 The predominant IL-36 γ -expressing cells in TLS are HEV-associated VEC | 109 |
| 3.4.4 IL-36 γ expression on the vasculature is associated with maintenance of TLS structures..... | 109 |
| 3.4.5 IL-1F5 expression in the TME is associated with immunosuppressive markers | 111 |
| 3.5 DISCUSSION..... | 112 |
| 3.6 ADDITIONAL SUPPORTING INFORMATION..... | 116 |
| 3.6.1 Materials and Methods | 116 |
| 3.6.2 Murine M1 macrophages exhibit a TLS-promoting phenotype..... | 116 |
| 3.6.3 Interpretation..... | 118 |
| 4.0 DISCUSSION AND PERSPECTIVES | 120 |
| 4.1 FURTHER DEFINING THE LINK BETWEEN IL-36γ AND TBET..... | 120 |
| 4.2 IL-36γ IS A NOVEL DRIVER OF THE ANTI-TUMOR IMMUNE RESPONSE ... | 121 |
| 4.3 ENDOGENOUS EXPRESSION OF IL-36γ IS LINKED TO A PRO-INFLAMMATORY PROFILE | 123 |
| 4.4 PERSPECTIVES | 124 |
| 4.4.1 The biologic function of IL-36 γ | 124 |
| 4.4.2 Tertiary lymphoid structures..... | 125 |
| 4.4.3 Combination immunotherapy..... | 126 |

| | |
|---|-----|
| 4.4.4 Alternative means of therapeutically introducing IL-36 γ into the TME..... | 128 |
| 4.4.5 Clinically relevant murine models | 130 |
| APPENDIX A. SUPPLEMENTARY FIGURES | 131 |
| APPENDIX B. SUPPLEMENTARY TABLES | 148 |
| BIBLIOGRAPHY | 155 |

LIST OF FIGURES

| | |
|---|----|
| Figure 1.1. PNA ^d biosynthesis. | 38 |
| Figure 1.2. Structure of classical and non-classical tertiary lymphoid structures..... | 43 |
| Figure 2.1. Characterization of therapeutic DC.Tbet. | 61 |
| Figure 2.2. DC.Tbet injected i.t. promote the rapid infiltration of lymphocytes and the development of PNA ^d blood vessels in association with enhanced locoregional induction of IL-36 γ | 64 |
| Figure 2.3. I.t.-delivered DC.Tbet mediates anti-tumor efficacy in secondary lymph node-deficient LTA ^{-/-} mice that is both CD4 ⁺ and CD8 ⁺ T cell-dependent. | 66 |
| Figure 2.4. The anti-tumor efficacy and TLS promoting activity associated with i.t. DC.Tbet-based therapy is ablated by the IL-36R antagonist IL-1F5 in vivo. | 70 |
| Figure 2.5. The anti-tumor efficacy and TLS promoting activity associated with i.t. DC.Tbet-based therapy is absent in the IL-36R ^{-/-} recipient mice. | 71 |
| Figure 2.6. DC.IL-36 γ produce/secrete bioactive IL-36 γ and upregulate intrinsic transcription of Tbet..... | 74 |
| Figure 2.7. I.t. delivery of DC.IL-36 γ is therapeutic and promotes TLS in wild-type, but not in IL-36R ^{-/-} hosts..... | 76 |
| Figure 2.8. The adaptive immune system is required for TLS formation. | 90 |
| Figure 2.9. CD62L-PNA ^d interaction is required for the therapeutic efficacy of DC.IL-36 γ treatment. | 92 |
| Figure 2.10. Proposed mechanism for the efficacy of DC.Tbet- and DC.IL-36 γ -based therapies. | 94 |

| | |
|---|-----|
| Figure 3.1. IL-36 γ is expressed by a variety of cell populations in the TME..... | 104 |
| Figure 3.2. M1 macrophages express high levels of IL-36 γ | 105 |
| Figure 3.3. Intratumoral macrophages are a source of local IL-36 γ | 106 |
| Figure 3.4. IL-36 γ ⁺ macrophages are associated with a proinflammatory TME..... | 108 |
| Figure 3.5. Expression of CD20 suggests presence of TLS in colorectal tumors. | 110 |
| Figure 3.6. Presence of the IL-36 receptor antagonist, IL-1F5, is not correlated with the density of CD20 ⁺ B cells in TLS. | 112 |
| Figure 3.7. M1 macrophages express genes linked to the promotion of tertiary lymphoid organogenesis..... | 118 |
| Figure S2.1. Human DC.Tbet cells upregulate expression of IL-36 γ | 131 |
| Figure S2.2. DC.mTbet express TLS-associated cytokines/chemokines and further potentiate their expression in the therapeutic TME. | 133 |
| Figure S2.3. LTA and CCL21 are upregulated in DC.Tbet/EGFP- vs. DC.EGFP-treated tumors. | 134 |
| Figure S2.4. Lymphocytes in TLS functionally resemble HEV in SLO..... | 135 |
| Figure S2.5. Phenotype of TIL from DC.Tbet/EGFP- versus DC.EGFP-treated tumors shows increased Type-1 functional polarity and decreased expression of exhaustion/anergic markers. | 136 |
| Figure S2.6. DC.IL-36 γ express TLS-associated cytokines/chemokines and further potentiate their expression in the therapeutic TME. | 137 |
| Figure S2.7. Lymphocytes in TLS functionally resemble HEV in SLO..... | 138 |
| Figure S2.8. MDSC, but not Tregs, are reduced in the TME after treatment with DC.Tbet/EGFP versus DC.EGFP..... | 139 |
| Figure S2.9. Expression of IL-1F5/IL-36RN and IL-1F10/IL-38 across human cancer types..... | 140 |
| Figure S3.1. Negative control staining..... | 141 |
| Figure S3.2. Representative gating strategy to identify T cells..... | 142 |

| | |
|--|-----|
| Figure S3.3. IL-36 γ ⁺ macrophages are not strongly correlated with most naïve and memory TIL subsets..... | 143 |
| Figure S3.4. Vasculature of secondary lymphoid organs express IL-1F5..... | 144 |
| Figure S3.5. IL-1F5 expression positively-correlates with expression of immunosuppressive genes in the TME. | 145 |
| Figure S3.6. Intratumoral expression of IL-36 γ is associated with a trend towards increased overall survival in several human cancers. | 146 |
| Figure S4.1. IL-36R-deficient DC.IL-36 γ confer superior therapeutic benefit versus WT DC.IL-36 γ | 147 |

LIST OF TABLES

| | |
|--|-----|
| Table 1.1. Presence and Prognostic Significance of TLSs in Cancer | 15 |
| Table 1.2. Lymphotoxin/LIGHT Receptors and Their Cell Expression Profiles..... | 20 |
| Table 1.3. IL-36R and IL-36 γ expression in the immune system..... | 51 |
| Table S2.1. Real-time PCR primers used in this study. | 148 |
| Table S2.2. Antibodies used in this study. | 149 |
| Table S3.1. Antibodies used for immunohistochemical and immunofluorescent imaging. | 151 |
| Table S3.2. Antibodies used for flow cytometric analyses. | 152 |
| Table S3.3. mRNA expression analysis of immune genes. | 153 |
| Table S3.4. Additional real-time PCR primers used in this study..... | 154 |

PREFACE

I would like to first thank all the members of the Storkus lab for their support, insight, and camaraderie. I've learned and laughed a lot with each of you, and couldn't have asked for a better group of people to work with over the past five years. I owe a special thanks to my mentor, Dr. Walt Storkus, for his direction and mentorship; and Jennifer, Ron, Lu, Subha, Kellsye, Manoj, and Emily for their friendship and scientific input and assistance that helped me grow as both a scientist and a person. I owe a sincere thanks as well to the members of my thesis committee, Drs. Lisa Butterfield, Binfeng Lu, Adrian Morelli, and Donna Stolz, for the guidance and resources that they provided me that allowed me to develop my research to the fullest potential. And I would like to thank the members of Teams 10, 13 and 15 at the Cordeliers Research Center, and especially to my mentor there, Dr. Catherine Sautès-Fridman, for welcoming me for 6 months and providing me the resources and support for a successful project as well as friendships that truly enhanced my stay in Paris.

Thank you to everyone who has supported me scientifically thus far – through high school, undergrad and grad school, I've had a constant stream of mentors and colleagues who helped get me to this point. Thank you as well to the several sources of individual funding I received during my training that allowed me to pursue this research and additional training experiences: the T32 in Autoimmunity and Immunopathology from NIAID, the Joy Cappel Young Investigator Award from Rockland

Immunochemicals, Inc., and the STEM Chateaubriand Fellowship of the Embassy of France in the United States.

Thanks to all of my friends in Pittsburgh who have been by my side and provided me friendship and encouragement throughout this process – you understand this process best, you've kept me sane during the toughest times, and I wouldn't have made it through without you. Thank you as well to the friends I made while in Paris for the camaraderie and adventures that made my time there truly one-of-a-kind. Finally, I'd like to thank my family for the constant encouragement to make the best decisions as I pursue my education and for being a source of support even and especially when I don't think I need it.

ABBREVIATIONS

Ad: Adenovirus

ADAM: A disintegrin and metalloproteinase

CCL: CC-motif chemokine ligand

CCR: CC-motif chemokine receptor

CM: Complete medium

CXCL: CXC-motif chemokine ligand

CXCR: CXC-motif chemokine receptor

DC: Dendritic cell

DcR3: Decoy receptor 3

DITRA: Deficiency in the IL-36 receptor antagonist

EGFP: Enhanced green fluorescent protein

EMRA: Effector, memory RA

GlcNAc6ST: N-acetylglucosamine 6-O-sulfotransferase

GlyCAM-1: Glycosylation-dependent cell adhesion molecule 1

GM-CSF: Granulocyte/macrophage colony-stimulating factor

HEV: High endothelial venule

HSV: Herpes simplex virus

HVEM: Herpesvirus entry mediator

IFN: Interferon

IHC: Immunohistochemistry

IL: Interleukin

IM: Invasive Margin

IRF: Interferon regulatory factor

i.p.: Intraperitoneal

i.t.: Intratumoral

LIGHT: Homologous to LT, inducible expression, competes with herpes simplex virus glycoprotein D for HSV entry mediator (HVEM), a receptor expressed on T lymphocytes, also known as TNFSF14

LPS: Lipopolysaccharide

LT: Lymphotoxin

MAdCAM-1: Mucosal vascular addressin cell adhesion molecule 1

MDSC: Myeloid-derived suppressor cell

MMP: Matrix metalloproteinase

MSI/MSS: Microsatellite instable/Microsatellite stable

NK: Natural killer

NKT: Natural killer T

NSCLC: Non-small cell lung cancer

PD-1: Programmed cell death-1

PD-L1: Programmed death ligand-1

PNAd: Peripheral node addressin

rAd: Recombinant adenovirus

s.c.: Subcutaneous

SLO: Secondary lymphoid organ

SMA: alpha-Smooth muscle actin

SMC: Smooth muscle cells

Tbet-ZsG: Tbet-ZsGreen

TC: Tumor core

TCM: Central memory T cell

TIL: Tumor infiltrating lymphocytes

Tfh: T follicular helper

Th: T helper

TLR: Toll-like receptor

TLS: Tertiary lymphoid structures

TME: Tumor microenvironment

TNF: Tumor necrosis factor

TNFRSF: TNF receptor superfamily

Treg: Regulatory T cell

VEC: Vascular endothelial cells

VEGF: Vascular endothelial growth factor

WT: Wild type

1.0 INTRODUCTION

1.1 IMMUNE RESPONSES IN THE TUMOR MICROENVIRONMENT

In their 2011 article, Hanahan and Weinberg updated the "hallmarks of cancer" to include "avoiding immune destruction." Indeed, it has become recognized over the past decade that the immune system plays a crucial role in tumor development and progression. Early in the formation of a tumor during the elimination and equilibrium phases, the immune system keeps a developing tumor at bay through the cooperation of innate and adaptive immune cells in recognizing tumor antigens, secreting Type-1-polarizing cytokines, and destroying the malignant cells. Subsequently, in the escape phase, the tumor evades immune system control by producing immunosuppressive molecules and downregulating intrinsic antigen presentation, thus preventing its recognition by immune cells (1).

Our understanding of how to at least partially reverse immune ignorance to evolving tumors has progressed in recent years. Most notably, inhibitors to PD-1 and PD-L1 negate negative signaling between tumor cells or tolerogenic myeloid cells and effector NK or T cells, and CTLA-4 blockade reverses T cell inhibition mediated through CD80 or CD86 molecules expressed on antigen presenting cells. While studies into the long-term efficacy of these therapies remains ongoing, early results indicate that their effectiveness may persist even after treatment is stopped, giving patients a chance at long-term survival without continued maintenance on treatment protocols. In light of these data, a major question still remains as to whether it is possible to not only induce broad-scale reversal of immunosuppression within the tumor microenvironment (TME), but to tailor the intratumoral immune response to be most effective at eliminating the tumor.

1.1.2 Tbet has a multitude of roles in the immune response, including the promotion of Type-1 immunity

Studies indicate that Type-1 immune responses, characterized by the expression of Tbet, IL-12p70, and IFN γ , are most effective at recognizing and destroying tumor cells (2). Tbet (i.e. TBX21) is a T-box family transcription factor expressed by a variety of innate and adaptive immune cells, including CD4⁺ and CD8⁺ T cells, NK cells, B cells, and dendritic cells (DC) (3,4). In particular, Tbet is best known as the master regulator of Type 1 immunity, though its role differs depending on the immune cell type in which it is expressed. Tbet is necessary for the transcription of the canonical Type-1 cytokine *IFNG* in CD4⁺ effector T cells (5) via a mechanism involving the suppression GATA-3 and downstream IL-4 and IL-5 expression to prevent skewing towards a Type-2

phenotype (6,7) as well as the downmodulation of Type-17-like responses (8). Forced overexpression of Tbet into polarized Th2 (CD4⁺) or Tc2 (CD8⁺) T cells converts these cells to a Type-1 phenotype, and they begin to express IFN γ (5,7) while suppressing secretion of IL-4 and IL-5 (5). Conversely, CD4⁺ effector T cells generated from Tbet^{-/-} mice express extremely low levels of IFN γ , but high levels of IL-4 and IL-5 compared to CD4⁺ T cells generated from WT mice (5). In CD8⁺ T cells, Tbet controls the transition from a naïve to effector phenotype after exposure to cognate antigen (9). Tbet is also important for promoting the infiltration of CD8⁺ T cells into the tumor versus lymph node following adoptive T cell therapy, where it also cooperates with Eomes to promote the development of effector and central memory T cells that protect the host against tumor re-challenge (10).

Tbet plays a similar role in DC to that it plays in CD4⁺ T cells, as it is required for the expression of IFN γ (but not other pro-inflammatory cytokines such as IL-12p40, IL-12p70, TNF, and IL-1). Indeed, Type-1 polarized DC (DC1) express similar levels of Tbet as do Th1 cells (4). Tbet is required for IFN γ expression by DC following stimulation with IL-12p70 and/or IL-18, as Tbet^{-/-} DC, but not their WT counterparts, fail to transcribe or secrete IFN γ following stimulation with these cytokines (4). Upon stimulation with IFN γ , DC can upregulate expression of Tbet, an effect that is not replicated when DC are stimulated with other classical activators such as LPS, TNF, or IL-1. Expression of Tbet by DC is also necessary for their ability to activate Th1 cells, as shown following OVA stimulation in an *in vivo* model (4) and downstream of TLR9 stimulation by CpG ODN in an *in vivo* model of *Listeria monocytogenes* infection (11); in both systems, protection is lost if DC lack expression of Tbet. There have also been reported roles for Tbet in B cells: Tbet appears to be required for the class switching of autoantibodies to IgG, independent of its role in T cells in both in mouse models of lupus pathogenesis (12) and an OVA vaccine model targeting melanoma (13). Intrinsic expression of Tbet by B cells appears to be predominantly found in the memory and plasmablast subsets (14), and is required for the migration of antibody-forming and germinal center B cells towards CXCL10, which is produced in high levels at sites of

inflammation (13). Tbet is also known to be expressed by human cytotoxic CD56^{dim} NK cells, iNKT cells, and some Eomes⁺ gamma-delta T cells (14).

1.1.3 DCs in cancer

1.1.3.1 Endogenous DCs Conventional DC can be naturally found within some types of human cancers, where they serve as a positive prognostic biomarker. In lung cancer, a high density of (mature) DC-LAMP⁺ DC, which are found exclusively within tertiary lymphoid structures (TLS), was found to be the best predictor of extended overall and disease-free survival (15). The density of DC-LAMP⁺ DC in patients with non-small cell lung cancer (NSCLC) was also positively correlated with the density of Tbet⁺ CD4⁺ T cells, an effect not observed when considering the Tbet⁺ CD8⁺ T cell compartment (16). In breast cancer patients, the presence of DC-LAMP⁺ DC in tumors was similarly linked to increased overall and disease-free survival. Notably, DC represent the primary source of the TLS-inducing cytokine lymphotoxin beta (LT β) in the TME over tumor cells, NK cells, T cells, and B cells. The density of DC-LAMP⁺ DC correlated with expression of the chemokines CCL19, CCL21, and CXCL13, all of which can independently promote the migration of T cells, B cells, and DC into tissue, and which are correlated with the density of T cells, B cells, and PNA⁺ HEV in the TME of breast cancer (17). A similar relationship between mature DC and TLS occurs in the setting of melanoma, where the densities of DC-LAMP⁺ DC and high endothelial venules (HEV) are strongly correlated with one another, with DC observed to localize around HEV (18).

1.1.3.2 DC-based immunotherapies Because of their role as the primary antigen presenting cell in inducing Type-1 immune responses, DC are frequently the basis of immunotherapies designed to treat or prevent cancer. Such therapies include DC-based vaccines, in which autologous DC are pulsed with tumor-derived peptides, including those derived from the tumor cells themselves (19–21) or from components of the TME, such as the tumor vasculature (22–24). These DC-based vaccines are generated *in vitro* by maturing autologous DC to increase expression of T cell stimulatory molecules, including CD80, CD86, and MHCII (19,21) and then loading these cells with target antigen for presentation of T cell epitopes in MHC complexes expressed on the DC surface. Injection of DC primed against tumor antigens activates a rapid Type-1 immune response that often leads to delayed tumor growth or tumor regression in murine models (19–24). Interestingly, the efficacy of these DC-based immunotherapies appears to require that they be conditioned under Type-1 conditions in order for the treatment to promote the expansion of tumor-specific CD8+ CTL versus T cells unable to exert effector function against target tumor cells (25). Vaccine-induced epitope spreading in the T cell repertoire, or therapeutic T cells invoked by the vaccine but reactive against tumor antigens not present in the vaccine, as a consequence of evolving rounds of antigen cross-priming, can also be observed (20,22) and may serve as a useful as a prognostic biomarker to identify patients most likely to respond well to treatment (26). Unfortunately, it has also been noted that tumors can escape from the therapeutically-induced immune response and continue to progress following DC-based vaccination. This supports the importance of generating poly-specific immune responses reactive against multiple tumor antigens to sustain therapeutic benefit and preclude the progression of antigen-escape variants.

Other DC-based immunotherapies are not antigen-specific, and instead are designed to bestow enhanced antigen presenting capability to these cells via stimulation with activating or Type-1-polarizing cytokines or engineering to force overexpression of immunostimulatory chemokines, cytokines, or transcription factors by these cells. Our lab has previously investigated whether DC engineered using an adenoviral vector to overexpress either *IL-12p70* (DC.IL12) or *Tbet* (DC.Tbet) are able to delay tumor

progression in a mouse model. Results from the CMS4 (BALB/c) sarcoma model indicate that DC.IL12 or DC.Tbet treatments are able to delay tumor progression, while treatment with DC.Tbet/IL12 (i.e., cells engineered to overexpress both *IL-12p70* and *Tbet*) leads to tumor regression and increased overall survival. Each of these treatments enhances CD8⁺ T cell reactivity to tumor cell- and tumor-associated stromal cell-derived antigens (27). Treatment with DC.Tbet has also been shown to delay tumor progression in the MCA205 (C57BL/6) sarcoma model, via a mechanism dependent on the local recruitment of CD8⁺ T cells and NK cells following treatment, but not the migration of injected DC to secondary lymph nodes (28). In the CMS4 as well as B16 models, the observed effect of DC.Tbet, DC.IL12, or DC.Tbet/IL12 treatments were enhanced by the loading of DC with tumor peptides prior to injection (27).

1.1.3.3 Perspectives on DC-based Immunotherapy DC-based vaccination strategies have shown minimal success both in the pre-clinical and clinical settings, and an additional disadvantage to peptide-based vaccines is that the same vaccine can not necessarily be applied across multiple tumor types, nor to different patients with the same type of tumor due to variations in tumor antigen expression and HLA haplotypes (29). The question remains as to how DC can best be employed to induce a protective immunity across a range of tumor types, regardless of the antigen expression profiles by heterogeneous populations of tumor cells.

1.2 THERAPEUTIC LYMPHOID ORGANOGENESIS IN THE TUMOR MICROENVIRONMENT

Aliyah M. Weinstein¹, Walter J. Storkus^{1,2,3}

From the ¹Department of Immunology, University of Pittsburgh School of Medicine, Pittsburgh, Pennsylvania, USA; ²Department of Dermatology, University of Pittsburgh School of Medicine, Pittsburgh, Pennsylvania, US; ³University of Pittsburgh Cancer Institute, Pittsburgh, Pennsylvania, USA

This section is adapted from text originally published in *Advances in Cancer Research* (2015; vol. 128). doi: 10.1016/bs.acr.2015.04.003. Both authors contributed to the manuscript.

1.2.1 Abstract

The inflammatory status of the tumor microenvironment (TME) has been heavily investigated in recent years. Chemokine and cytokine signaling pathways such as CCR7, CXCR5, lymphotoxin, and IL-36, which are involved in the generation of secondary lymphoid organs (SLO) and effector immune responses, are now recognized as having value both as prognostic factors and as immunomodulatory therapeutics in the context of cancer. Furthermore, when produced in the TME, these mediators have been shown to promote the recruitment of immune cells, including T cells, B cells, DCs, and other specialized immune cell subsets such as follicular DCs and T follicular helper (Tfh) cells, in association with the formation of tertiary lymphoid structures (TLS) within or adjacent to sites of disease. Although TLS are composed of a heterogeneous collection of immune cell types, whose composition differs based on cancer subtype, the qualitative presence of TLS has been shown to represent a biomarker of good prognosis for cancer patients. A comprehensive understanding of the role each of the driver pathways plays within the TME may support the rational design of future immunotherapies to selectively promote/bolster TLS formation and function, leading to improved clinical outcomes across the vast range of solid cancer types.

1.2.2 Introduction

In recent years, a growing body of literature has established important roles for inflammatory immune cells in the etiology of a wide variety of diseases, including infectious virus-associated diseases, autoimmune diseases such as psoriasis and arthritis, and cancer. More recently, work in this field has expanded in an attempt to elucidate critical signaling pathways involved in initiating and fine-tuning inflammatory immune cell activity within affected tissue sites. It has become clear that an array of chemokines (e.g. CXCL13, CCL19, CCL21, and members of the TNF family) and cytokines (e.g. IL-36R and LT β R agonists) play important roles in the recruitment, activation, and function of immune cells within inflamed/diseased tissue microenvironments. The orchestration of these factors culminates in the development of organized networks of innate and adaptive immune cells within the TME, that have commonly been referred to as TLS. Here, we will attempt to provide a better understanding of these pathways to provide a foundation for the design of next-generation immunotherapies that will allow for the selective targeting of inflammatory pathways at the appropriate time and location during disease evolution to prevent, deter, or eradicate cancer *in vivo*.

1.2.3 Development of TLS in Chronically-Diseased Tissues

Our understanding of the dynamics of how immune cells infiltrate and persist as an operational unit within the TME has evolved considerably over the past decade, and now encompasses a paradigm in which TLS develop at the periphery of or within tumor lesions to limit disease progression and/or as a consequence of effective treatment

intervention. TLS are distinct from primary and secondary lymphoid organs as they do not form during embryonic development and instead can originate in any non-lymphoid tissue that has been subject to prolonged/chronic inflammation (30). TLS express chemokines including CCL19, CCL21, and CXCL13 that recruit naive and effector CD4⁺ and CD8⁺ and memory CD4⁺ T cells, B cells, and NK cells to sites of inflammation (31). The primary cell populations found within TLS are DCs, B cells, and naive and memory T cells (32). For example, lymphocytic aggregates and an upregulation of associated chemokines have been observed in the affected tissues of individuals with chronic inflammatory diseases such as Sjögren syndrome, rheumatoid arthritis, multiple sclerosis, myasthenia gravis and Hashimoto's thyroiditis (33), as well as cancer (15,34–36).

1.2.3.1 TLS: Organizational structure Interestingly, it has been observed that there is not a uniform distribution of TLS within inflammatory peripheral tissue microenvironments. For instance, in the setting of oral squamous cell carcinoma, approximately one third of tumors presenting with TLS were missed when only one section of the tumor was evaluated by pathologists (37). In Merkel cell carcinoma, most tumor-infiltrating CD8⁺ T cells and TLS were located at the tumor periphery, with the presence of TLS correlating with an increased CD8⁺-to-CD4⁺ T cell ratio at the margin, but not in the center, of the tumor mass (38). Similarly, in breast cancer, TLS are sometimes observed proximal to the stroma, and within an individual lymphoid structure, the number of lymphocytes decreased as a function of proximity to the center of the tumor, with the most actively proliferating lymphocytes localized to a small area adjacent to the stroma (39). In other models of breast cancer, TIL are observed in the tumor stroma, but not embedded within the tumor tissue itself (40). In metastatic colorectal cancer, B cell infiltrates were localized to the outer edges of the tumor lesion (41). These data suggest that the TME is architecturally heterogeneous with regard to the presence and localization of TIL/TLS, and that diverse signals likely contribute to determining the anatomic locations in which TLS are “seeded”. In this regard, studies have shown that the same signals controlling lymphocyte recruitment to sites of inflammation may play drastically different roles under normoxic (characteristic of the tumor outer cortex/margin) versus hypoxic (characteristic of the tumor core) conditions. For example, signaling via the CCL21/CCR7 axis has been shown to promote angiogenesis in inflammatory microenvironments (42), and new blood vessel formation is one mechanism that facilitates tumor growth and metastasis. In ovarian cancer, hypoxia induced an increase in intrinsic CCR7 expression by tumor cells, with CCL21 signaling in the hypoxic TME contributing to an upregulation of N-cadherin and the matrix metalloproteinase MMP-9, which are known to promote cell migration and invasiveness (43). In patients with non-small cell lung cancer (NSCLC), a similar effect has been observed, as expression of MMP-1 and ADAM metalloproteinase with thrombospondin type 1 motif, 2 (ADAMTS2) in PBMCs was correlated with poor clinical outcome (44).

The organizational structure of TLS in tumors can vary substantially. While classical lymphoid structures are comprised of a B cell follicle (i.e. a germinal center) intertwined with a network of follicular DC, intratumoral B cell infiltrates have been observed in which the B cells are heterogeneously “sprinkled” throughout the tissue instead of being localized within focused aggregates. This has been observed in human oral squamous cell carcinoma (37) and breast cancer (40) tissues, and in tissue sections of murine MCA205 fibrosarcomas (36), in association with more beneficial disease outcomes. Thus, the establishment of higher order structure in TLS in or near tumors *in vivo* may not be a critical factor to the development of effective anti-tumor immune response. It may only be required that the infiltrating effector cells and antigen (cross)-presenting cells interact productively within the TME.

1.2.4 TLS in cancer: Clinical Correlates of Disease Progression and Response to Treatment

In the cancer setting, the presence of TLS in the TME correlates with increased disease-free survival in patients, with similar results obtained in murine tumor models (see **Table 1.1**). These structures allow for the activation, expansion and differentiation of tumor antigen-specific B and T cells within the tumor itself, leading to a more effective anti-tumor immune response even in the absence of therapeutic intervention (31,45). In melanoma, a 12-gene signature has been characterized that predicts both the presence of TLS within a tumor and increased survival. This signature includes genes that encode for CCL19, CCL21, and CXCL13, as well as CCL4, CXCL9, and CXCL10 (46). In patients with oral squamous cell carcinoma, the presence of TLS is associated with a decrease in tumor-associated death (37). In Merkel cell carcinoma, the presence of TLS correlated with significantly increased recurrence-free survival compared with patients whose tumors did not contain TLS (38). In lung cancer, TLS arise spontaneously and confer a beneficial phenotype to patients (45). In these patients, both the density of

mature (DC-LAMP⁺) DC (15) and follicular DC (47) can be used as markers for increased survival. Tumors containing fewer mature DC demonstrate a corresponding decrease in Type 1-polarized CD4⁺ T cells (15), suggesting that TLS within the TME are crucial locations for generating effective Type-1 anti-tumor immune responses and that a diminished ability to prime a Type-1 response allows for tumor growth. Supporting this contention, in lung cancer, the presence of mature DC within TLS was a better predictor of patient survival than the presence of CD8⁺ T cells in TLS, with high densities of mature DC also correlating with increased expression of genes related to Type-1 effector cell polarization and cytotoxicity in the TME (48,49), and patients with intratumoral TLS have an increased likelihood of survival compared to those who do not (15,47). In primary HER2⁺ breast cancer, infiltration of lymphocytes corresponded to a decrease in the recurrence rate of tumors and a more favorable patient outcome. This was marked by an increase in intratumoral levels of chemokines associated with the development of lymphoid structures - including CCR7, CCL19, CXCL9, CXCL10, CXCL13, and LIGHT - and levels of genes associated with lymphocytes- such as ZAP70, CD8, CD28, and Lck (50).

In patients with metastatic colorectal cancer, an increased number of discrete TLS within the TME correlates with an increase in overall survival and a decrease in disease recurrence compared with patients presenting with less immune cell infiltrates; these groups can be stratified based on the presence of TLS or the level of CD45⁺ or CD20⁺ tumor-infiltrating cells (41), indicating that interactions between B cells and other lymphocyte populations play a role in mediating anti-tumor immunity. B cell infiltration also corresponded with a more favorable prognosis in breast cancer. The number of B cells found within the TME correlated with an increase in cancer specific survival and disease free survival in patients (40). B cells in the TME undergo antigen-driven proliferation, somatic hypermutation, and affinity maturation within the tumor, and these cells co-localize with T cells, follicular DC, and plasma cells into structures resembling tertiary lymphoid structures (51). In a subsequent study of breast cancer patients, an additional marker of overall survival related to the presence of TLS was determined to be the presence of T follicular helper cells, a subset of CD4⁺ T cells that produces

CXCL13 and recruits B cells to sites of inflammation (39). In this study, the presence of CXCL13 was also positively correlated with IFN γ expression, suggesting that T follicular helper cells play a role in initiating Type 1 immune responses. B cells have independently been shown to be required for the generation of anti-tumor CTL responses, especially in melanoma. Depletion of B cells before inoculation of B16 melanoma into mice led to an increase in primary tumor burden and in number of lung metastases, indicating that B cells are important for the initial immune response generated against a tumor. The increase in tumor growth was concurrent with a decrease in IFN γ - and TNF α -secreting T cells in the TME as well as a decrease in the number of T cells found in the periphery and in the tumor draining lymph node (52). Of note, it was also observed that the T cells present within tumors with high numbers of tumor infiltrating lymphocytes were more likely to be T follicular helper cells or Type 1-polarized CD4⁺ cells (39). These data support the idea that orchestrated interactions between immune cell subtypes within the tumor are critical to the generation of protective anti-tumor immune responses.

Interestingly, some tumors that arise in highly inflammatory microenvironments benefit from the infiltration of regulatory T cells (Tregs) as opposed to effector immune cells into the TME. In particular, in the cases of head and neck cancer and colorectal cancer, the presence of intratumoral Treg has been reported to convey good clinical prognosis (53,54).

Furthermore, the presence and magnitude of tumor infiltrating lymphocytes (TIL) in the TME has been strongly associated with the effectiveness of a range of chemo- and immuno-therapeutic agents. Many immunotherapeutic strategies currently being investigated in clinical trials involve immune checkpoint blockade, including the use of antibodies capable of inhibiting signaling through CTLA-4 or PD-1 into T cells. Interestingly, it appears that these therapies may work, at least in part, via increasing the ability of newly-arrived CD8⁺ TIL to be primed and then mature into protective anti-tumor T effector cells. Priming of CD8⁺ T cells in the tumor draining lymph nodes or the trafficking of circulating T effector cells into the TME appear less important to clinical outcome than the priming of resident TIL after blockade of CTLA-4, PD-L1, or IDO (55).

Similarly, the presence of T follicular helper cells in breast cancer TME predicts for superior responsiveness to pre-operative chemotherapy (39). More broadly, the presence of TLS or CXCL9 expression in the TME of patients with breast cancer is a statistically significant predictor of a higher incidence of complete response to neoadjuvant chemotherapy (56).

Table 1.1. Presence and Prognostic Significance of TLSs in Cancer

| Cancer subtype | Location of TLS | Inflammatory infiltrates | Anti-inflammatory infiltrates | Predictive outcome of TIL/TLS presence | References |
|--------------------------|---|--|-------------------------------|--|------------------|
| Bladder carcinoma | proximal to tumor cell nests | CD3 ⁺ T cells, including CTL; CD20 ⁺ B cells; follicular DC; mature CD208 ⁺ DC | N/A | increased anti-tumor immune response; no correlation with invasion, metastasis, or poor prognosis | (57,58) |
| Breast cancer | proximal to/tumor stroma; peritumoral | lymphocytes; B cells; T cells; follicular DC; plasma cells; T follicular helper cells | N/A | decreased disease recurrence; increased response to chemotherapy | (39,40,50,56,59) |
| Colorectal carcinoma | tumor periphery | B cells; Type 1-polarized memory T cells; CD8 ⁺ T cells; CD45RO ⁺ T cells; follicular DC | Tregs | inflammatory cells: equivocal (either disease progression and recurrence, or anti-tumor immune response and low-risk, early-stage disease); Tregs: improved survival | (31,53,54,60,61) |
| Gastric cancer | invasive margin; tumor core | B cells; Bcl6 ⁺ germinal center B cells; CD4 ⁺ , including Th1, T cells; CD8 ⁺ T cells; follicular DC | FoxP3 ⁺ Tregs | increased overall survival; relapse-free survival | (62,63) |
| Head and neck cancer | tumor stroma; tumor periphery; intratumorally | macrophages; CD4 ⁺ T cells; CD8 ⁺ T cells | FoxP3 ⁺ Tregs | effector T cells: increased overall survival; Tregs: decreased local recurrence | (53,64) |
| Hepatocellular carcinoma | liver parenchyma | T cells; B cells; neutrophils; NK cells; macrophages; follicular DC | Tregs | Increased recurrence; decreased overall survival | (65) |

| | | | | | |
|------------------------------|------------------------------------|--|---|---|---------------|
| Lung cancer (NSCLC) | tumor stroma | mature DC; follicular DC; CD62L ⁺ and naive CD4 ⁺ and CD8 ⁺ T cells; B cells; follicular DC | N/A | increased survival | (15,45,47–49) |
| Melanoma | peritumoral stroma; intratumorally | B cells; T cells; CD86 ⁺ DC | N/A | increased survival | (46,52) |
| Merkel cell carcinoma | tumor periphery | CD8 ⁺ T cells; B cells; APC | N/A | increased survival; recurrence-free survival | (38) |
| Metastatic colorectal cancer | tumor periphery | CD45 ⁺ T cells; CD20 ⁺ B cells | N/A | increased overall survival; decreased disease recurrence | (41) |
| Oral squamous cell carcinoma | peritumoral stroma | B cells; follicular DC | N/A | increased survival | (37) |
| Pancreatic cancer | Intratumoral; peritumoral | Th1 and Th17 cells; CD8 ⁺ T cells; B cells; DC; follicular DC | low infiltrate of Tregs and macrophages | increased overall and disease-free survival | (66–68) |
| Renal cell carcinoma | peritumoral | mature DC; CD3 ⁺ T cells | N/A | increased survival; increased disease-free survival; increased overall survival | (69) |

1.2.5 Cues for TLS Development

While the precise sequence of signals that serve to control TLS development has yet to be completely elucidated, especially in the context of the TME, certain signaling pathways classically known to recruit immune cells into inflammatory tissue microenvironments appear to be involved.

1.2.5.1 The requirement for lymphotoxin signaling in the evolution of TLS in the

TME Lymphotoxin (LT)- α / β signaling through the LT β R is required for the establishment and maintenance of lymphoid structures. LT α and LT β are members of the TNF family and share common receptors and signaling pathways with other members of their family. The lymphotoxin ligands are expressed predominantly by immune cell subsets, while the receptors are found on epithelial cell populations. The receptor-ligand interactions promote the organization of immune cells and stromal cells within lymphoid structures (70). The LT α /LT β subunits exert their biologic function by forming three distinct trimeric molecules, each with different receptor specificity. The homotrimer of lymphotoxin alpha, LT α_3 , is a secreted protein that signals through TNFR1, TNFR2, and HVEM (70,71). Two membrane bound heterotrimers can also form from the lymphotoxin subunits: LT $\alpha_1\beta_2$ and LT $\alpha_2\beta_1$, with LT $\alpha_1\beta_2$ being the predominant form. LT $\alpha_1\beta_2$ signals through the lymphotoxin beta receptor (LT β R), while LT $\alpha_2\beta_1$ is able to bind TNFR1 and TNFR2 but does not have a clear biologic role in signaling through these receptors (70). The receptors TNFR1 and TNFR2 have broad expression throughout the body. The lymphotoxin beta receptor is expressed by stromal cells, epithelial cells, monocytes, and DC. HVEM is expressed by T cells, DC, macrophages, and epithelial cells (**Table 1.2** and ref. (72)). Specifically, signaling through the LT β R is required for HEV differentiation and for the formation of organized SLO. Blockade of signaling through the LT β R results in decreased lymphocyte migration into lymph nodes in a model of collagen-induced arthritis, and this appears due to impaired expression of adhesion molecules PNA β and MAdCAM on HEV (73). A similar decrease in lymphocyte trafficking is observed in Peyer's patches in the absence of LT β R-mediated signaling (74). In the spleen, signaling through the LT β R is required for the segregation of B cells and T cells into distinct zones, and for the generation of follicular DC and the formation of B cell follicles (75). LT β R-associated signaling also plays a key role in TLS formation. In mice that constitutively express both LT α and LT β in the pancreas, the T and B cell chemokines CCL19, CCL21 and CXCL13 were more predominantly expressed, L-selectin $^+$ (aka CD62L $^+$; binds PNA β and MAdCAM) cells were more abundant, and T and B cell zones within the immune infiltrate were more pronounced

than in mice only expressing $LT\alpha$ (76). In the TME, PNA_d and L-selectin expression is exclusively found within TLS and not elsewhere in the stroma or the tumor tissue, and the two co-localize with each other (45). L-selectin is important for the trafficking of naïve (77,78) of central memory T cells (79), in conjunction with CCL19 and CCL21 gradients that signal through CCR7 on these cells (31,79). Lymphotoxin- α / β induce the production of CCL19, CCL21, and CXCL13 (80). Specifically, lymphotoxin- α is required for CCL19, CCL21, and CXCL13 expression, while $LT\beta$ is most critically required for CXCL13, but less so CCL19 or CCL21, expression (81). This appears to be a result of the differential receptor binding ability of the lymphotoxins and the downstream signaling components being activated (70). Such pathways appear to involve a positive feedback loop in the spleen, where cells expressing the $LT\beta R$ and CXCL13 recruit B cells, with activated B cells subsequently expressing $LT\alpha_1\beta_2$, begetting further expression of CXCL13 by stromal cells (80). A similar biologic circuit has been shown to exist between $LT\alpha_1\beta_2$ and CCL19 and CCL21 in both SLO and TLS (80,82). Blockade of signaling through the $LT\beta R$ using a soluble decoy receptor blocks the recruitment of both B cells and $CD8^+$ T cells into lymphoid organs (73).

Table 1.2. Lymphotoxin/LIGHT Receptors and Their Cell Expression Profiles.

This table describes the receptor binding capabilities of the TNF family member ligands that play critical roles in tertiary lymphoid organogenesis.

| Ligands | Receptor | Function | Receptor Expression | References |
|--|--------------|-----------|--|------------|
| TNF α ; LT α_3 ; LT $\alpha_2\beta_1$ | TNFR1 | Signaling | Widespread | (70,72,83) |
| TNF α ; LT α_3 ; LT $\alpha_2\beta_1$ | TNFR2 | Signaling | Widespread | (70,72,83) |
| LT $\alpha_1\beta_2$; LIGHT | LT β R | Signaling | Stromal cells; epithelial cells; monocytes; DC | (71,72,83) |
| LIGHT; LT α_3 | HVEM | Signaling | T cells; DC; macrophages; NK cells; epithelial cells | (72,83) |
| LIGHT | DcR3 | Decoy | Secreted | (84) |

Surprisingly, tumor and stromal cells may also express and respond to signaling through the LT β R. Induction of this signaling pathway by the natural ligand LT $\alpha_1\beta_2$ or by cross-linking with LT β R-Ig can induce the secretion of the pro-inflammatory mediators IL-8 and CCL5 by both melanoma (A375) and fibroblast (WI38VA13) cell lines *in vitro* (85). The effect of LT β R signaling on non-immune cell subsets is predicted to have an additional role in promoting anti-tumor immunity besides its role in the formation of TLS.

1.2.5.2 EnLIGHTening Protective Immunity in TLS Both stromal and immune cell populations respond to LIGHT (also known as TNFSF-14). LIGHT, expressed by T cells, immature DC, and macrophages (72), is related to the lymphotoxins and is able to signal through several receptors of the TNF superfamily, including the LT β R on stromal cells and HVEM (also known as TNFRSF-14; ref (71)) on T cells. In regard to the generation of an immune response, LIGHT is required for CD8⁺ but not CD4⁺ T cell proliferation and differentiation (86). Mice lacking LIGHT were shown to have impaired CD8⁺ T cell responses to bacterial infection (86), indicating a requirement for LIGHT in the generation of productive Type 1 immune responses. Furthermore, LIGHT is able to synergize with IFN γ to enhance the production of CXCL9, CXCL10, and CXCL11, which serve to recruit and polarize CXCR3⁺ Type-1 immune cells (87).

In the context of tumor immunology, expression of LIGHT appears to have a broadly beneficial role in reducing tumor burden and improving survival. In breast cancer patients, LIGHT expression correlates with the generation of TLS in the TME. Expression of LIGHT mRNA was 5 times greater in the newly-formed structures than in normal lymph nodes isolated from the same patient (88), suggesting that LIGHT may be a driver in the formation of TLS in the cancer setting. Ectopic introduction of LIGHT into the TME has been shown to promote the development of anti-tumor immunity in numerous models of cancer. Forced expression of LIGHT in a fibrosarcoma model (Ag104L^d) resulted in increased signaling through the LT β R on stromal cells in the TME, leading to upregulated expression of CCL21 and MAdCAM-1 by these cells. Treated tumors also exhibited increased CD8⁺ T cell infiltration that ultimately led to the rejection of established disease (89,90). A similar result was observed in established murine melanoma (B16) and colon (MC38) cancers (90). Intratumoral vaccination with a recombinant adenovirus encoding the cDNA for LIGHT (Ad.LIGHT) is able to incite anti-tumor immune responses against B cell lymphoma (91), cervical cancer (92), and breast cancer (90). In the B cell lymphoma model, treatment with Ad.LIGHT induces expression of CCL21 and recruitment of T cells into the TME, increases overall survival from primary tumor challenge, and protects treated mice against normally lethal tumor re-challenge (91). When applied in combination with a HPV16-VRP vaccine in cervical

cancer models, Ad.LIGHT is able to increase circulating levels of anti-tumor T cells, promote CD8⁺ T cell infiltration into the TME, regulate tumor growth, and increase overall survival, when compared with vaccines alone (92). Ad.LIGHT injected into established murine 4T1 breast cancers results in diminished lung metastasis after surgical removal of the primary tumor (90). Together, these results suggest that Ad.LIGHT is able to initiate a systemic, tumor antigen-specific immune response that is protective. Work evaluating treatment with mesenchymal stem cells engineered to overexpress LIGHT (MSC-L) has also shown an inhibition tumor growth following treatment in both gastric (93) and breast (94) cancer models. In the breast cancer model, the efficacy of MSC-L was dependent on the ability of lymphocytes to be recruited into the TME via LT β R-dependent signaling events (94). Interestingly, another study evaluating LIGHT/HVEM signaling determined that advanced stage gastric cancer patients expressed significantly lower levels of HVEM on the surface of their leukocytes, and higher serum levels of soluble HVEM shed from leukocytes when compared to healthy controls (95). Prior studies reported the presence of robust levels of soluble HVEM in the serum of patients with autoimmune diseases such as psoriasis, dermatitis, and arthritis (96), suggesting that soluble HVEM may represent a marker of ongoing chronic inflammatory conditions. In addition, low levels of HVEM have been shown to drive the generation of dominant Type-2-polarized immune responses in patients with cutaneous T cell lymphoma, in association with disease progression (87). Low levels of LIGHT production in metastatic colorectal cancer lesions has been linked to a decreased number of intratumoral T cells compared to normal tissue (97). This immunosuppression could be reversed by introducing LIGHT into the system as an interventional strategy. In support of this possibility, forced expression of LIGHT in the mouse TRAMP-C2 model of prostate cancer overcomes Treg-mediated immunosuppression and synergizes with a biologic vaccination strategy (PSCA TriVax) to activate DC and recruit effector T cells into the TME (98). In particular, synergy between LIGHT and PSCA TriVax suggest that LIGHT plays a role in the generation of autoimmune responses, which in the context of cancer may promote a reduction in tumor burden. HVEM, the receptor for LIGHT, is also able to bind BTLA, a molecule found on T effector cells that enhances their ability to be suppressed by Tregs (99).

Thus, in the immunosuppressive TME, LIGHT may compete with BTLA for binding of HVEM, thereby limiting the ability of Tregs to suppress immune effector cells (99). Furthermore, LIGHT has the capacity to bind to decoy receptor 3 (DcR3), a soluble receptor that is expressed by many tumors, including those located in the esophagus, stomach, colorectal, pancreatic, lung, brain, renal, ovarian, blood, hepatocellular, and oral cavity (100). DcR3 is related to two other decoy receptors of the TNF family that bind but do not induce signaling upon binding their ligand. Since DcR3 sequesters LIGHT, an additional avenue of translational research aims to engineer a mutant LIGHT that is unable to bind DcR3 but retains its ability to signal through HVEM and LT β R to induce more potent anti-tumor immune responses. Of note, LIGHT that is unable to bind DcR3 is better able to induce the apoptotic death of tumor cells (101), with its effects on immune cell subsets to be determined. LIGHT does appear to have detrimental effects in tumors that arise due to chronic inflammation. In livers infected with hepatitis or with virally-induced hepatocellular carcinoma, levels of LTA, LT β , LIGHT and LT β R are increased, and chronic hepatitis in this model can be alleviated by treatment with LT β R-Ig, which serves as a sink for LT β R ligands (102).

LIGHT has also been shown to play a role in NK cell involvement in anti-tumor immunity. NK cells constitutively express HVEM, and forced expression of LIGHT in the TME mediates recruitment of NK cells to the tumor from the periphery and activation of these cells, including secretion of IFN- γ . Strikingly, this study observed a requirement for both activated NK cells and IFN γ in inducing an anti-tumor CTL response at later time points: peak NK cell infiltration was observed at 10 days post-tumor inoculation, while peak CD8 $^+$ T cell levels occurred 22 days post tumor inoculation. This unique role for NK cells in CD8 $^+$ T cell activation is not observed in SLO such as the spleen (103). NK cells have also been shown to induce the maturation of DC using a similar pathway: upon recognition of target cells, NK cells upregulate their cell surface expression of LIGHT, and LIGHT-expressing NK cells were able to induce upregulation of CD86 on the surface of autologous DC in a cytokine-independent manner (104). Thus in addition to playing a role in the recruitment of lymphocytes to the TME, LIGHT appears to also

have a direct role in priming anti-tumor immune responses, pointing to LIGHT as a potential therapeutic agent to be explored in the clinic.

1.2.5.3 The Importance of CCR7 Agonists for TLS Evolution in the TME CCL19 (i.e. EBV-induced molecule 1 ligand chemokine/ELC or MIP-3 β) and CCL21 (i.e. secondary lymphoid chemokine/SLC) are constitutively expressed by stromal cells and serve to recruit CCR7⁺ cells to sites of inflammation (105). Within the immune repertoire, CCR7 is expressed on naive and memory T cells, B cells, DC, and NK cells (31,106,107). In a mouse model involving the forced expression of CCL19, CCL21a, or CCL21b in peripheral tissues, each single chemokine was sufficient to induce immune cell infiltration into the pancreas (82,108), but not into the skin or the central nervous system (108,109). CCL19/CCL21-induced infiltrated tissue contained HEV and organized networks of stromal cells (82), consistent with the TLS paradigm. Some cancers have evolved mechanisms to antagonize the host-protective effects of CCR7-mediated immune cell chemotaxis. HPV-induced cervical cancer manipulates its local microenvironment by secreting IL-6, which inhibits NF κ B and CCR7 expression by mature DC and instead upregulates the pro-tumorigenic MMP-9 metalloproteinase. Such effects are reversible as a consequence of treatment with neutralizing anti-IL-6 antibodies (110). However, CCR7 has also been reported to have detrimental effects in certain cancers. In hepatocellular carcinoma, signaling by both CCL19 and CCL21 promoted the proliferation and invasion of tumor cells, while CCRL1/CCX-CKR, a naturally occurring receptor sink for the CCR7 ligands, was able to mitigate these effects (111). CCRL1 is unable to induce intrinsic intracellular signaling pathways, but it mediates the internalization and degradation of CCL19 and disallows its agonism of CCR7 (112). Melanoma cells have been shown to express CCL19 and CCR7, and expression of CCR7 correlates with metastasis, especially to the liver (113). Thus in certain cases, it appears that tumor cells have established mechanisms to use the body's natural chemokine gradients to benefit their own survival. While in many instances their roles are considered as parallel or redundant, expression of CCL19 and CCL21 in different organs may be under the control of different signaling pathways. For example, blockade of signaling through the LT β R causes a decrease in CCL19, but not CCL21, levels in lymph nodes (73). These results suggest that signaling pathways involving these chemokines include both shared and differential components and that these differences may be organ-dependent.

Chemotaxis of naive B cells towards a CCL21 gradient is mediated in part by Type-1 IFN α . Specifically, IFN- α is able to diminish the ligand-induced receptor internalization of CCR7 in the presence of CCL21, allowing for B cells in pro-inflammatory microenvironments to traffic more efficiently during the generation of antigen-specific humoral immune responses (107). In mice, three isoforms of CCL21 exist. CCL21a differs from CCL21b and CCL21c based on the presence of a serine instead of a leucine at position 65, whereas the exon sequences of CCL21b and CCL21c are identical and may represent splice variants (114). Humans express just one isoform of this protein, which contains a leucine at position 65 but performs the same functions as all three mouse isoforms. The tissue distribution of CCL21 varies between mouse and humans as well: in humans, CCL21 expression is found predominantly in lymphoid tissues including the lymph nodes, spleen, and appendix, while in mice, CCL21 is more broadly expressed and is found at the highest levels in spleen and lung (115). Within lymphoid structures, CCL21 is expressed by stromal cells and endothelial cells, especially those that make up HEV (106), and allow for the recruitment of CCR7-expressing immune cells towards a gradient. In a normal skin microenvironment, subcutaneous injection of CCL21 led to the recruitment of lymphocytic infiltrates into the skin at the site of injection 4 days later. CCL21 injection also led to an increased T cell (and DC) recruitment to the draining lymph node, and this recruitment also peaked 4 days post-injection (116). In melanomas treated with DC engineered to ectopically express CCL21 (i.e. DC.CCL21), TLS developed at the site of DC delivery, and expression of IFN γ by CD4⁺ and CD8⁺ T cells was observed, concurrent with a reduction in tumor burden in treated patients (36,117). In this situation, priming of anti-tumor effector T cells takes place within the TLS, as DC.CCL21 do not migrate to the tumor draining lymph node. Instead, naive T cells are recruited to the TME from the peripheral circulation, and begin to express CD25 (IL-2R α) within 24 hours of arrival (117). Interestingly, some tumors intrinsically express CCL21, in association with an immunosuppressed TME. This may be the result of CCL21 recruitment of CCR7⁺ Tregs that can mitigate the clinical benefits of inflammatory immune effector cells (118). In the setting of melanoma, tumor cell secretion of CCL21 promotes tumor immune escape through the production of TGF- β and the recruitment of Tregs and myeloid derived

suppressor cells (MDSC; ref. (119)). A similar result has been observed in a pancreatic islet beta cell tumor model, in which forced overexpression of CCL21 in the tumor cells led to enhanced tumor progression and significantly higher numbers of Tregs found within the TME (120). This latter result was dependent on host tissue expression of CCR7. CCL21-CCR7 signaling has also been reported to have a pro-angiogenic effect. In a model of rheumatoid arthritis, a CCL21 gradient caused migration of CCR7⁺ micro-vascular endothelial cells. CCL21 also leads to the secretion of pro-angiogenic factors, such as VEGF, Ang-1, and IL-8, by fibroblasts and macrophages. Neutralization of CCL21 or blockade of CCR7 abrogated micro-vascular endothelial cell migration *in vivo* (42). Thus in the context of cancer, the pro-angiogenic capability of CCL21 signaling may mediate tumor progression, as *de novo* blood vessel formation is required for tumor growth and metastasis.

CCL19 is expressed by stromal cells in lymphoid organs, as well as by mature DC (121). Like CCL21, the transcription of CCL19 is regulated by two NF κ B binding sites and one interferon-stimulated response element in its promoter region. The inhibition of NF κ B activation partially down-regulates transcription of IFN γ and CXCL10 by DC (122). However, CCL19 also stimulates the proliferation and metastasis of breast cancer cells, which can only be alleviated by interfering with CCR7 receptivity on tumor cells (123). Increased levels of CCL19 and CCR7 are also known to be expressed by prostate cancer tissues, and signaling by CCL19 through CCR7 expressed on prostate cancer cells induces cell proliferation (124). CCR7 is expressed by gastric cancer cells, with higher levels of CCR7 expression associated with lymph node metastasis, higher stage tumor, and poor overall survival. Treatment of human gastric cancer cells with CCL19 induced the expression of MMP-9 and decreased levels of E-cadherin, consistent with a shift towards a pro-metastatic phenotype (125). In ovarian cancer, CCR7⁺ tumor status was correlated with advanced disease stage and with lymph node metastasis, and these clinical parameters were linked to increased expression of MMP-9 and N-cadherin (43) that were subsequently determined to be dependent upon CCL19 signaling (125).

DC are also recruited to lymphoid organs and activated via CCR7 ligand gradients. After the acquisition of antigen in its local microenvironment and the provision of activation

(danger or maturation) signals, DC upregulate CCR7 on their surface and become competent to migrate in response to secondary lymph node chemokines, CCL19 or CCL21 (116,126). The ability of DC to migrate in response to a CCR7 ligand gradient was found to be partially dependent on MMP-9 expression by the DC (126). In addition to recruiting DC to sites of inflammation, CCL21 boosts the T cell-priming function of DC. Human DC treated with recombinant CCL21 and subsequently peptide pulsed and co-cultured with CD8⁺ T cells were better able to stimulate IFN γ release from the T cells than peptide-pulsed DC that were not treated with CCL21. The T cells also expressed slightly elevated levels of perforin, granzyme B, and FasL. Interestingly, this benefit of CCL21 treatment required CXCL10 signaling during the T cell priming phase (127).

Interestingly, however, in a murine model of metastatic melanoma, the intratumoral presence of elevated levels of CCL21 at the time of adoptive T cell therapy resulted in increased survival, proliferation, and effector function of transferred T cells and led to prolonged survival of CCR7⁺ T cell-treated mice compared to mice treated with transferred T cells alone (128). In a lung cancer model, injection of recombinant CCR7 into tumors led to complete tumor regression concurrent with trafficking of CD4⁺ and CD8⁺ T cells to the tumor and to the tumor draining lymph node (129). This effect was dependent upon T cell recruitment (129) and the recruiting cytokines/chemokines CXCL9, CXCL10, and IFN γ (130). In the LoVo model of human colorectal cancer, treatment with recombinant CCL19 suppressed tumor growth *in vivo* concurrent with increased serum levels of IL-12 and IFN γ via a T cell-independent mechanism that involved DC and NK cells (131). Furthermore, results from non-tumor models support a beneficial role for CCL21 in generating protective Type 1 immune responses. CCL21 can co-stimulate effector CD4⁺ and CD8⁺ T cells, induce T cell proliferation, and induce a Type 1 polarized immune response characterized by secretion of IFN γ and not IL-4 or IL-5 (132). When taken together, these results suggest a dual function for CCR7 and its ligands CCL19 and CCL21 in anti-tumor immunity, as CCR7 signaling may promote the formation of TLS and the recruitment and survival of immune effector cells in an inflammatory microenvironment, or the recruitment of suppressive immune cells such as Tregs and MDSCs and the secretion of regulatory cytokines, depending on context. The

precise signals involved with determining the pro- versus anti-tumor impact of CCR7 and its ligands have not yet been elucidated.

1.2.5.4 The Importance of CXCR5 agonists in TLS evolution

CXCL13, also known as BLC, is critical for the formation of SLO and TLS. Its receptor, CXCR5 is expressed on the surface of B cells, and these cells migrate towards gradients of CXCL13 expressed by follicular DC or stromal cells in lymphoid organs (106). Mice deficient in either CXCL13 or CXCR5 lack structured lymphoid organs including lymph nodes, Peyer's patches and spleen, which appears to be due to a lack of follicular DC networks that are required for the organization of recruited B cells into follicles/germinal centers (80). CXCL13 is under the transcriptional control of $LT\beta R$ -mediated signaling in all SLO (73), and signaling by CXCL13 through CXCR5 leads to increased cell surface expression of $LT\alpha_1\beta_2$ (80). The CCR7 ligands CCL19 and CCL21 also promote elevated expression of $LT\alpha_1\beta_2$ on the surface of B cells, though to a lesser extent than does CXCL13 (80). In response to infection, DC and $CD4^+$ T cells are able to upregulate CXCR5, and this promotes the recruitment of B cells to sites of immune priming in lymphoid organs (133). Forced expression of CXCL13 in non-lymphoid organs leads to the formation of lymphoid-like structures and the recruitment of immune cells into affected tissue sites (134). Interestingly, CXCL13 expression within lymphoid organs appears to be required not only for B cell migration to lymphoid organs, but for antigen presentation to B cells at these sites as well (135).

Like CCR7 ligand chemokines, CXCL13 appears to play multiple roles within the TME. Although CXCL13 is crucial for the recruitment of immune cells into sites of inflammation, it can also mediate the invasion and metastasis of many types of cancer. Colon cancer cell lines commonly express the CXCR5 receptor, and are able to proliferate and migrate in response to CXCL13 gradients in a CXCR5-dependent manner (136). The migratory capacity of these colon cancer cells appears to be mediated downstream of CXCR5 signaling by the matrix metalloproteinase MMP-13 (136), consistent with results observed in human colon cancer patients (137). A similar

result has been observed in prostate cancer, as primary prostate cancer tissues and prostate cancer cell lines both express CXCR5. After treatment with CXCL13, prostate cancer cell lines upregulate MMP-1, MMP-2, and MMP-9, and are able to migrate towards a CXCL13 gradient in a CXCR5-dependent manner (138). In the Myc-CaP and TRAMP prostate cancer models *in vivo*, CXCL13 is upregulated by myofibroblasts in the tumor stroma downstream of TGF- β in response to hypoxia, and this promotes metastasis and the development of more aggressive, hormone-independent tumors (139). Many subtypes of human lung cancers also express CXCR5. Specifically, adenocarcinomas and squamous cell carcinomas, but not healthy lung tissues, express CXCR5 (140). Furthermore, patients with lung adenocarcinomas or squamous cell carcinomas present with increased serum levels of CXCL13 when compared to healthy patients, and CXCR5-expressing lung cancer cell lines are able to migrate towards a CXCL13 gradient *in vivo* (140). Some breast cancer patients have been shown to express elevated levels of CXCL13 in both the TME and systemically in the peripheral blood (141). In particular, patients with metastatic breast cancer present with significantly higher serum levels of CXCL13 when compared to normal controls and to patients whose tumors were resected, suggesting that CXCL13 may be a potential biomarker capable of detecting early metastatic disease in these patients (141). Both CXCR5 and CXCL13 have also been shown to be expressed by patients with infiltrating ductal carcinoma, and their co-expression correlates with lymph node metastasis and an up-regulation in expression of MMP-9 in these patients, supporting a role for the CXCR5-CXCL13 axis in promoting epithelial to mesenchymal transition of breast cancer cells (142).

Speaking to the prognostic value of CXCL13 expression, in colorectal cancer, both CXCR5 and CXCL13 may be upregulated in malignant compared to normal tissues, and patients with higher expression of CXCR5 and CXCL13 present with a lower 5-year overall survival and lower 5-year progression free survival when compared to disease stage-matched patients whose tumors were negative for CXCR5 and CXCL13 (143). In a clinical trial for HER2-positive breast cancer, the presence of CXCL13 on tumor infiltrating lymphocytes was associated with a lower occurrence of complete response to

treatment (144). However, other groups have reported a beneficial role for CXCL13 and CXCR5 in breast cancer. In particular, there was a positive correlation observed between high intratumoral CXCL13 or CXCR5 expression and increased disease free survival in high risk HER2-positive, estrogen receptor-low breast cancer patients (145). In hormone receptor-positive invasive ductal carcinoma, patients with grade I non-triple negative breast cancer presented with higher intratumoral levels of CXCL13 compared to patients with higher grade (grade II/III) or triple negative tumors (146). Interestingly, interferon regulatory factor 5 (IRF5), a regulator of CXCL13, is present in some but not all breast cancers, and media conditioned *in vitro* by IRF5-positive tumors is able to recruit B- and T-cells while IRF5-negative tumor conditioned media is not (146), suggesting that these tumors may secrete CXCL13 *in vivo*, generating a gradient to recruit lymphocytes into the TME. Thus in the cancer setting, increased CXCL13/CXCR5 expression- especially in patients with metastatic disease- may in fact represent a mechanism by which protective immune responses are actively recruited into disease sites.

Overall, work evaluating the role of chemokine signaling in the context of tumor progression suggests that chemokine/chemokine receptor expression may not be entirely beneficial or entirely harmful to the patient. Instead, chemokine expression may coordinately mediate immune cell recruitment into the TME and promote the metastasis of tumor cells, as many forms of tumor/tumor cell lines have been shown to express chemokines or chemokine receptors. Thus in the context of generating novel therapeutics to cancer, it will be important to balance the positive and the negative effects of enhancing or inhibiting signaling through these pathways. Specifically, it may be useful to stratify patients based on expression of chemokines/chemokine receptors to optimize the benefits of targeted (immuno)therapies.

1.2.6 Therapeutic Manipulation of TLS in Cancer Patients: Establishing a Paradigm for Anti-Tumor Efficacy

Our own work in murine models suggests that forced overexpression of cDNA encoding the Type 1 transactivator Tbet within the TME is therapeutic in the cancer setting. In particular, we have shown that DC engineered to (over)express Tbet (i.e. DC.Tbet) inhibit the growth of CMS4 (BALB/c) and MCA205 (C57BL/6) sarcomas *in vivo* after intratumoral injection, leading to the prolonged overall survival of treated tumor-bearing mice (27,28). This result is dependent upon the presence of host lymphocytes and NK cells, as RAG1^{-/-} mice and mice depleted of either CD8⁺ T cells or NK cells were not protected from tumor growth by treatment with DC.Tbet (28). As T cells and NK cells must be able to traffic to the site of the tumor, it stands to reason that early chemokine signaling plays a key role in the mechanism by which intratumoral delivery of DC.Tbet leads to the recruitment of Type 1-polarized immune cells into the TME. In support of this hypothesis, DC.Tbet (but not control DC) cells express increased transcript levels for numerous chemokines, including CCL1, CCL4, CCL8, CCL12, CCL17, CCL25, CCL28, and CXCL12 (28). Furthermore, DC.Tbet treatment leads to an upregulation of CXCL9 and CXCL10 in the TME as late as 21 days post tumor inoculation (27). As a set, these chemokines are attractants for T cells, B cells, and NK cells as well as for DC and monocytes. These results provide a framework by which DC.Tbet promotes a rapid (hours) and sustained (days to weeks) chemokine response to actively recruit and retain immune cells in TLS within the effectively treated TME.

1.2.7 Conclusions and Future Directions for Clinical Translation

Chemokine expression within the TME and the development of TLS can often, but not always, represent a positive prognostic marker in patients with solid tumors. Due to the

differential requirements for effector and regulatory immune cell subsets within the TME of a diverse array of cancer types (see **Table 1.1**), immunotherapies designed to promote the recruitment of immune cells into the TME, or those targeting chemokine pathways, must still be evaluated on an empirical “case-by-case” basis. Examples of controversial effects of TLS include the positive effect of TLS presence in metastatic, but not primary, colorectal carcinoma, or the benefit of both Treg and effector T cell infiltration in head and neck cancer (53,64), which traditionally arises as a result of prolonged inflammation at the site of disease. Future avenues of research must elucidate whether the presence or absence of certain chemokines, cytokines, or cell populations within the TLS can predict a patient’s ability to mount a successful anti-tumor immune response secondary to treatment. Although trends in the prognostic value of TLS are seen within cancer subtypes, it is likely that a better method of stratifying patients for immunotherapy will be to evaluate the specific immune cell infiltrates and chemokines expressed at the time of diagnosis, in hopes of determining whether the enhancement or suppression of the immune response therapeutically is the best course of treatment.

Therapeutic agents targeting TLS-relevant chemokine pathways have thus far been evaluated in mouse tumor models, with forced expression of LIGHT or CCL21 both mediating beneficial therapeutic outcomes against a variety of solid tumors. Further analyses of the pathways involved in beneficial immune responses within the TME have identified additional immunomodulatory agents that may prove to be clinically important targets of immunotherapy.

In summary, recent advances in our understanding of chemokine and cytokine pathways and their role in the generation of lymphoid organs have allowed for a greater appreciation of the dynamic crosstalk between immune cell types that occurs within TLS that form in or proximal to the TME. This paradigm provides a set of biologic endpoints that should be achieved in order to render improved clinical benefit as a consequence of (immuno)therapeutic intervention in cancer patients. Specifically, intratumoral delivery or promotion of TLS-facilitating factors, applied as single agents via viral vectors or transduced cells (e.g. DC) or direct injection of recombinant proteins into accessible

tumor lesions, may allow for the preferential manipulation of protective-over-regulatory TIL within tumor-associated TLS. Under such conditions, TLS-primed/expanded anti-tumor immune effector cells may confer systemic clinical benefits (i.e. locoregional treatment of a single lesion may beget circulating immune-mediated regulation of disseminated disease) with minimal anticipated off-target toxicities.

1.3 BIOSYNTHESIS AND FUNCTIONAL SIGNIFICANCE OF PERIPHERAL NODE ADDRESSIN IN CANCER-ASSOCIATED TLS

Aliyah M. Weinstein¹, Walter J. Storkus^{1,2,3}

From the ¹Department of Immunology, University of Pittsburgh School of Medicine, Pittsburgh, Pennsylvania, USA; ²Department of Dermatology, University of Pittsburgh School of Medicine, Pittsburgh, Pennsylvania, USA, ³University of Pittsburgh Cancer Institute, Pittsburgh, Pennsylvania, USA

This section is adapted from text that was published in *Frontiers in Immunology*. doi: 10.3389/fimmu.2016.00301. Both authors contributed to the manuscript.

1.3.1 Abstract

Peripheral node addressin (PNAd) marks HEV, which are crucial for the recruitment of lymphocytes into lymphoid organs in non-mucosal tissue sites. PNAd is a sulfated and

fucosylated glycoprotein recognized by the prototypic monoclonal antibody MECA-79. PNAd is the ligand for L-selectin, which is expressed on the surface of naïve and central memory T cells, where it mediates leukocyte rolling on vascular endothelial surfaces. Although PNAd was first identified in the HEV of peripheral lymph nodes, recent work suggests a critical role for PNAd in the context of chronic inflammatory diseases, where it can be used as a marker for the formation of tertiary lymphoid structures (TLS). TLS form in tissues affected by sustained inflammation, such as the tumor microenvironment (TME), where they function as local sites of adaptive immune cell priming. This allows for specific B- and T-cell responses to be initiated or reactivated in inflamed tissues without dependency on SLO. Recent studies of cancer in mice and humans have identified PNAd as a biomarker of improved disease prognosis. Blockade of PNAd or its ligand, L-selectin (aka CD62L or LECAM-1), can abrogate protective anti-tumor immunity in murine models. Here, we examine the pathways regulating PNAd biosynthesis by the endothelial cells integral to HEV and the formation and maintenance of lymphoid structures throughout the body, particularly in the setting of cancer.

1.3.2 Pathways regulating PNAd expression

1.3.2.1 Signaling through the lymphotoxin beta receptor is required for HEV differentiation Lymphotoxin beta receptor (LT β R) signaling drives expression of adhesion molecules and chemokines involved in the recruitment of circulating lymphocytes into lymphoid organs, including CCL21, CXCL13, MAdCAM-1, and PNAd (76). Specifically, expression of LT β R on endothelial cells in peripheral lymph nodes is required for their development into HEV, with high endothelial cells functioning as lymphoid tissue organizer cells (LTo). Endothelial cell-specific deletion of LT β R leads to a reduction in: i.) MECA-79 staining, ii.) CCL19, CCL21 and GlyCAM-1 expression, and iii.) the ability to assume cuboidal morphology, by endothelial cells in peripheral lymphoid organs (**Figure 1.1A** and ref. (147)). *In vivo* work using bone marrow chimeric mice deficient in LT α in their hematopoietic compartment also implicates a role for LT β R-mediated signaling in the maintenance of HEV, as these mice exhibit profoundly reduced lymph node cellularity (148).

LT $\alpha_1\beta_2$ and LIGHT can bind and signal through the LT β R, while a related ligand, LT α_3 , can signal through TNFR1, TNFR2, and HVEM. All three ligands can be produced by CD11c⁺ DC (148). However, each ligand appears to have a distinct role in regulating PNAd expression. In SLO, LIGHT appears to have little impact on PNAd expression (73). Using a transgenic model of lymphotoxin overexpression in the pancreas, it was observed that LT α and LT β play distinct roles in the formation of TLS. LT $\alpha_1\beta_2$ controls luminal PNAd expression, while LT α_3 controls abluminal PNAd expression (76). These differences in ligand function appear to relate to their impact on the level of GlcNAc6ST expression by endothelial cells. GlcNAc6ST-2 expression was reduced if only LT α but not LT β was present, with HEV in LT $\beta^{-/-}$ animals (that retained GlcNAc6ST-2) expressing PNAd (76). LT $\alpha^{-/-}$ animals were deficient in GlcNAc6ST-2 expression on HEV, although they retained PNAd expression (149). Blockade of LT β R signaling also decreases transcription of GlcNAc6ST-2 in lymph nodes by 10-fold, with GlcNAc6ST-1, FucT-VII and FucT-IV levels also coordinately reduced, thereby limiting post-translational modification of PNAd and inhibiting its ability to be recognized by L-selectin (73).

Lymphocytes are also able to secrete lymphotoxin ligands (73,147). Interestingly, the requirement for T or B cells themselves in HEV activation in SLO is equivocal. Reports suggest that neither cell type is required for HEV differentiation (73), although it has also been observed that *Rag*^{-/-} mice exhibit decreased expression of GlcNAc6ST-2 compared to WT mice (150).

1.3.2.2 Post-translational modifications are required for L-selectin recognition of PNA_d Members of the PNA_d family of addressins include GlyCAM-1, CD34, sgp200, podocalyxin, endomucin, and nepmucin: however, not all PNA_d ligands appear to be required for lymphocyte trafficking (151,152). For example, lymphocyte trafficking to peripheral lymph nodes remains unaltered in CD34^{-/-} (153) or GlyCAM1^{-/-} (154) mice, suggesting redundancy in the functional roles of PNA_d family members. In order for PNA_d to be recognized by MECA-79 as well as its receptor, L-selectin, a series of post-translational modifications must first occur (**Figure 1.1**). Specifically, while PNA_d undergoes sulfation and glycosylation (155), it is sulfation of the 6 sialyl Lewis X motif that renders these molecules recognizable by the MECA-79 antibody (156). Fucosylation of the Core 2 branched O-glycan serves as the recognition site of PNA_d by L-selectin (**Figure 1.1B**) (157,158).

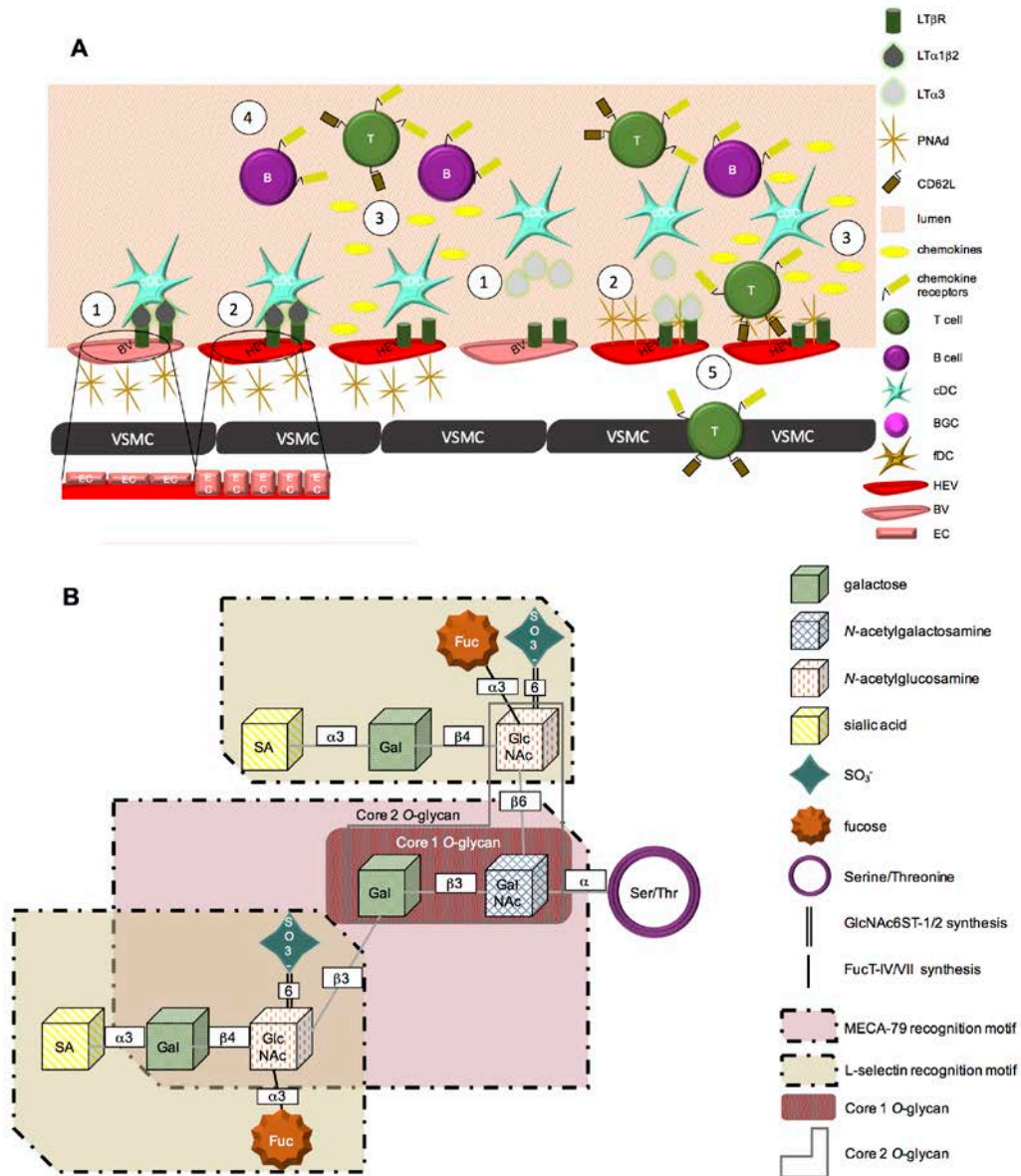


Figure 1.1. PNAAd biosynthesis.

(A) (1) LT β R is expressed on blood vessel endothelial cells. Membrane-bound LT α 1 β 2 or secreted LT α 3 secreted from cDC can signal through this receptor. (2) LT β R-mediated signaling promotes a physical change in vascular endothelial cells from a flat to cuboidal morphology. This signaling cascade also leads to the expression of PNAAd on the surface of vascular endothelial cells, promoting HEV status. (3) LT β R signaling

further induces HEV secreted chemokines, including CCL19, CCL21, and CXCL13. (4) Chemokines form gradients and “decorate” the blood vessel wall, initiating the recruitment of CCR7⁺ T cells or CXCR5⁺ B lymphocytes from the peripheral blood circulation into chronically inflamed tissues. (5) L-selectin on the surface of T cells is able to bind PNA_d on the surface of HEV. These cells are then able to adhere to the vessel wall and extravasate into the tissue. **(B)** PNA_d is synthesized from a Core 1 O-glycan. The extended Core 1 O-glycan serves as the MECA-79 recognition motif. The fucosylated Core 2 O-glycans are able to be recognized by L-selectin. Sulfation of the extended Core 1 and Core 2 O-glycans at the sixth position is mediated by GlcNAc6ST-1 and -2; α 3 fucosylation is added by FucT-IV and -VII.

1.3.2.2.1 Sulfation GlcNAc6ST-1 and GlcNAc6ST-2 are members of the GalNAc6ST-6-O-sulfotransferase subfamily of glycosyl sulfotransferases that are critical to the transfer of sulfate groups to galactose or GlcNAc at the 6 position, with this sulfation of carbohydrate motifs on PNA_d required for it to be presented at the cell surface and to be recognized by the MECA-79 antibody and by its natural ligand, L-selectin (159).

Though related, GlcNAc6ST-1 and GlcNAc6ST-2 have different roles in the sulfation of PNA_d. Using mice deficient in either single sulfotransferase, it was shown that GlcNAc6ST-2 controls luminal expression of PNA_d while GlcNAc6ST-1 controls expression of PNA_d on the abluminal vascular surface (160,161).

GlcNAc6ST-2 is expressed by mature, but not immature, HEV. Using a Cre-recombinase model, Kawashima and colleagues observed that expression of GlcNAc6ST-2 is activated in HEV cells recognized by the MECA-79 antibody (i.e., expressing PNA_d) but not in cells reactive only with the MECA-367 antibody (recognizing MAdCAM-1) (162). This is consistent with observations that GlcNAc6ST-1 and -2 have little impact on cellular expression of MAdCAM-1, a canonical marker of immature HEV in SLO within non-mucosal tissue sites (163).

1.3.2.2.2 Glycosylation A family of alpha(1,3)fucosyltransferases control the fucosylation of E-, P-, and L-selectin ligands (164). In particular, FucT-VII and FucT-IV play distinct roles in the generation of L-selectin ligands on the surface of HEV. FucT-IV is required for the expression of L-selectin ligands on the surface of HEV, whereas the primary role of FucT-VII appears to be in its contribution to enhancing GlyCAM-1-mediated tethering of rolling lymphocytes. The specific role of FucT-VII temporally follows glycosylation and sulfation of the glycoprotein and is involved in capping the molecule to produce the preferred ligand recognized by L-selectin. Double knockout of both FucT-VII and FucT-IV in mice reduced lymphocyte recruitment to SLO by over 80% when compared to FucT-VII^{-/-} mice. (165).

1.3.3 Markers of high endothelial venules

Two sets of adhesion molecules dominantly modulate lymphocyte recruitment to SLO/TLS depending upon which site in the body the cells are trafficking to: recruitment to peripheral lymph nodes is dependent upon the L-selectin/PNAd interaction, while recruitment to mucosal sites requires the $\alpha_4\beta_7$ integrin/MAdCAM-1 interaction (166). The same high endothelial cells that express PNAd or MAdCAM-1 also express CCL21, a CCR7 ligand. Supporting the importance of PNAd- and CCL21-expressing HEV for the recruitment of lymphocytes, the majority of lymphocytes in HEV-expressing tissues are spatially located within approximately 20 microns of HEV (167). CCL21 preferentially recruits CCR7⁺ CD4⁺ L-selectin⁺ (naïve) T cells, which can interact with PNAd on the cells of the HEV. CCL21, like PNAd, is under the control of intrinsic LT β R-mediated signaling during HEV development (but not in mature lymphoid tissues) (73,76).

1.3.4 Immune Cell Recruitment by HEV

PNAd binds L-selectin expressed on the surface of lymphocytes. This interaction is required for the recruitment of lymphocytes into SLO (168). Post-translational modifications of PNAd family members are critical for this interaction. For example, B cell recruitment to peripheral lymph nodes is dependent on sulfation of PNAd (163). The velocity of T and B cell rolling is also dependent upon sulfation of L-selectin ligands on lymph node endothelial cells, with adherence of lymphocytes to the vessel wall decreased in GlcNAc6ST-deficient animals (163). This may also be controlled by the presence of DC within SLO, as the velocity of lymphocyte rolling in CD11c-DTR mice was significantly increased, and the percentage of lymphocytes able to adhere to the vessel wall was decreased, in these mice after treatment with diphtheria toxin to delete DC. The HEV of DC-depleted mice regained expression of MAdCAM-1, and after reconstitution with adoptively-transferred CD11c⁺ DC, these HEV recovered classical cuboidal morphology, suggesting that DC-produced factor(s) is/are required for the maturation of HEV (148).

The CCR7-CCL21 axis is also important for lymphocyte recruitment into lymphoid organs. Mice deficient in CCR7 have impaired migration of B and T cells, as well as DC, to SLO including lymph nodes and Peyer's patches. This limits primary immune responses against infectious agents (169). Expression of CCL21 by high endothelial cells is controlled by a pathway unique to these cells versus high endothelial cells expressing alternate addressins. Specifically, heparan sulfate, a glycosaminoglycan primarily found on the surface of vascular endothelial cells, is required for CCL21 expression on HEV (170). Using an *Ext1*-flox/flox mouse crossed with a GlcNAc6ST-2-cre transgenic mouse to delete a glycosyltransferase necessary for the synthesis of heparan sulfate in PNAd-expressing cells, expression of CCL21 on the surface of HEV was abrogated (167).

1.3.5 Tertiary Lymphoid Organs

Although the pioneering work identifying PNAd and the pathways controlling its expression were initially studied in the context of SLO, recent literature supports an important role for PNAd in TLS (aka ectopic lymphoid structures) that develop in peripheral tissue sites impacted by chronic inflammation. Overall, TLS have varying degrees of similarity to SLO. Classical TLS closely resemble SLO in their cellular composition, with TLS containing a network of follicular DCs and germinal centers in which B cells reside, proliferate and differentiate (**Figure 1.2A**). Non-classical TLS also contain some degree of B cell infiltration, but they do not exhibit an follicular DC “framework” (37), with only diffuse, sparse B cell distributions being observed (**Figure 1.2B**) (36,40).

The L-selectin-PNAd interaction controls lymphocyte recruitment to TLSs. In particular, PNAd upregulation in affected tissues is observed in the settings of allergic contact dermatitis, lymphoid hyperplasia, and a variety of types of skin lesions and cutaneous lymphomas; i.e. diseases characterized by robust lymphocytic infiltrates into peripheral tissues (171). The CCR7 signaling axis also plays a role in TLS formation. Most importantly, CCR7-mediated signals are required for the clustering of DC in peripheral tissues. Interactions between DC and T cells proximal to blood vessels appears required for the acquisition of PNAd+ HEV in peripheral tissues (149).

Notably, $LT\beta R$ -mediated signaling controls the formation of HEV in peripheral tissues (34,149). Akin to the roles that lymphotoxin signaling plays in the control of PNAd expression in SLO, $LT\alpha 3$ -dependent signaling has been reported to dominantly control PNAd expression on HEV within the TME in murine melanoma models (34), while in human breast cancer, $LT\beta$ (produced by DC-LAMP+ DC) appears to play a comparable dominant role (17).

TLS have been observed in a variety of chronic inflammatory diseases, including arthritis (172), gastritis and ulcerative colitis (158,173), atherosclerosis (174), and cancer (31). As the development of TLS in chronic/autoimmune diseases has been well-reviewed (33,175), we will now focus on the emerging field of TLS formation in solid tumors.

1.3.5.1 TLS in Cancer Cancer-associated TLS characteristically contain PNA⁺ vessels, and are commonly localized to the outer margin (versus the core) of the tumor lesion (176). With the exception of reports for TLS predicting a worse prognosis in patients with renal cell carcinoma (RCC) (177) and some cases of colorectal cancer (178), the vast weight of the literature has correlated the presence of TLSs in human solid tumors with better clinical prognoses (32). Both classical and non-classical TLS have been reported within the TME (**Figure 1.2**). Of these 2 forms of TLS, however, the presence of classical TLS in tumors may provide a superior index for improved prognosis when compared to the presence of only non-classical TLS in the TME (37). These results suggest that systematic analysis of PNA⁺ expression and TLS status in tumor biopsies may be a useful addition to current clinical criteria used to predict patient outcomes.

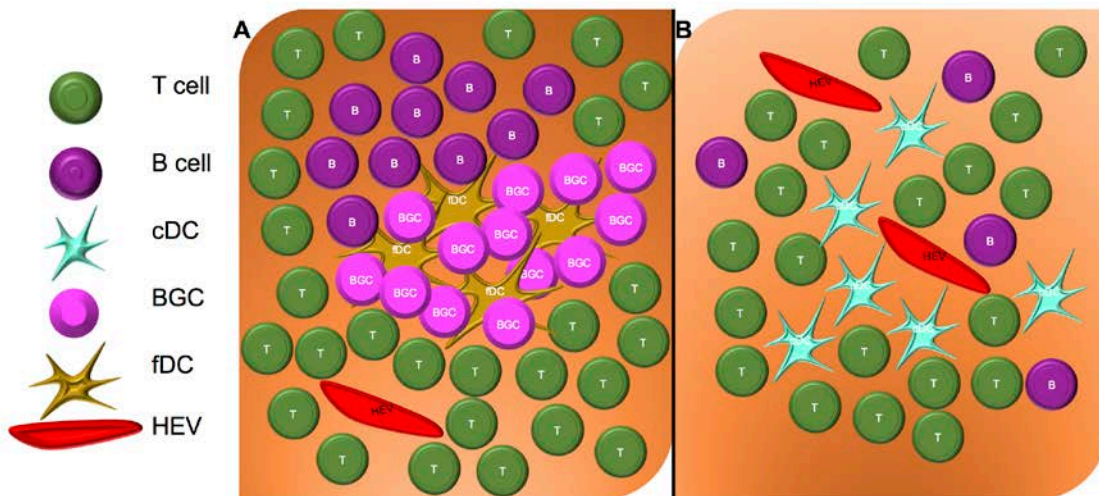


Figure 1.2. Structure of classical and non-classical tertiary lymphoid structures.

(A) Classical TLS contain a nucleated core of follicular DC and germinal center B cells (BGC), surrounded by an HEV-containing T cell zone. **(B)** Non-classical TLS do not contain follicular DC or BGC, but may contain sparse B cell, T cell, and DC infiltrates surrounding HEV.

1.3.5.1.1 Lung Cancer In non-small cell lung cancer (NSCLC), PNA^{d+} vessels have been identified exclusively within TLS (45). In these tumors, the composition of cells within the TLS specifically correlates with patient prognosis. While T cells (all tumor-infiltrating L-selectin⁺ T cells, comprised of both naïve and central memory CD4⁺ and CD8⁺ cells) are localized to TLS (45,48), overall T cell infiltrate and density appears to play a minor role in patient outcome when evaluated independently of other prognostic markers. Instead, the density and proximity of mature DC to TLS within the tumor may be most important, and patients with high DC-LAMP⁺ mDC infiltrates exhibit markedly extended overall survival (48). These findings are further supported by gene array data indicating that *CXCR4*, a gene associated with DC migration towards CXCL12 gradients, is strongly correlated with increased overall survival in NSCLC patients (44). Unlike T cells, B cells do appear to play a significant protective role against lung cancer, and their presence can be used as a positive prognostic marker of overall survival. Interestingly, DC and B cell density in TLS can be used as a coordinate prognostic marker for patients with greatest overall survival. In NSCLC, B cells organize into germinal center-like structures containing CD21⁺ follicular DC. These B cells proliferate and differentiate *in situ*, leading to locoregional secretion of IgG and IgA antibodies reactive against tumor-associated antigens (47).

1.3.5.1.2 Skin cancers TLS have been identified in both primary and metastatic melanoma, where they have been observed to contain PNAd⁺ vessels (179,180). TLS in primary melanomas can be either classical or non-classical TLS. In metastatic melanoma, these structures are primarily composed of CD3⁺ T cells and mature (DC-LAMP⁺) DC proximal to PNAd⁺ HEV (181). Plasma B cells may also be present in such TLS, with these cells producing Th-dependent IgG and IgA antibodies specific for tumor-associated antigens (179,181). In primary cutaneous melanoma, the presence of intratumoral HEV has been correlated with robust lymphocytic infiltration and tumor regression. Furthermore, if the high endothelial cells making up HEV have a cuboidal morphology, indicative of functional HEV, a positive correlation with CCR7, CCL19, and CCL21 expression within the tumor has also been observed (182).

The presence of TLS also portends better clinical outcome (recurrence free and overall survival) in the setting of Merkel cell carcinoma. These structures are also characterized by an increased CD8⁺/CD4⁺ T cell ratio at the tumor periphery and by a co-clustering of T and B cells within these anatomic sites (38).

1.3.5.1.3 Colon Cancer TLS in human colon cancer have been detected in both the colon crypt and at the invasive front of the tumor, as well as in the peritumoral region (61,183). They contain immune cell types typically observed in SLO, including B cells, CD21⁺ follicular DC, T cells, and mature DC marked by DC-LAMP⁺, with CD31⁺ vascular endothelial cells and LYVE-1⁺ lymphatic vessels also noted (61,183). T cells and mature DC represent positive prognostic markers in both primary (32) and metastatic (177) colorectal cancer. In such tumors, the B cells may not organize into germinal center-like structures (61,183). These TLS appear to function as local sites for the priming and expansion of both B and T cells, based on the expression of the Ki-67 marker in *de facto* germinal centers in these diseased tissues (183).

1.3.5.2 Therapeutic induction of TLS Recent work from our group suggests that intratumoral TLS can be induced therapeutically via adoptive transfer of gene-modified DC, leading to reduced tumor progression. Following intratumoral injection of Type 1-polarized DC (DC engineered to overexpress Tbet, i.e. DC.Tbet) into established murine sarcomas or colon carcinomas, CD4⁺ and CD8⁺ T cell recruitment to the TME is observed within 2 days, with an upregulation of PNA⁺ expression detected by 5 days after treatment. This suggests that PNA⁺-independent events control early T cell recruitment to the TME, and that T cell-dependent factors may consequently result in PNA⁺ upregulation on tumor-associated VEC (28,36). Once established, PNA⁺ vessels become surrounded by dense infiltrates of both CD11c⁺ DC and CD3⁺ T cells, with these non-classical TLS principally localized near the tumor periphery for at least two weeks following initial therapeutic intervention (36). The presence of DC in TLS is consistent with prior studies of SLO demonstrating that DC accumulation proximal to HEV is required for the subsequent optimal homing of lymphocytes into SLO (148).

1.3.6 Future Perspectives

Although there appears to be some variability in the cellular composition across tumor types, TLS in the TME contain PNA⁺ HEV typically surrounded by dense B cell and/or

DC infiltrates. Importantly, the presence of intratumoral or peritumoral TLS has been almost universally linked with superior clinical prognosis in patients with solid forms of cancer. Though T cells are also present in intratumoral TLS, their presence has thus far proven equivocal as a prognostic biomarker (184). The spontaneous formation of TLS has been observed in a variety of human cancers, including those reviewed above as well as oral squamous cell carcinoma (37,185), gastric cancer (176,186), bladder cancer (57), breast cancer (40,51,56), and others (31,187,188). Thus, it may ultimately be best to employ PNA^d as well as B cell and DC infiltration in the TME as biomarkers to stratify patients based on TLS status, i.e. to differentiate individuals that may respond better to treatment intervention, including immunotherapies (based on superior locoregional immune competency). Furthermore, because TLS may be induced therapeutically (at least in murine models), it is also intriguing to speculate on the possibility that protective TLS may be conditionally sponsored in patients receiving chemo- or immuno-therapies (189), and that such structures may be used to monitor/predict the patient's outcome and prospective treatment management.

1.4. THE IL-36 CYTOKINE SUBFAMILY IN IMMUNE-MEDIATED PATHOGENESIS

This section is partially adapted from text originally published in *Advances in Cancer Research* (2015; vol. 128). doi: 10.1016/bs.acr.2015.04.003. Both authors contributed to the manuscript.

1.4.1 The IL-36 cytokines share unique characteristics with other IL-1 family cytokines

The IL-36 family of cytokines is comprised by a recently identified IL-1 sub-family that supports the generation of pro-inflammatory immune responses. These cytokines share sequence similarities and three-dimensional structures with known IL-1 family members such as IL-1 α and IL-1 β , and were in fact assayed using genomics approaches to identify sequences homologous to IL-1 and IL-1Ra (190,191). The IL-36 subfamily consists of three agonists (IL-36 α , IL-36 β and IL-36 γ , previously referred to as IL-1F6, 8 and 9, respectively), one full antagonist (IL-36Ra/IL-1F5), and one partial antagonist (IL-38) that signal through a heterodimeric receptor consisting of IL-1Rrp2, a unique receptor, and IL-1RAcP, a co-receptor shared with the IL-1 and IL-33 receptors. Like all IL-1 family members, the IL-36 agonists and IL-1F5 require processing before they become fully active biologically. Indeed, specific truncation of the N-terminus of each of these proteins results in a 10³-10⁵ fold increase in biologic activity when compared to unprocessed, full-length protein (192,193).

Similar to other IL-1 family members, the IL-36 family cytokines lack a signal sequence that directs classical secretion from the cell (191). Instead, both the cleavage and secretion of the IL-36 cytokines occurs through a pathway that is also involved in the secretion of IL-1 β and IL-18, i.e. pyroptosis. This is a pro-inflammatory form of cell death that is distinct from apoptosis and requires the processing of the pro-forms of these cytokines by the non-canonical inflammasome, with the participation of caspase-1 (194,195) and caspase-3/7 (195) for cytokine transcription and release from the cell, respectively. The IL-36 cytokines themselves are not involved in activating the cell death pathway, however; instead, recognition of pathogens or danger signals through Toll-like receptors and NOD-like receptors on antigen presenting cells activate caspase-1, with the secondary release of these pro-inflammatory cytokines from producer cells undergoing pyroptosis propagating Type-1 immune responses (196). In immune cells, IL-36 expression is also induced downstream of IL-18 and Tbet (197); in epithelial cells,

IL-36 is classified as an alarmin and is induced by cathelicidins such as CRAMP/LL-37 (198).

An additional unique characteristic of IL-1 family cytokines is their ability to translocate to the nucleus, where they exert functions largely independent of their effects as secreted factors (199,200). We and others have observed that IL-36 γ is able to enter the nucleus of DC (35) and epithelial cells (201), though the function of nuclear IL-36 γ has yet to be described. This parallels the biology of several other IL-1 family members, as IL-1 α (202,203), IL-1 β (200,204,205), IL-33 (206,207), and IL-37b (208) can all enter the nucleus. Once in the nucleus, these cytokines can regulate transcription (202,207), for example through association with the heterochromatin as in the case of IL-33 (207). Interestingly, nuclear translocation of IL-1 α appears to be partially dependent on receptor binding and the subsequent translocation of the bound complex to the nucleus (203); the prodomain of IL-1 α is also able to translocate to the nucleus (209).

1.4.2. IL-36R signaling

A growing body of literature describes that the three IL-36R agonists, IL-36 α , IL-36 β , and IL-36 γ , can be produced by different immune and non-immune cell types and/or under different physiologic conditions (210). Of particular interest to this work is IL-36 γ ; a summary of the immune cells capable of producing this cytokine is presented in **Table 1.3**. Besides its expression by immune cells, high levels of IL-36 γ are secreted by keratinocytes (195,198,211), other epithelial cell populations in the gut (201) and lung (212,213), and colonic myofibroblasts (214). Once released from producer cells, the IL-36 cytokines have effects on IL-36R⁺ cell types throughout the body. Numerous immune cell subsets express IL-36R (**Table 1.3**); outside of the immune compartment, predominant IL-36R expression in humans occurs in the skin, while in mice, receptor expression is more broadly distributed throughout organs including the prostate, esophagus, uterus, seminal vesicle, and paw (192). Human and murine fibroblasts also

express IL-36R (201,215–217); reports of expression by intestinal epithelial cells appear equivocal in humans but have proven reproducible in mice (201,218).

Despite speciation in the range of cell types expressing the IL-36 receptor (i.e. between mice and humans), IL-36 ligands appear to induce similar immune responses in both species. Downstream effectors of IL-36 signaling include NF κ B, MAPK, ERK1/2, and Jnk. This leads to secretion of IL-6, IL-8 and GM-CSF by IL-36-treated mouse and human transformed cell lines (192). Interestingly, in a mouse model of fibrosarcoma (MC57-SIY), NF κ B signaling is required in both CD4⁺ and CD8⁺ T cells for priming of a Type 1 immune response (as measured by secretion of IFN γ and TNF α , and specific lysis of target cells) and control of tumor growth (219). This suggests a possible mechanism by which signaling through the IL-36 receptor via NF κ B may promote anti-tumor immunity.

IL-36 induces the activation and maturation of human and mouse DC. In response to treatment with IL-36 agonists, murine DC upregulate CD80, CD86, and MHCII (220), and human DC upregulate CD83, CD86, and HLA-DR. Furthermore, IL-36 signaling leads to increased secretion of IL-1 β and IL-6 by human DC (221) and IL-1 β , IL-6, IL-12p40, and IL-12p70 by murine DC (220), strong indications that IL-36 plays a critical role in promoting states of both acute and chronic inflammation.

Naive murine CD4⁺ T cells constitutively express the IL-36 receptor and mature in response to IL-36 signaling. In particular, IL-36 (but not other IL-1 family members or IL-12p70) specifically induces IL-2 secretion and the proliferation of naive CD4⁺ T cells (222). Treatment of CD4⁺ T cells with recombinant IL-36 β in the presence of antigen leads to the secretion of pro-inflammatory cytokines/chemokines and the induction of a canonical Type-1 effector cell phenotype characterized by expression of Tbet and secretion of IFN γ (222). In the presence of IL-12p70, IL-36 can induce secretion of IFN γ by CD4⁺ T cells (222). However, the local cytokine milieu plays a role in conditioning the cellular response to IL-36R agonism. In the absence of IL-12p35, signaling through the IL-36 receptor instead leads to transcription of GATA3 and secretion of IL-4 in T cells (222). Notably, mice deficient in expression of IL-36R exhibit impaired IFN γ , IL-6, TNF α ,

and nitrite responses to bacterial challenge (222), suggesting that IL-36 plays a crucial role in the initiation of adaptive immunity *in vivo*. It is worth noting that IL-36R expression is lost in mature Th1-, Th2-, and Th17-polarized CD4⁺ T cells (222). Indeed, IL-36R signaling appears to suppress polarization of naïve murine CD4⁺ T cells into the Th17 subset (218,222).

Although expression of the IL-36R by human T cells appears to differ based on subtype and environmental condition (222–224), DC treated with rhIL-36 induce effects on the responding human T cell repertoire that appear similar to those induced directly on murine T cells by rmlIL-36. For example, IL-36 α -treated DC enhance allogeneic CD3⁺ T cell proliferation to a degree greater than mitogen-activated T cells (225), with human T cells expanded with IL-36-conditioned DC also secreting increased levels of IFN γ (225). Stimulation of naïve CD8 T cells in the presence of IL-12 plus either IL-36 β or IL-36 γ can stimulate IFN γ production by the T cells in the absence of TCR ligation (224). Indeed, human T cells primed in the presence of IL-36 are likely to be Type 1 polarized, since IL-36 β treatment of DC leads to their secretion of IL-12 and IL-18, which then prompt the transcriptional activation of *Tbet* in responder T cells (225). IL-36R expression between human naïve, effector, and memory T cell subsets has not been sufficiently investigated; however, early data is emerging about the different subsets of Th17 cells. One study demonstrated that cytokine secretion by human memory Th17 cells that have seen *Candida albicans* is inhibited by the addition of either IL-1F5 or IL-38 into the culture (193), indirectly suggesting that these cells express IL-36R. Effector Th17 cells from the blood and lesional skin of psoriasis patients also appear capable of responding to IL-36 signaling (226).

Table 1.3. IL-36R and IL-36 γ expression in the immune system

The immune cell subsets expressing IL-36R and IL-36 γ are summarized here. Green box, reported to express; yellow box, conflicting reports in the literature/subset-dependent; red box, reported to not express; black box, no reports.

| <i>Species</i> | IL-36R | | IL-36 γ | |
|-------------------------|-----------------------|-----------------------|-------------------|---------------|
| | Mouse | Human | Mouse | Human |
| DC | (220,227) | (221,225,228) | (35,197,220,229) | (197,215) |
| macrophages | (220,227) | (228) | (197,227,230,231) | (197,215,230) |
| monocytes | | (221,228) | | (215,232) |
| pDC | | (225,228) | | (233) |
| neutrophils | (220,227) | (221,234) | (227) | |
| NK cells | (223) | (228) | | |
| CD4+ T cells | (220,222,224,235,236) | (221,228,237,238) | (220) | (232,238,239) |
| CD8+ T cells | (220,223,224) | (221,223,228,237,240) | (220) | (232,238,239) |
| γ/δ T cells | (223) | (241) | | |
| B cells | (220,227,236) | (228,237) | | (215) |

1.4.3 IL-36 as an Early Inflammatory Mediator of Lymphoid Organogenesis in Tissues, Including Cancer

In the context of disease, IL-36 family cytokines have been implicated in the pathogenesis of several autoimmune diseases. Most notably, IL-36 signaling plays a major role in skin autoimmune diseases such as psoriasis and dermatitis. Pustular psoriasis may arise from DITRA (deficiency in the IL-36 receptor antagonist), a deficiency in IL-1F5 (242). A murine model of this disease is characterized by massive immune cell infiltrate into skin lesions of IL-1F5-deficient mice. This infiltrate consists of

CD45⁺ lymphocytes, neutrophils, and macrophages that are recruited into the diseased skin in an IL-36R-dependent manner (229). Mutations in IL-1F5 have also been observed in patients presenting with acute generalized exanthematous pustulosis (AGEP), a drug-induced side effect that presents with skin lesions containing robust lymphocytic infiltrates (243,244). It has been hypothesized that individuals with loss-of-function mutations in IL-1F5 are more likely to develop lesional skin diseases. Similar immune infiltrates have been observed in patients presenting with pustular psoriasis, although in this disease setting, the dominant driver of pathogenesis appears to be locoregional overexpression of IL-36R agonist cytokines that leads to increased activation of MAPK and NF κ B signaling in lesional skin (245). Supporting this, several studies evaluating human and murine models of psoriasis have observed overexpression of the IL-36 cytokines in diseased skin and reported that disease that is exacerbated in the absence of IL-1F5 expression (215,246).

IL-36 signaling has more recently been reported to play opposing roles in the gut pathogenesises colitis and Crohn's disease (215,235,247). In patients with Crohn's disease, expression of IL-36 α , IL-36 γ , and IL-38 were positively correlated with each other, and in the cohort evaluated, 7/16 patients appeared to have elevated levels of IL-36 γ in affected bowel tissue (215). IL-36 γ also appears to inhibit the development of peripheral CD4⁺ T regulatory cells in the gut, instead promoting Th9 cell expansion and subsequent colitis pathogenesis (235). In a murine model of dextran sodium sulfate (DSS)-induced colitis, one study indicated that signaling through the IL-36R was necessary for the resolution of intestinal damage, in a mechanism that appears to be dependent upon neutrophil recruitment to the site of damage to clear commensal bacteria (247); another showed that mice deficient in the IL-36R presented with less severe disease progression, including less weight loss, a lower disease activity index, and maintenance of normal colon pathology (218). While in both studies results indicated that IL-36R signaling was required for the infiltration of immune cells, including neutrophils, into the diseased tissue, in the latter study, this infiltrate was associated with inflammation and disease progression. Increased expression of *IL36A* and *IL36G* was also observed in the colon 6D following the onset of disease. In an investigation of

pediatric inflammatory bowel disease, however, no difference was observed in *IL36G* expression between normal mucosa, patients with ulcerative colitis, and patients with Crohn's disease (*IL36A* expression was significantly increased; ref. (218)). Therefore, in the gut, it appears as though IL-36 signaling can play opposing roles depending on the particular cells involved in the etiology of each disease state.

The role of IL-36R agonists in the pathogenesis of arthritis also remains contentious. Clinical reports suggest that patients with psoriatic arthritis and rheumatoid arthritis express elevated levels of IL-36 α in their synovial lining when compared to patients with osteoarthritis, with IL-36 α expression correlated with increased production of IL-6 and IL-8 in the affected joints (248). Expression of both the IL-36R and IL-36 α is increased in the human TNF transgenic mouse model of inflammatory arthritis (*hTNFtg*), concurrent with lymphocytic infiltration into the joints; however, blockade of signaling through the IL-36 receptor using an antagonist antibody did not relieve inflammation (249). A similar result was observed in a collagen-induced arthritis (CIA) model (216). Thus, in arthritis, IL-36 is likely a contributing factor in disease pathogenesis, but not necessarily a dominant driver as it is in skin autoimmune conditions.

Notably, IL-36 is a downstream target of Tbet (197), with a positive-feedback loop allowing for IL-36 to induce secondary transcription of Tbet as well (220). In human myeloid cells, silencing of Tbet by siRNA decreased expression of IL-36 γ , and expression of IL-36 γ by DC was also dependent upon IL-18/IL-18R signaling via MAPK- and NF κ B-dependent pathways. Specifically, the promoter region of IL-36 γ contains both Tbet and NF κ B binding sites, with IL-18 signaling inducing Tbet binding to the IL-36 γ promoter (197). Tbet is also expressed in both human and murine DC, where it has been shown to be critical to DC1 functional polarization and the ability of these APC to activate Type-1 T cell responses *in vivo* (4). Interestingly, DC.Tbet generated from *CCR7*^{-/-} hosts appeared most effective in preventing tumor growth, strongly suggesting that their preferred biology was manifest in the TME and not the TDLN (28). Indeed, the anti-tumor efficacy of i.t.-delivered DC.Tbet appears critically dependent upon TIL recruitment, activation, expansion and differentiation within the TME. In this context, IL-

36 has been shown to bolster T cell proliferation and cytokine secretion, including secretion of IFN γ (220). Furthermore, CCL1 and CXCL10- chemokines observed to be upregulated by DC.Tbet cells- are known to be upregulated by wild-type DC after stimulation with IL-36R agonists (220). Thus we believe that IL-36 is a key early mediator of TLS development in inflamed tissues and that purposeful instigation of IL-36 delivery or production in the TME (via administration of DC.Tbet or an equivalent modality) will have the potential to evolve both humoral and cellular immunity that is protective and/or therapeutic to the cancer-bearing host.

Consistent with the observation that overexpression of IL-36 in tissues correlates with increased immune cell infiltration, results from our laboratory suggest that IL-36 γ plays a role in the induction of chemokines that can rapidly recruit T and B cells into the inflammatory microenvironment of therapeutically-managed tumors. In contrast to concerns for pathologic autoimmunity resulting from such immune infiltrates in psoriasis, arthritis, and inflammatory bowel models, this is a highly-preferred biologic outcome in the context of cancer. We are currently evaluating the ability of IL-36 γ to drive Type 1 anti-tumor immune responses and TLS formation *in vivo*, when used as a single agent or in the context of combination immunotherapies.

2.0. TBET AND IL-36 γ COOPERATE IN THERAPEUTIC DC-MEDIATED PROMOTION OF ECTOPIC LYMPHOID ORGANOGENESIS IN THE TME

Aliyah M. Weinstein¹, Lu Chen¹, Emily A. Brzana², Prashanti R. Patil², Jennifer L. Taylor², Kellsye L. Fabian¹, Callen T. Wallace³, Sabrina D. Jones², Simon C. Watkins³, Binfeng Lu¹, David F. Stroncek⁴, Timothy L. Denning⁵, Yang-Xin Fu⁶, Peter A. Cohen⁷ and Walter J. Storkus^{1,2,8-10}

From the ¹Department of Immunology, University of Pittsburgh School of Medicine (UPSOM), Pittsburgh, PA 15213; ²Department of Dermatology, UPSOM, Pittsburgh, PA 15213; ³Department of Cell Biology and Physiology, UPSOM, Pittsburgh, PA 15213; ⁴Department of Transfusion Medicine, Clinical Center, NIH, Bethesda, MD 20892; ⁵Center for Inflammation, Immunity & Infection at Georgia State University, Atlanta, GA 30303; ⁶Departments of Pathology and Immunology, UT Southwestern Medical Center, Dallas, Texas 75390; ⁷Department of Hematology/Oncology, Mayo Clinic, Scottsdale, AZ 85259; ⁸Department of Pathology, University of Pittsburgh School of Medicine, Pittsburgh, PA 15213; ⁹Department of Bioengineering, UPSOM, Pittsburgh, PA 15213; ¹⁰University of Pittsburgh Cancer Institute, Pittsburgh, PA 15213

This text was published in *OncolImmunology*. doi: 10.1080/2162402X.2017.1322238. A.M.W., B.L., T.L.D., P.A.C., S.C.W. and W.J.S. designed experiments. A.M.W., L.C., E.A.B., P.R.P., J.L.T., K.L.F., C.T.W., S.D.J., and D.F.S. performed experiments.

A.M.W., J.L.T., B.L., S.C.W., T.L.D., Y.X.F., P.A.C., and W.J.S. interpreted data. A.M.W. and W.J.S. wrote the paper. All authors read and agreed on the final version of the submitted manuscript.

2.1 ABSTRACT

We have previously reported that direct injection of DCs engineered to express the Type-1 transactivator Tbet (i.e. DC.Tbet) into murine tumors results in anti-tumor efficacy in association with the development of structures resembling tertiary lymphoid structures (TLS) in the TME (TME). These TLS contained robust infiltrates of B cells, DC, NK cells and T cells in proximity to PNA⁺ blood vessels; however, they were considered incomplete, since the recruited B cells failed to organize into classic germinal center-like structures. We now report that anti-tumor efficacy and TLS-inducing capacity of DC.Tbet-based i.t. therapy is operational in peripheral lymph node-deficient LTA^{-/-} mice, and that it is highly dependent upon a direct Tbet target gene product, IL-36 γ /IL-1F9. Intratumoral DC.Tbet fail to provide protection to tumor-bearing IL-36R^{-/-} hosts, or to tumor-bearing wild-type recipient mice co-administered rIL-1F5/IL-36RN, a natural IL-36R antagonist. Remarkably, the injection of tumors with DC engineered to secrete a bioactive form of mIL-36 γ (DC.IL-36 γ) also initiated therapeutic TLS and slowed tumor progression *in vivo*. Furthermore, DC.IL-36 γ cells strongly upregulated their expression of Tbet, suggesting that Tbet and IL-36 γ cooperate to reinforce each other's expression in DC, rendering them competent to promote TLS formation in an “immunologically normalized”, therapeutic TME.

2.2 INTRODUCTION

Preferred clinical endpoints for cancer immunotherapies include the activation and recruitment of Type-1 T effector cells into tumors, the sustained (poly)functionality of these T cell populations, and the coordinate reduction of operational antagonism mediated by regulatory cells (Treg and MDSC) and tumor cells in the immunosuppressive TME (TME) (250–255). Anti-tumor T cell (cross)priming is conventionally believed to occur in tumor-draining secondary lymph nodes (256–258); however, recent findings suggest that the induction of T effector cells from naïve precursors can occur in and around tumor lesions *in vivo*, within so-called TLS (36,45,48,53,183). The presence of TLS in a broad range of cancer types has been reported to represent a harbinger of improved clinical prognosis (e.g. extended OS, PFS, RFS), in association with the presence of robust populations of TIL (15,16,36,45,48,183,259,260).

In contrast to tissue-draining SLO, TLS are not encapsulated and can be found embedded within almost any non-lymphoid tissue (261), typically under conditions of persistent inflammation, as seen in the settings of chronic infectious disease, autoimmunity, transplantation and cancer (261–264). A canonical feature of TLS is the presence of PNA⁺ high-endothelial venules (HEV) (76,261), specialized vascular structures that allow for the preferential adhesion and recruitment of CD62L(L-selectin)⁺ naïve and central memory T cells and DCs into peripheral lymphoid sites (76,265). Notably, in a study of 225 primary melanomas, Martinet and colleagues reported that the density of HEVs correlated positively with the degree of tumor infiltration by naïve and Type-1-polarized T cells, as well as, DC-LAMP⁺ mature DC (18), with these recruited immune cell populations found to loosely cluster around HEV (179). Furthermore, B cells infiltrating primary melanomas were not organized into formal

germinal centers (GC) as is typical of SLO, suggesting a state of “incomplete” lymphoid organogenesis in the observed TLS (179).

We have previously reported that DC engineered to express the Type-1 transactivator protein Tbet/TBX21 (i.e. DC.Tbet) exhibit Type-1 functional polarization (266), and that when delivered directly into tumor lesions in mice, these biologic products promote rapid (within hours) infiltration by lymphocytes and NK cells, and the development of TLS within days (28,36). We now show that the abilities of i.t.-delivered DC.Tbet to slow tumor growth and to promote TLS within the TME are highly IL-36 γ -dependent, as this therapy fails to achieve either endpoint when applied in wild-type hosts that are co-administered IL-36R antagonist IL-1F5 or when applied to tumor-bearing IL-36R^{-/-} recipient mice.

IL-36 γ (aka IL-1F9) is a recently identified member of the IL-1 family that we now report to be profoundly upregulated in DC after infection with rAd.Tbet (but not control Ad), presumably due to the direct transcriptional action of Tbet on the IL-36 γ promoter (197). Interestingly, we noted that DC engineered to express a secreted, bioactive form of mIL-36 γ (i.e. DC.IL-36 γ) upregulate their expression of Tbet, suggesting a positive feedback loop formed between Tbet and IL-36 γ . Like DC.Tbet, when delivered into the established TME, DC.IL-36 γ also promoted the rapid development of TLS and slowed tumor growth. These results support the utility of Tbet- and IL-36 γ -based therapeutics in the cancer setting and may provide clues for the roles of IL-36R agonist cytokines (i.e. IL-36 α , IL-36 β and IL-36 γ) in disease-associated TLS formation in alternate chronic inflammatory states, such as autoimmune arthritis, diabetes and psoriasis (263,264,267,268), among others.

2.3 RESULTS

2.3.1 DC.Tbet overexpress pro-inflammatory gene products, including IL-36 γ .

Day 5 cultured, bone-marrow derived DC from C57BL/6 mice were infected with rAd.mTbet to generate DC.Tbet. To investigate the effect of Tbet overexpression in DC, molecular profiling of DC.Tbet versus control DC.null was performed, leading to the identification of a range of differentially-expressed gene transcripts, including a number of pro-inflammatory cytokines and chemokines (**Figure 2.1A**). Notably, IL-36 γ and IL-12p40 were two of the most overexpressed gene transcripts in DC.Tbet when compared to control DC in both mice and humans (**Figs. 2.1A, S2.1**), whereas other transcripts such as CXCL9 and IL-1 β were not consistently elevated in DC.Tbet in an evolutionarily-conserved manner (thus limiting their likely translational relevance). Both Tbet and IL-36 γ protein expression could be detected in murine DC.Tbet by IFM (**Figure 2.1B**), and DC.Tbet secreted higher levels of mIL-12p70 (**Figure 2.1C**) and mIL-36 γ (**Figure 2.1D**) than control engineered DC. We then confirmed that injection of DC.Tbet cells into established s.c. MCA205 sarcomas on days 7 and 14 post-tumor inoculation resulted in slowed tumor growth when compared to i.t. therapy using PBS or control DC. ψ 5 cells (**Figure 2.1E**).

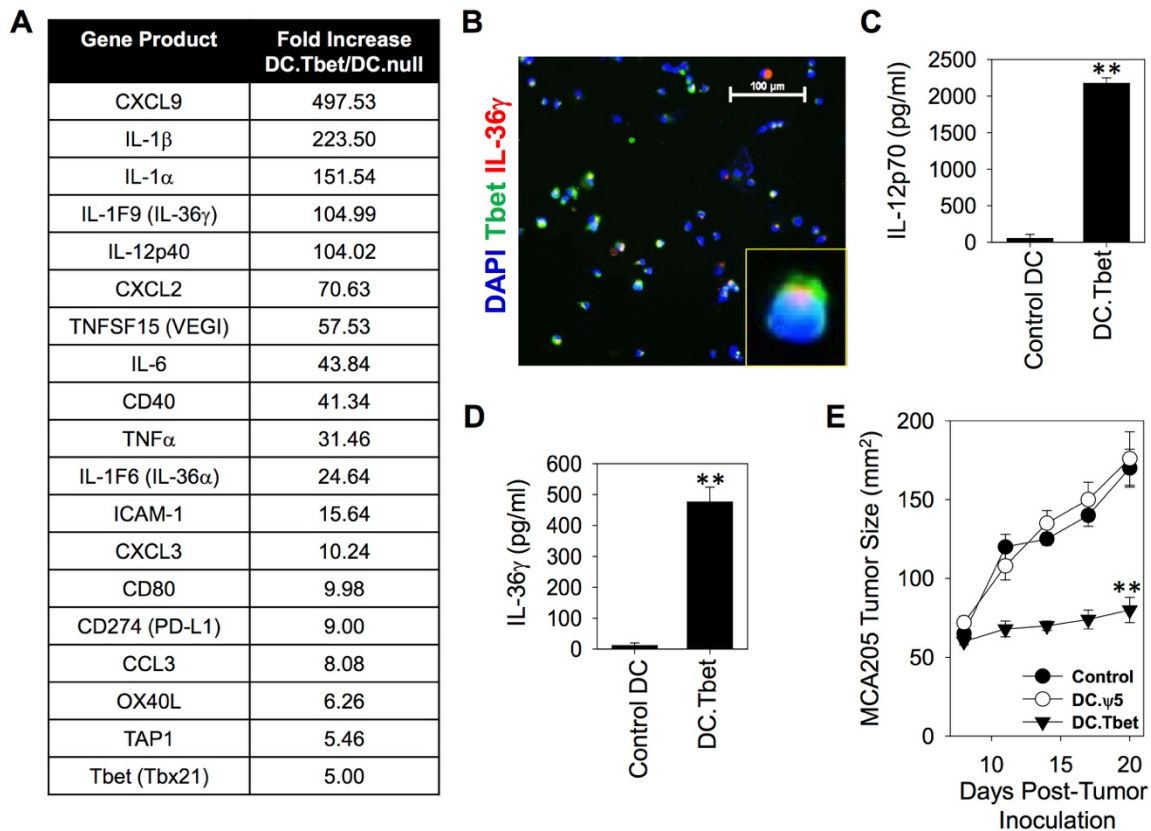


Figure 2.1. Characterization of therapeutic DC.Tbet.

Bone marrow-derived DC were generated in GM-CSF + IL-4 cultures for 5-6 days, before being infected for 48h with rAd.mTbet or control rAd.EGFP or empty rAd.ψ5, or they were left untransduced, as indicated. In **A**, DC were treated, as indicated, with the addition of LPS + IFN γ for the second 24h of infection. Affymetrix gene array analyses were performed on DC.Tbet (**A**), with transcripts increased >5-fold compared to control DC reported. DC.Tbet generated from Tbet-ZsG (H-2^b) reporter mice were then analyzed by IFM for intracellular expression of the Tbet reporter (green) and IL-36 γ (red), with DAPI staining of nuclei (**B**). DC.Tbet or control DC were cultured at 4×10^5 cells/mL. After 48h of infection, supernatant was harvested and mIL-12p70 (**C**) or

mIL-36 γ (**D**) production was analyzed by ELISA. **p < 0.05 for DC.Tbet versus control DC (t-test). In **E**, DC.Tbet, control DC. ψ 5, or PBS were then injected intratumorally into mice bearing d7 established s.c. MCA205 sarcomas on days 7 and 14 post-tumor inoculation. Tumor size was measured over time. **p < 0.05 for DC.Tbet versus PBS or control DC. ψ 5 treatment on days \geq 11 (ANOVA). Data are representative of those obtained in 2 independent experiments performed in each case.

2.3.2 i.t. delivery of DC.Tbet results in rapid infiltration of lymphocytes and development of TLS in vivo.

To investigate the longitudinal cellular and molecular changes occurring within the therapeutic TME, MCA205 sarcomas were harvested from tumor-bearing wild-type C57BL/6 mice or syngenic (H-2^b) Tbet-ZsG reporter mice at various time points after i.t. delivery of DC.Tbet cells. Immunofluorescence microscopy analyses revealed early (by 4-10h post-treatment) infiltration of treated tumors by T cells (both CD4⁺ and CD8⁺) that continued to increase in their abundance through 24h post-treatment (**Figure 2.2A**). Many of these TILs appeared to exhibit Type-1 functional polarization, based on their expression of the Tbet reporter in Tbet-ZsG recipient models (**Figure 2.2A**). In stark contrast, B cells (identified by their CD19⁺ or B220⁺ phenotypes) though present in the TME by 5 days following treatment with DC.Tbet, did not contribute significantly to TIL composition early or late (**Figure 2.2A-C**). Interestingly, although not evident at 4-24 hours post-i.t. injection of DC.Tbet, PNA⁺ vessels became readily detectable in MCA205 tumors beginning on day 5 after treatment and persisted until at least 5 days following the second treatment with DC.Tbet (i.e. d12 after first injection of DC.Tbet; **Figure 2.2B, 2.2C**). Immunofluorescence imaging also revealed strong local production of IL-36 γ in MCA205 tumors beginning at 4h after i.t.-based DC.Tbet therapy, with

sustained intratumoral IL-36 γ observed through 5 days following the second treatment with DC.Tbet (**Figure 2.2D, 2.2E**). Since PNAd⁺ HEV in peripheral tissues have been linked to the formation of TLS in chronically-inflamed tissues (171,257,261,262), we next analyzed whether injected DC.Tbet and/or the therapeutic TME expressed a transcript profile consistent with TLS formation. We observed that DC.Tbet at the time of injection into mice expressed higher levels of mRNA encoding CCL19, CCL21, LIGHT and LTA (but not CXCL13), when compared to control DC. ψ 5 (**Figure S2.2A**). Notably, we found that each of these transcripts was differentially upregulated in the TME within 4-10 days of DC.Tbet vs. control DC. ψ 5 injection (**Figure S2.2B**), at least circumstantially implicating the involvement of additional DC.Tbet-conditioned tumor stromal cells (or tumor cells themselves) as principal pro-TLS transcript sources over time *in vivo*.

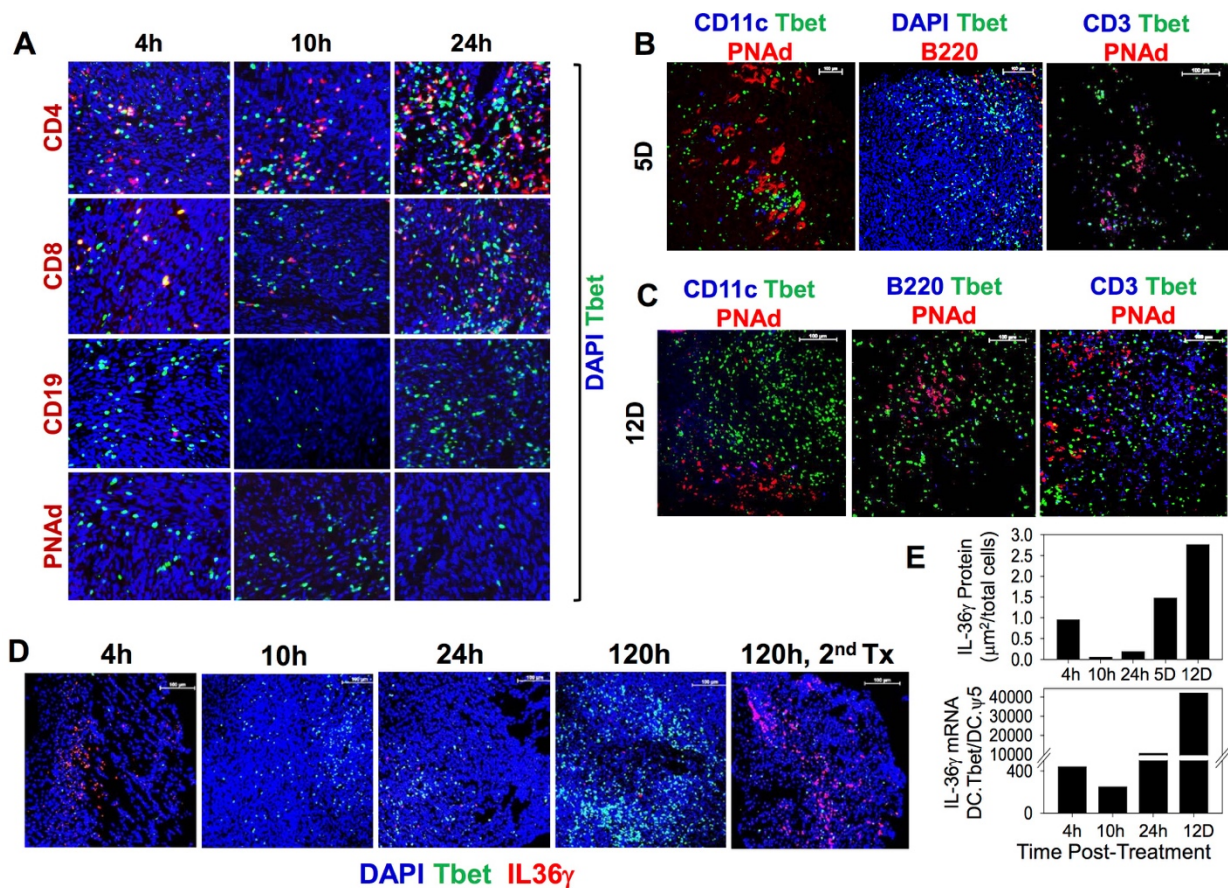


Figure 2.2. DC.Tbet injected i.t. promote the rapid infiltration of lymphocytes and the development of PNAAd⁺ blood vessels in association with enhanced locoregional induction of IL-36γ.

MCA205 tumor-bearing wild-type C57BL/6 mice or Tbet-ZsG reporter mice were treated by i.t. delivery of 1×10^6 DC.Tbet or DC.ψ5 7 days post-tumor inoculation. In **A**, tumors were harvested from Tbet-ZsG mice at 4h, 10h or 24h after treatment with DC.Tbet and tissue sections analyzed by IFM for CD4⁺ T cells, CD8⁺ T cells, CD19⁺ B cells, and PNAAd⁺ HEV. In **B** and **C**, expression and localization of peripheral node addressin (PNAAd), CD11c⁺ DC, CD3⁺ T cells, and B220⁺ B cells were analyzed in tumor sections

from Tbet reporter mice on days 5 (**B**) and 12 (**C**) post-treatment with DC.Tbet. In **D**, day 5 (post-DC.Tbet treatment) tumor sections from Tbet-ZsG mice were analyzed by IFM for co-expression of the Tbet reporter (green) and IL-36 γ (red, using a specific polyclonal antibody). In **E**, IL-36 γ protein levels were assayed by quantification of fluorescence from IFM, or transcript levels were assayed by real-time PCR in total tumor RNA isolated from wild-type C57BL6/J hosts, at the indicated time points following DC.Tbet or DC. ψ 5 treatment. Data are representative of those obtained in 2-3 independent experiments performed in each case.

2.3.3 Therapeutic anti-tumor efficacy of i.t. DC.Tbet is not dependent on host LTA.

Given evidence for the development of TLS in the TME of DC.Tbet-treated C57BL/6 wild-type mice, we next examined whether SLO were necessary for the observed therapy benefits of this treatment strategy. MCA205 sarcomas were established in peripheral lymph node-deficient LTA^{-/-} mice (269), and treated with i.t. delivered DC.Tbet or control DC. ψ 5 as outlined in **Figure 2.1D**. We noted that the treatment of MCA205 sarcomas with DC.Tbet was comparably efficacious in both LTA^{-/-} and C57BL/6 wild-type host animals (**Figure 2.3A**). Furthermore, based on the results of repeat experiments involving the co-administration of depleting anti-CD4 or anti-CD8 antibodies, we conclude that therapeutic protection mediated by DC.Tbet in LTA^{-/-} mice is both CD4⁺ T cell- and CD8⁺ T cell-dependent (**Figure 2.3B**).

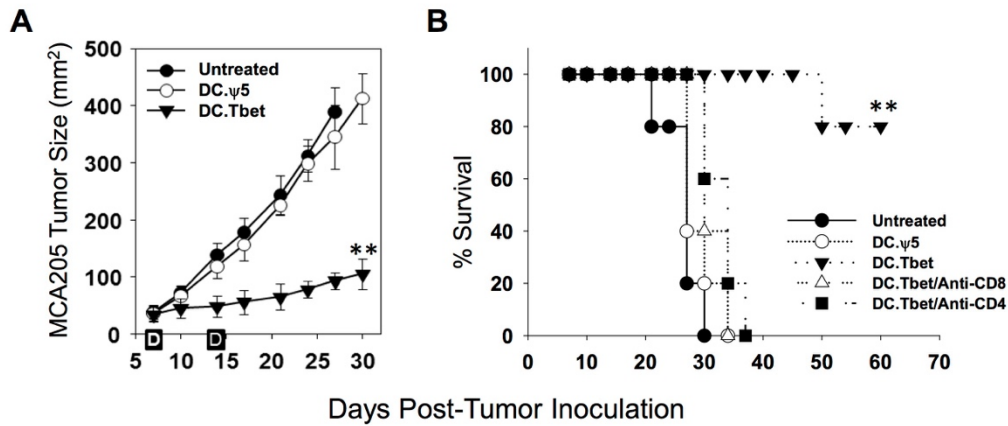


Figure 2.3. I.t.-delivered DC.Tbet mediates anti-tumor efficacy in secondary lymph node-deficient $LTA^{-/-}$ mice that is both $CD4^{+}$ and $CD8^{+}$ T cell-dependent.

In **A**, lymphotoxin- α ($LTA^{-/-}$) mice bearing established day 7 MCA205 sarcomas were left untreated, or they were treated (**D**) on days 7 and 14 by i.t. injection of 10^6 DC.Tbet or control DC. ψ 5 cells alone, with tumor size (mean \pm SD from 5 mice/group) then monitored over time. In **B**, this same model was left untreated, or treated on days 7 and 14 with DC. ψ 5 or DC.Tbet cells (\pm systemic i.p. administration of depleting anti-CD4 or anti-CD8 mAbs) and time-to-euthanasia (as an index of overall survival) reported over time. $**p < 0.05$ for DC.Tbet versus all other cohorts (ANOVA). Data are representative of those obtained in 2 independent experiments performed.

2.3.4 Ablation of IL-36R signaling abrogates the therapeutic anti-tumor efficacy of i.t. DC.Tbet.

Although mouse and human DC.Tbet produce high levels of IL-36 γ and IL-12 transcripts and protein (**Figures 2.1 and S2.1**), our previous work demonstrated that the therapeutic benefits of such treatments were maintained even if the injected DC.Tbet were generated from syngenic IL-12p35^{-/-} or IL-12p40^{-/-} mice (28). Subsequent mechanistic analyses were therefore focused on the study of DC.Tbet-associated IL-36 γ and its receptor IL-36R. To determine whether the therapeutic benefits of i.t.-delivered DC.Tbet were IL-36R-dependent, wild-type C57BL/6 mice were treated on days 7 and 14 after s.c. injection of MCA205 sarcomas, in the absence or presence of (i.t.) co-delivered rIL-1F5 (aka IL-36RA or IL-36RN), a natural IL-36R antagonist (192,211). As depicted in **Figure 2.4**, we observed that rIL-1F5 co-delivery effectively blocked the ability of i.t. DC.Tbet to slow tumor growth (**Figure 2.4A**), to sponsor the development of PNA⁺ HEV in the TME (**Figure 2.4B**), or to recruit/retain CD4⁺ and CD8⁺ TIL (**Figure 2.4C**).

To further confirm the importance of IL-36R on host (tumor stromal/immune) cells to the anti-tumor efficacy of i.t.-delivered DC.Tbet in an alternate tumor model, we established s.c. MC38 colon carcinomas in syngenic (H-2^b) C57BL/6 wild-type or IL-36R^{-/-} mice, before treating them i.t. on days 7 and 14 with DC.Tbet/EGFP or control DC.EGFP (i.e. rAd.EGFP was used to engineer both DC cohorts to mark these injected cells for subsequent tissue imaging studies). As shown in **Figure 2.5A**, consistent with data obtained in the MCA205 sarcoma model, treatment of established MC38 tumors with DC.Tbet/EGFP but not DC.EGFP resulted in significant slowing in tumor growth. Also consistent with data obtained in the MCA205 model, we noted that transcripts associated with PNA⁺ HEV/TLS development and immune cell trafficking (particularly

LTA and CCL21) were increased in the TME of MC38-bearing mice treated i.t. with DC.Tbet/EGFP vs. control DC/EGFP (**Figure S2.3**). Although data from MCA205 models in LTA^{-/-} recipient animals argued against a major role for host LTA in the therapeutic efficacy of i.t.-delivered DC.Tbet (**Figure 2.3**), to determine the broader role(s) of LTβR agonist cytokines (from either the injected DC.Tbet cells or the host TME) on the anti-tumor action of DC.Tbet, we established s.c. MC38 tumors in C57BL/6 mice, before treating them i.t. on days 7 and 14 with LTβR-Ig or an isotype control antibody in concert with control DC.EGFP or DC.Tbet/EGFP. As shown in **Figure 2.5B**, MC38 tumors in mice co-treated with LTβR-Ig and DC.Tbet/EGFP exhibited similar rates of slowed progression (through day 18 of the experiment) when compared to mice treated with DC.Tbet/EGFP plus an isotype control antibody. These data suggest that LTβR agonists do not play a pivotal role in DC.Tbet-associated anti-tumor efficacy.

As was the case in our MCA205 tumor models, i.t. injections of DC.Tbet into established s.c. MC38 tumors in C57BL/6 mice led to the development of PNA⁺ HEV surrounded by CD3⁺ T cell and CD11c⁺ DC infiltrates within 5 days of initiating treatment with DC.Tbet/EGFP, but not control DC.EGFP (**Figure 2.5C**). We also confirmed that the therapeutic benefit and TLS formation associated with i.t. delivery of DC.Tbet/EGFP into MC38 tumors was negated in IL-36R^{-/-} recipient mice (**Figure 2.5D, 2.5E**), whereas TLS were readily apparent in H&E stains of DC.Tbet/EGFP-treated tumors in wild-type C57BL/6 recipient animals (**Figure 2.5E**). In MC38-bearing C57BL/6 wild-type hosts, TLS persisted within the TME for at least 6 days following the second injection of DC.Tbet/EGFP (**Figure 2.5F**), and these TLS contained injected EGFP⁺ DC located proximal to PNA⁺ vessels (**Figure 2.5G**). Prior reports in the field have documented the proximity of lymphocytes to PNA⁺ HEV in SLO and, critically, identified a role for PNA⁺ in maintaining lymphocyte proximity to HEV (167). Consistent with previous observations for approximately 30-40% of lymphocytes residing within 20 μm of an HEV in SLO, we observed a similar distribution pattern in tumor-associated TLS after i.t. treatment with DC.Tbet/EGFP cells (**Figure S2.4A-E**). Specifically, we noted that 31.99% of CD3⁺ T cells, 48.46% of B220⁺ B cells and 21.65% of CD11c⁺ DC within the TME treated with DC.Tbet were located within 20 μm of a PNA⁺ vessel (**Figure S2.4F**).

However, as we also discerned in the MCA205 model, B cells in this therapeutic TME failed to organize into formal germinal-center like structures (**Figure S2.4A**). Tumors treated with DC.Tbet/EGFP also contained a higher frequency of CD3⁺ T cells versus tumors treated with control DC.EGFP (**Figure S2.5A**), with increased numbers of Tbet⁺ T cells within the TME after i.t. delivery of DC.Tbet/EGFP (**Figure S2.5B**). Interestingly, CD3⁺ TIL in DC.Tbet/EGFP-treated tumors contained a lower abundance of exhausted/aneergic T cells as suggested by their decreased expression profiles for the PD-1, CTLA4 and TIM-3 checkpoint molecules, versus CD3⁺ TIL isolated from control treated mice (**Figure S2.5C**).

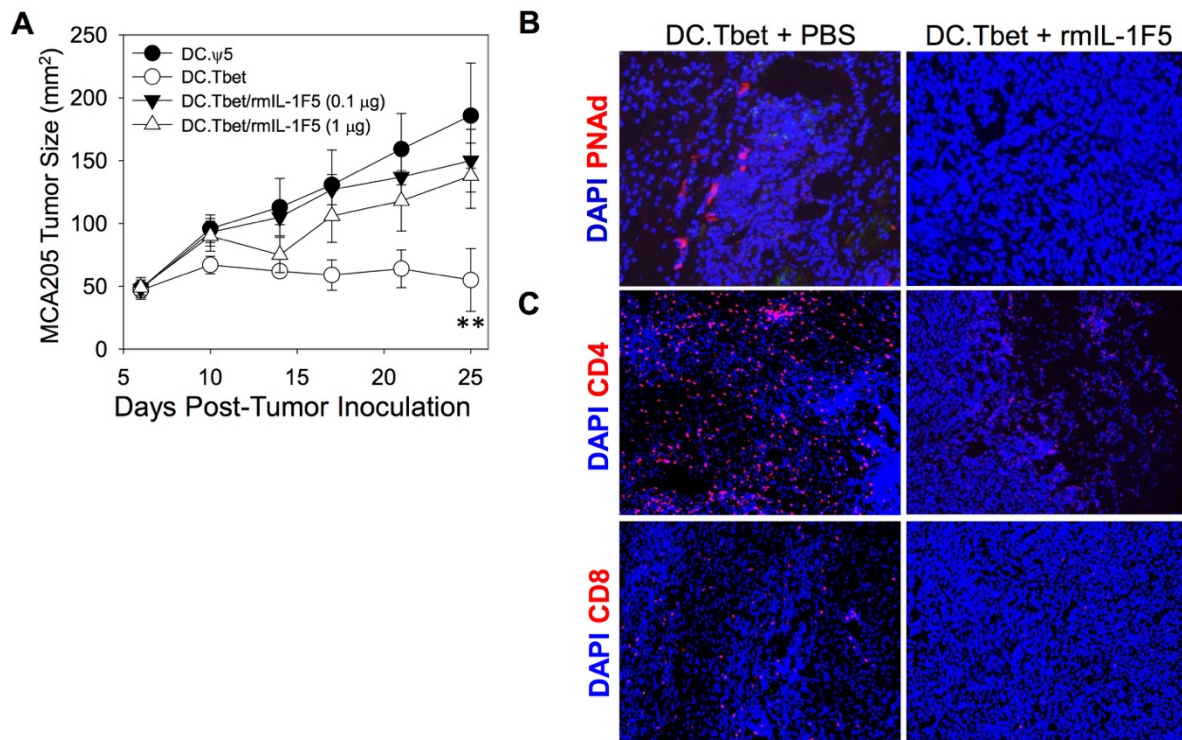


Figure 2.4. The anti-tumor efficacy and TLS promoting activity associated with i.t. DC.Tbet-based therapy is ablated by the IL-36R antagonist IL-1F5 in vivo.

WT C57BL6/J mice bearing established day 7 MCA205 sarcomas were left untreated, or they were treated on days 7 and 14 by i.t. injection of 10^6 DC.Tbet or DC. ψ 5 alone or with DC.Tbet plus co-injection (i.t.) of rmlL-1F5 (0.1 μ g or 1 μ g in 50 μ l PBS) followed by (i.t.) injections of the respective doses of IL-1F5 alone in 50 μ L PBS on days 8, 9, 15, and 16, with tumor growth (**A**) monitored over time (n = 5 mice/group). **p < 0.05 for DC.Tbet vs. all other cohorts (ANOVA) on days \geq 17. In **B** and **C**, tumors were harvested from the indicated treatment cohorts on day 25 post-tumor inoculation (i.e. 9 days following the final injection of rmlL-1F5) and analyzed by IFM for the presence of PNA⁺ vessels (**B**) and CD4⁺ T cells and CD8⁺ T cells (**C**). Data are representative of 3 independent assays performed in each case.

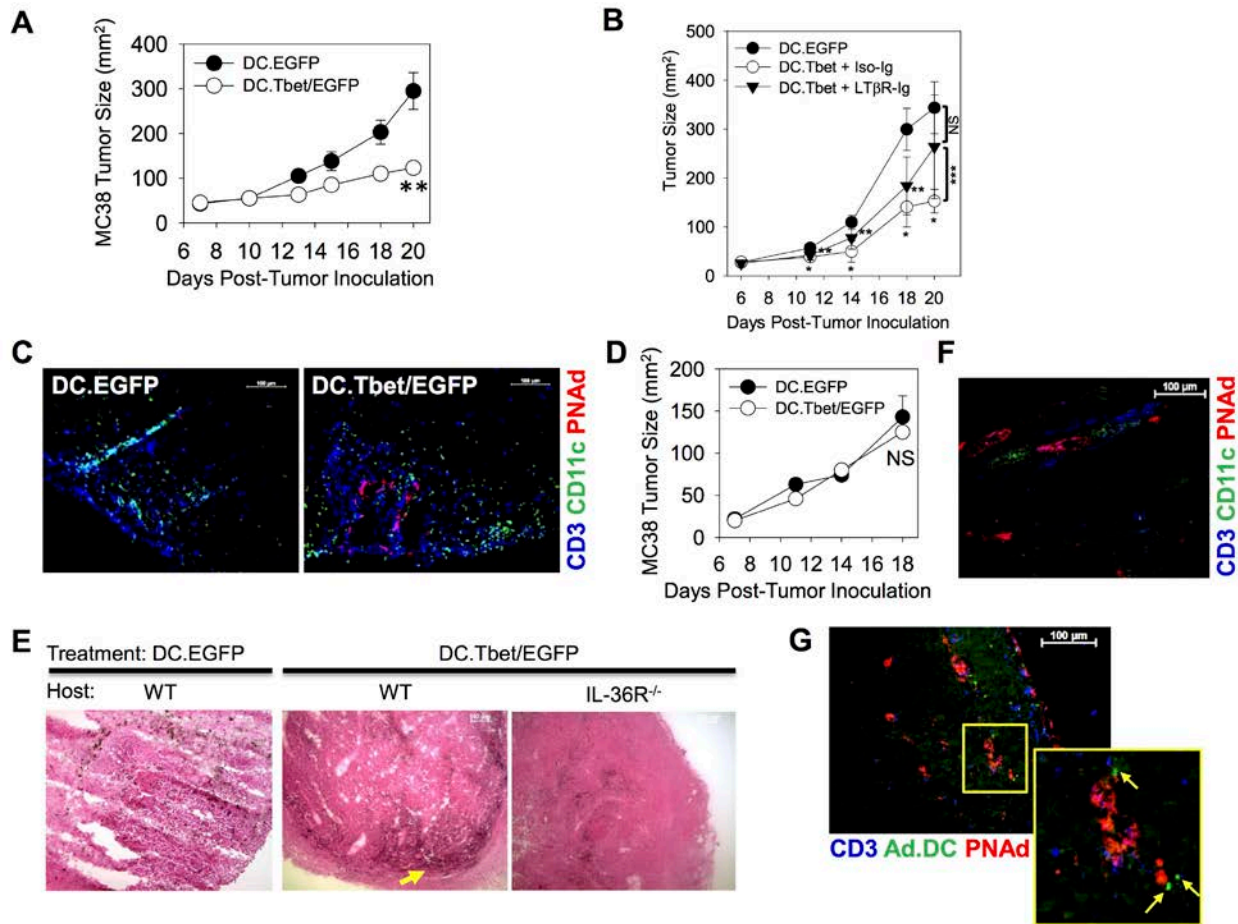


Figure 2.5. The anti-tumor efficacy and TLS promoting activity associated with i.t. DC.Tbet-based therapy is absent in the IL-36R^{-/-} recipient mice.

10⁵ MC38 colon carcinoma cells were injected into the flanks of syngenic wild-type C57BL/6 (A) mice and allowed to establish. Tumor-bearing mice were randomized into groups of 5 animals/cohort on day 7 post-implantation, with all cohorts exhibiting comparable mean tumor size. These animals were then left untreated, or were treated on days 7 and 14 by i.t. injection of 10⁶ control DC.EGFP or DC.Tbet/EGFP, with tumor growth subsequently monitored over time (n = 5 mice/group). **p < 0.05 for DC.Tbet vs. all other cohorts on days ≥ 13 for C57BL/6 recipients. In B, the experiment from A was repeated, with the addition of co-treatment cohorts including LTβR-Ig (100 μg) or an isotype control antibody (100 μg), injected i.t. 3 hours prior to each injection of DC.Tbet.

* $p < 0.05$ for DC.Tbet + Iso-Ig vs. DC.EGFP on days ≥ 11 ; ** $p < 0.05$ for DC.Tbet + LT β R-Ig vs. DC.EGFP on days 11-18 (NS on day 20); *** $p < 0.05$ for DC.Tbet + Iso-Ig vs. DC.Tbet + LT β R-Ig on day 20. In **C**, tumors harvested 5 days following with DC.Tbet/EGFP or control DC.EGFP were cryosectioned and analyzed by IFM for the presence of PNA $^+$ HEV, CD3 $^+$ T cells, and CD11c $^+$ DC (**C**). In **D**, 10^5 MC38 colon carcinoma cells were injected into the flanks of syngenic IL-36R $^{-/-}$ and allowed to establish and were treated as described in **A**. $p = NS$ for DC.Tbet vs. control cohorts in IL-36R $^{-/-}$ mice at all time points (ANOVA). In **E**, day 18-21 tumors harvested from the indicated treatment cohorts were cryosectioned and then H&E stained as described in Materials and Methods. Robust TIL populations (**C**, **E**) were observed in cortical regions of MC38 tumors, only in DC.Tbet-treated C57BL/6 hosts. In **F** and **G**, DC.Tbet/EGFP-treated tumors were harvested from wild-type C57BL6/J hosts at day 20 and analyzed by IFM for the presence of PNA $^+$ HEV, CD3 $^+$ T cells, and CD11c $^+$ DC (**F**) or PNA $^+$ HEV, CD3 $^+$ T cells, and DC.Tbet/EGFP (**G**). Data are representative of those obtained in 3 independent experiments performed in each case.

2.3.5 DC engineered to secrete bioactive rmlIL-36 γ (DC.IL-36 γ) recapitulate the effects of i.t. DC.Tbet treatment in vivo.

We next asked whether ectopic IL-36 γ production by DC would allow these cells to phenocopy DC.Tbet in their ability to effectively treat established tumors after i.t. injection, in association with the promotion of “non-classical” TLS within the TME. We first designed and produced a recombinant adenoviral vector encoding a fusion protein consisting of the human CD8 signal sequence followed by a full agonist form of mIL-36 γ chain (i.e. amino acid positions G13-S164 found in the processed, bioactive form of this cytokine) (192). This vector was then used to generate and characterize DC.IL-36 γ

(**Figure 2.6**), before subsequently applying them as an i.t.-delivered cellular therapy (**Figure 2.7**).

Predictably, DC.IL-36 γ displayed a robust increase in mL-36 γ mRNA transcript (**Figure 2.6A**) and protein (**Figure 2.6B**) levels when compared with control DC. Molecular profiling of DC.IL-36 γ versus control DC was performed, leading to the identification of a panel of upregulated chemokines and cytokines (**Figure 2.6C**). Consistent with data from DC.Tbet cells, DC.IL-36 γ at the time of injection expressed elevated levels of CCL21 and LTA, as well as LIGHT (**Figure S2.6**). Remarkably, DC.IL-36 γ strongly upregulated their expression of Tbet when compared to control DC, although this level of elevated transcription (**Figure 2.6D**) and protein production (**Figure 2.6E**) did not quite reach that observed in DC.Tbet. IL-36 γ was secreted from DC.IL-36 γ (and DC.Tbet) but not control DC (**Figure 2.6F**), and the IL-36 γ secreted by DC.IL-36 γ was bioactive based on its ability to upregulate Tbet reporter expression in splenic T cells isolated from Tbet-ZsG mice (**Figure 2.6G**). When visualized by IFM, DC.IL-36 γ cells were determined to co-express Tbet and IL-36 γ (**Figure 2.6H**).

We subsequently determined that i.t. delivery of DC.IL-36 γ slows MC38 tumor growth in C57BL/6 wild-type hosts (**Figure 2.7A**) and promotes the development of TLS with MC38 tumors (**Figure 2.7B**) to a degree similar to that observed for DC.Tbet-based therapy (**Figure 2.5**). Euclidean distance analyses of fluorescence microscopy images revealed that 39.62% of CD3⁺ TIL, 60.09% of B220⁺ B cells and 37.32% of CD11c⁺ DC were located within 20 μ m of PNA⁺ vessels within the TME of animals treated with DC.IL-36 γ (**Figure S2.7**). Transcripts associated with TLS formation, including LTA, LIGHT, CCL19, CCL21, and CXCL13, were coordinately upregulated within 1-5 days following DC.IL-36 γ treatment. As expected, DC.IL-36 γ -based therapy was ineffective in limiting tumor progression or in facilitating TLS formation in MC38 tumors established in IL-36R^{-/-} recipient animals (**Figure 2.7C, 2.7D**). Given the coordinate upregulation of Tbet transcription and protein production in DC.IL-36 γ (**Figure 2.6D, 2.6E**), we next analyzed whether DC.IL-36 γ developed from Tbet^{-/-} bone marrow remained effective as an anti-tumor agent in wild-type recipients. As shown in **Figure 2.7E**, DC.IL-36 γ /EGFP

developed from wild-type or Tbet^{-/-} bone marrow were equally efficacious as a therapy versus DC.EGFP when injected directly into MC38 tumors. Thus, DC expressing ectopic IL-36 γ do not require intrinsic Tbet expression to mediate anti-MC38 benefit after i.t. delivery.

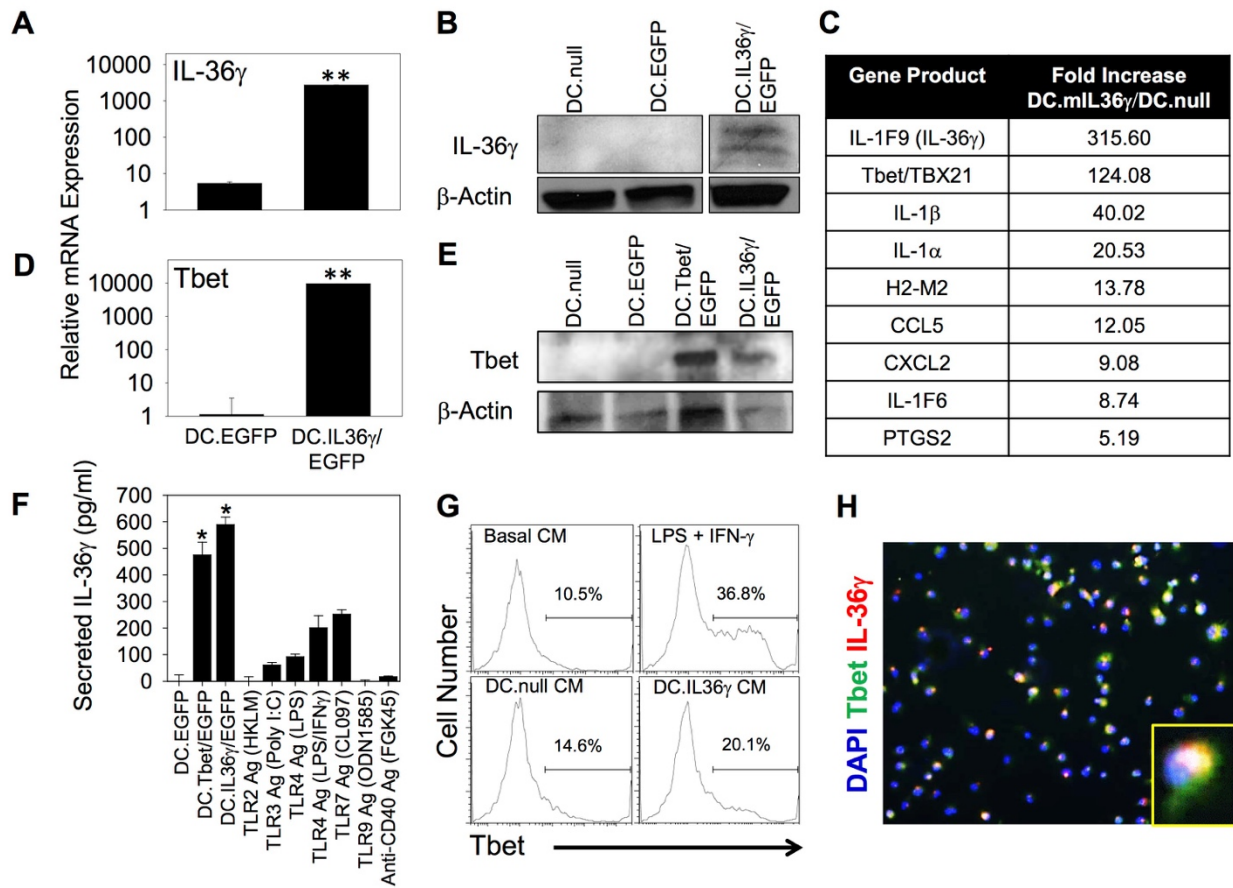


Figure 2.6. DC.IL-36 γ produce/secrete bioactive IL-36 γ and upregulate intrinsic transcription of Tbet.

Real-time PCR (**A**) and Western blot analysis (**B**) for IL-36 γ were performed on lysates of DC.IL-36 γ /EGFP versus control DC.null or DC.EGFP to confirm transduction efficacy. In **C**, Affymetrix gene array analyses were performed as outlined in Materials and Methods, with transcripts increased >5-fold compared in DC.IL-36 γ versus control DC.null reported. In **D** and **E**, real-time PCR (**D**) and Western blot analysis (**E**) for Tbet were performed on lysates of DC.IL-36 γ /EGFP and/or DC.Tbet/EGFP and/or control DC.EGFP and/or control DC.null. In **A** and **D**, mean \pm SD data are reported; ** $p < 0.05$ (t-test). In **F**, DC were differentiated for 5 days *in vitro*, with CD11c⁺ cells then isolated and either transduced with rAd to express EGFP, mTbet, and/or mIL-36 γ , or untransfected control DC were treated for 24h with the indicated TLR agonists or agonist anti-CD40 (FGK45) antibody. Cell-free supernatants were then analyzed by mIL-36 γ ELISA. * $p < 0.05$ for DC.Tbet and DC.IL-36 γ vs. all other treatment groups (ANOVA). In **G**, cell-free supernatants were recovered from engineered DC and analyzed for bioactivity by addition to cultures of bulk splenocytes isolated from Tbet (ZsG) reporter mice; i.e. 10⁶ splenocytes were cultured in 200 μ L of basal media (negative control), media containing LPS + IFN γ (positive control) or cell-free media harvested from DC.null or DC.IL-36 γ cells 48h after rAd infection. After overnight culture, splenocytes were analyzed by flow cytometry for upregulation of intracellular Tbet reporter expression. In **H**, DC.IL-36 γ cells were analyzed by IFM as described in **Figure 1B** to detect coordinate expression of Tbet and IL-36 γ protein. All data are representative of those obtained in 2-3 independent experiments performed in each case.

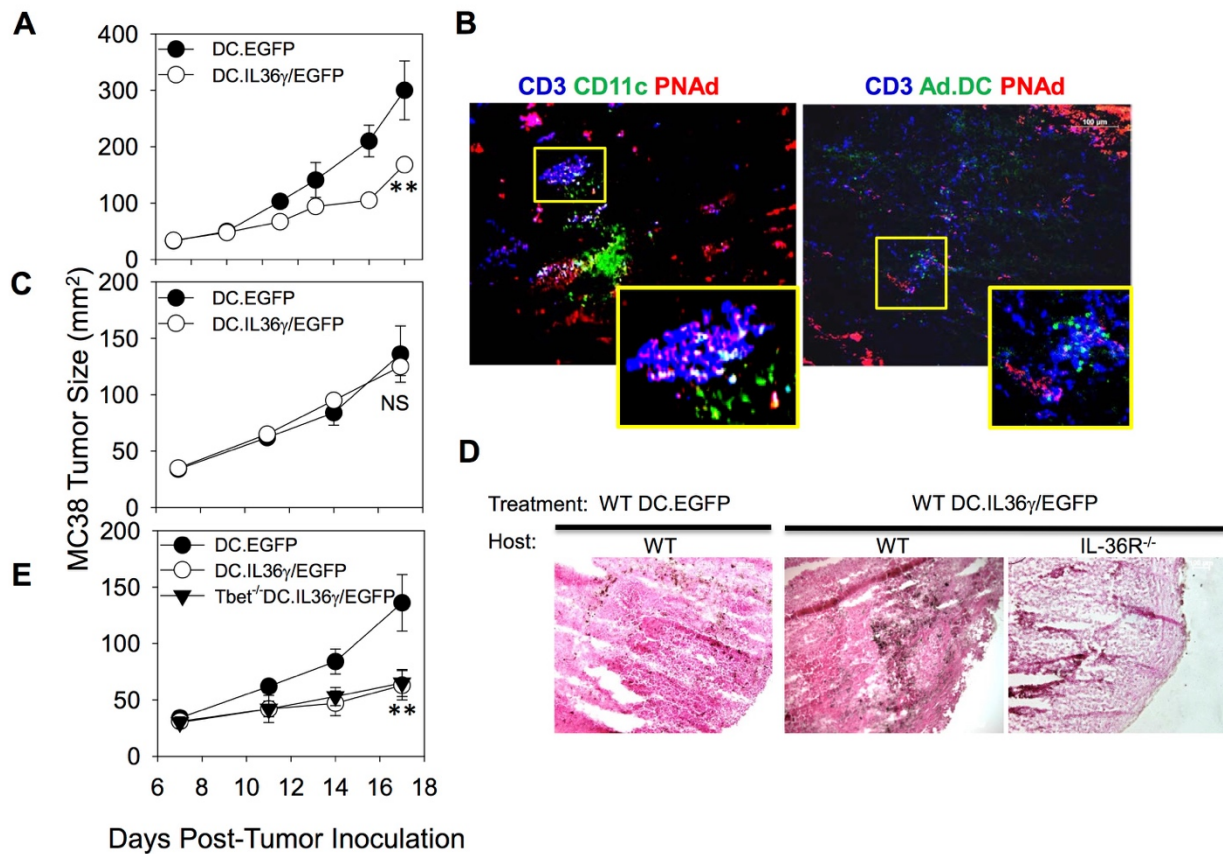


Figure 2.7. I.t. delivery of DC.IL-36 γ is therapeutic and promotes TLS in wild-type, but not in IL-36R^{-/-} hosts.

10⁵ MC38 colon carcinoma cells were established s.c. in the flanks of syngenic wild-type C57BL/6 (A) mice. After randomization of the tumor-bearing animals on day 7 to cohorts (5 mice/group) exhibiting comparable mean tumor sizes, mice were treated by i.t. injection with 10⁶ control DC.EGFP or DC.IL-36 γ /EGFP on days 7 and 14, and tumor growth monitored over time. $**p < 0.05$ for DC.IL-36 γ /EGFP vs. DC.EGFP on days ≥ 11 (ANOVA). After euthanasia on day 20 post-tumor inoculation, tumors were cryosectioned and analyzed by IFM for the presence of TLS based on the presence of PNAAd⁺ HEV surrounded by CD3⁺ T cells, CD11c⁺ DC, and DC.IL-36 γ /EGFP in the tumor cortex (B). In C, the experiment performed in A was repeated in IL-36R^{-/-} host

animals. *NS* for DC.IL-36 γ /EGFP versus DC.EGFP at all time points (ANOVA). In **D**, MC38 tumor sections harvested on d18 (IL-36R^{-/-} hosts) or d20 (WT C56BL/6J hosts) post-treatment with DC.IL-36 γ /EGFP or control DC.EGFP were then H&E stained to identify TIL in the cortical regions of the tumors. In **E**, BMDC generated from wild-type or Tbet^{-/-} mice were infected with control rAd.EGFP or rAd.mIL36 γ /EGFP and injected i.t. into established MC38 tumors in wild-type C57BL/6 mice on days 7 and 14 and tumor growth (mean \pm SEM in mm²) was monitored over time. ***p* < 0.05 for WT or Tbet^{-/-} DC.IL-36 γ /EGFP vs. DC.EGFP on days \geq 11; *NS* for WT versus Tbet^{-/-} DC.IL-36 γ /EGFP at all time points (ANOVA). Data are representative of those obtained in 2-3 independent experiments performed in each case.

2.4 DISCUSSION

A major novel finding in our report is that the therapeutic benefits of i.t. delivered DC.Tbet therapy are tied to the ability of these gene-modified cells to promote TLS formation in the cortical region of progressive tumors via a process that is strictly dependent on IL-36 γ , an IL-1 family member cytokine associated with a range of chronic inflammatory diseases including psoriasis, arthritis, and diabetes, among others (263,264,267,268). Indeed, while development of TLS within tumors and slowed tumor growth resulted from the injection of DC.Tbet directly into established MCA205 sarcoma or MC38 colon carcinoma lesions in syngenic C57BL/6 mice, these processes failed to occur after DC.Tbet treatment of tumors in IL-36R^{-/-} hosts or in wild-type mice that received co-injections of the IL-36R antagonist IL-1F5 (aka IL-36Ra/IL-36RN). Surprisingly, IL-36 γ -dependent TLS formation in the TME did not appear to require significant participation by LT β R ligand cytokines based on the results of studies

integrating i.t. co-delivery of antagonist LT β R-Ig (**Figure 2.5B**) or the use of LTA^{-/-} host animals (**Figure 2.3**). In this regard, recent results from Engelhard's group suggest that induction of HEV and early stages of TLS development in i.p. B16.OVA melanomas are LT β R-independent, but LT α_3 /TNFR-dependent (34). Future studies using TNFR1/2^{-/-} recipient animals will help in delineating the role of the LT α_3 /TNFR signaling axis in the antitumor efficacy of i.t.-delivered DC.Tbet (or DC.IL-36 γ).

The anti-tumor benefits mediated by i.t. delivery of DC.Tbet were associated with the rapid infiltration of tumors (within hours) by Tbet⁺ CD4⁺ and CD8⁺ T cells and by locoregional production of cytokines (LTA, LIGHT) and chemokines (CCL19, CCL21 >> CXCL13) classically linked to TLS formation (34,45,48,261,262). Tumor-infiltration by B cells and the development of PNA⁺ HEV in the tumor cortex were subsequently observed by 5 days after treatment with DC.Tbet (but not with control DC). Notably, though present in the TME, B cells were not observed to coalesce into formal germinal centers in treated tumors at any time during the performance of our studies. This result is consistent with previous reports of "incomplete"/"non-classical" lymphoid neogenesis of TLS detected in primary human melanoma (179) and oral squamous cell carcinoma (37). These TLS are instead defined by the presence of PNA⁺ HEV and the proximity of DC and B/T cells to the therapeutically-induced HEV (**Figure S2.4**), based on a paradigm established for SLO by Tsuboi *et al* (167).

The presence of Tregs in TLS has been recently described by Joshi *et al.* (270), where these suppressive cells were observed to localize proximal to DC, B cells, and other T cell subsets within these structures. In our studies, Tregs (i.e. CD4⁺FoxP3⁺) were notably rare events in MC38 tumors, and the frequency of tumor-infiltrating Tregs was statistically equivalent in DC.Tbet/EGFP- versus DC.EGFP-treated tumors (**Figure S2.8A**). In striking contrast, we observed that levels of CD11b⁺Gr1⁺ MDSC in MC38 tumors were reduced after i.t. treatment with DC.Tbet/EGFP versus DC.EGFP (**Figure S2.8B**). When taken in the context of our findings for reduced levels of immune checkpoint molecules associated with TIL exhaustion/anergy in our treatment models (**Figure S2.5C**), this may support the general capacity of i.t.-delivered DC.Tbet to promote TLS in the context of an "immunologically normalized" TME.

In “classic” TLS formation, B cell nucleation/GC formation appears to critically depend on the action of Tfh cells (261–263,271) and follicular DCs (37). As such, we would hypothesize that B cell nucleation/GC formation may fail after treatment with DC.Tbet or DC.IL-36 γ based on the absence or dysfunction of Tfh and follicular DC within the TME. We will evaluate this supposition in prospective studies in each of our tumor models. In this same vein, we also previously reported early infiltration of NK cells into the TME of DC.Tbet-treated MCA205 tumors (36). We are prospectively evaluating whether any deficiency in Tfh cell numbers/function may be related to the recruitment of NK cells that have been reported to inhibit Tfh numbers/function (272) or alternatively to the inability of DC.Tbet or DC.IL-36 γ cells, or an IL-36 γ -rich microenvironment, to sponsor the differentiation or survival of Tfh cells in TLS induced within the treated TME.

An additional major finding in our studies reflects the apparent cooperativity of Tbet and IL-36 γ in therapeutic DC, with ectopic expression of either gene product promoting the robust upregulation of the alternate gene product in transfected DC. Hence, in addition to the aforementioned transactivation of IL-36 γ by Tbet in DC.Tbet (**Figure 2.1A** and (197)), we also observed strong upregulation of Tbet mRNA/protein expression in DC.IL-36 γ versus control DC (**Figs. 2.6C-E**). This is suggestive of a positive feed-back loop in their molecular regulation, at least in myeloid DC. Like DC.Tbet, DC.IL-36 γ were capable of mediating potent anti-tumor effects and promoting TLS formation when injected directly into established tumors in wild-type C57BL/6 host animals. We also observed that the therapeutic anti-tumor benefits of DC.Tbet were lost when applied to tumor-bearing IL-36R^{-/-} mice, and that DC.IL-36 γ derived from Tbet^{-/-} bone marrow remained effective in suppressing the progressive growth of tumors in wild-type C57BL/6 mice. These findings support the cooperativity of Tbet and IL-36 γ underlying the anti-tumor efficacy observed for this DC-based cellular therapy, with IL-36 γ being down-stream of Tbet in the underlying operational paradigm.

While our findings suggest the Tbet- and IL-36 γ -dependency of therapeutic efficacy (TLS formation and slowed tumor growth *in vivo*) associated with i.t. delivery of DC.Tbet or DC.IL-36 γ , it remains unclear as to whether DC provide more than a “vessel” to

deliver the key Tbet-/IL-36 γ -dependent signals into the therapeutic TME. We are currently investigating the comparative treatment benefits associated with mTbet and mIL-36 γ recombinant protein/gene (rAd)-based therapies applied locoregionally in the setting of well-established MCA205 and MC38 murine tumor models. It is also both practical and pertinent to ask whether *in vitro* conditioning of DC (in the absence of genetic engineering) is capable of yielding IL-36 γ -secreting cells that might be competent to recapitulate the therapeutic benefits of DC.Tbet or DC.IL-36 γ upon delivery into the TME. As shown in **Figure 2.6F**, DC cultured with agonists for TLR3, TLR4 and TLR7 (but not TLR2, TLR9 or CD40) were capable of stimulating increased secretion of IL-36 γ from DC, albeit to far lower levels than those achieved from DC.Tbet or DC.IL-36 γ . Nevertheless, it will be important that prospective translational modeling includes a comparison of DC.Tbet/DC.IL-36 γ versus TLR-agonized DC as therapeutic agents. Furthermore, it has also been reported that cathelicidin anti-microbial peptides including LL-37 (in humans) and CRAMP (in mice) promote robust production of IL-36 γ by keratinocytes in the skin (198), with both proteins found prevalently in psoriatic plaques (273,274). As a consequence, it will be informative to determine whether local application of CRAMP to our tumor models begets IL-36/IL-36R-dependent TLS development as well as therapeutic benefit.

Even though DC.Tbet preferentially produce IL-36 γ (over alternate IL-36R agonists IL-36 α and IL-36 β), an additional remaining question is whether i.t. administration of IL-36 α or IL-36 β , or neutralizing antibodies against the natural IL-36R antagonists (i.e. IL-1F5/IL-36RA/IL-36RN or IL-1F10/IL-38; (193)), which might be used to agonize IL-36R-dependent signaling in the TME, would prove therapeutic against well-established tumors. In our murine gene array analyses of DC.Tbet and DC.IL-36 γ (**Figs. 2.1A, 2.6C**), IL-36 α transcription is upregulated, albeit to a lesser extent than is IL-36 γ (8-20 fold versus 105-316 fold, respectively), supporting the reported co-regulation of these two IL-36R agonists (220) and suggesting that administration of IL-36 α might lead to effects similar to those observed following IL-36 γ -based therapy. Interestingly, a meta-analysis has recently revealed an association between tumor expression of IL-1F5 and

poor clinical prognosis in cancer patients (240), and IL-1F5 (and to a lesser extent IL-38) appears to be commonly expressed at the protein level in the TME of a broad range of cancer histologies (**Figure S2.9**). Prospective experiments using i.t. delivery of DC.IL-36 α , DC.IL-36 β or (positive control) DC.IL-36 γ +/- blocking anti-IL1F5 or anti-IL-1F10 antibodies will attempt to clarify these issues in our murine tumor models. Future studies will also elucidate which tumor stromal/immune cell populations respond to IL-36R agonism in the therapeutically-effective TME.

Although not critical to the therapeutic benefits observed in our tumor models (28), it is also notable that DC.Tbet and DC.IL-36 γ secrete high-levels of IL-12p70 (**Figs. 2.1C, 2.6H** and (266)), which is known to be induced by IL-36R-mediated signaling (220). IL-12 has recently been reported to upregulate IL-36R expression on CD8⁺ T cells and to promote the development of improved Type-1 antigen-specific immunity under conditions of aerobic glycolysis (240) (a characteristic of the progressor TME) (193), providing further support for the reinforcing nature of Tbet- and IL-36 γ -associated (immune)biologies within the purview of cancer immunotherapy. Tsurutani *et al.* (240) also suggest that IL-2 and costimulation potently upregulate CD8⁺ T cell expression of IL-36R, which could foreshadow the superior anti-tumor activity of combined immunotherapies integrating DC.Tbet or DC.IL-36 γ with i.) systemic or locoregional administration of rIL-2 and/or ii.) costimulatory agonists or immune checkpoint inhibitors (i.e. to improve the ratio of co-stimulatory/co-inhibitory signals into anti-tumor effector cells) and/or iii.) adoptive T cell or CAR-T cell-based therapy (to promote extended Type-1 polarization and functionality of the transferred anti-tumor effector cells).

In conclusion, our findings support the utility of Tbet- and IL-36 γ -driven, IL-36R-dependent therapies to recondition the TME by fostering the development of non-classical TLS and an “immunologically normalized” microenvironment (i.e. fewer MDSC, lower expression of immune checkpoint molecules on CD3⁺ TIL) in association with delayed tumor growth in both wild-type and peripheral lymph node-deficient hosts. Such approaches would be expected to promote improved cross-priming of anti-tumor T effector cells within the TME, as well as to condition the TME to preferentially recruit

vaccine-primed or ACT T cells into tumor sites when applied in combination protocols. The further inclusion of immune checkpoint blockade or regulatory cell depletion/antagonists would also be expected to improve the fate of the TLS-sponsored anti-tumor T cell repertoire. Such combination regimens are currently being investigated in our pre-clinical models, with the intent to inform future clinical trial designs for the treatment of patients with solid forms of cancer.

2.5 MATERIALS AND METHODS

2.5.1 Study design.

The objectives of these studies were to test the hypothesis that early infiltration of immune cells into the TME and formation of TLS correlated with delayed tumor progression as a consequence of DC.Tbet-based therapy, and to identify downstream mediators of these effects. Once IL-36 γ was identified as a potential candidate (**Figure 2.1A**), we sought to characterize its role in mediating anti-tumor immunity and immune cell recruitment to the TME. The sample sizes and endpoints were determined based on previously published work (28,36) and Institutional Animal Care and Use Committee (IACUC) guidelines. In all *in vivo* experiments, cohorts of mice were randomized 7 days following tumor inoculation. Experiments were replicated as described in individual figure legends. All experiments were performed in an unblinded fashion.

2.5.2 Mice.

Female 6-8 week old wild-type C57BL/6 (H-2^b) mice, as well as, LTA^{-/-} and Tbet/TBX21^{-/-} mice (all on the B6 background) were purchased from the Jackson Laboratory (Bar Harbor, ME). IL-36R^{-/-} and Tbet-ZsGreen (Tbet-ZsG) reporter mice (275) were kindly provided under MTAs from AMGEN and Dr. Jinfang Zhu (NIH/NIAID), respectively, from stocks maintained at Taconic. All animals were handled under aseptic conditions per an IACUC-approved protocol and in accordance with recommendations for the proper care and use of laboratory animals.

2.5.3 Tumor cell lines and culture.

The MCA205 sarcoma and MC38 colon carcinoma (H-2^b) cell lines were purchased from the American Type Culture Collection (ATCC) These cell lines were free of *Mycoplasma* contamination and were maintained in complete medium (CM: RPMI-1640 media supplemented with 10% heat-inactivated fetal bovine serum, 100 µg/mL streptomycin, 100 U/mL penicillin, and 10 mmol/L L-glutamine, all reagents purchased from Invitrogen, at 5% CO₂ tension in a 37°C humidified incubator.

2.5.4 Recombinant adenoviruses (rAd).

E1/E3-substituted, replication-defective (Ad5-derived) recombinant adenoviruses encoding EGFP (rAd.EGFP), murine Tbet (rAd.mTbet), as well as the empty control Ad.ψ5 vector, have been described previously (27). To generate the rAd.mIL36γ vector,

the nucleotide sequence encoding a fusion protein composed of the hCD8 α signal peptide fused to the N-terminus of the bioactive mIL-36 γ (G13–S164) protein was isolated by PCR amplification from the pcDEF3.hCD8/mIL36 γ plasmid (223) using specific primers (forward: 5'-AAAGTCGACGCCATGGCCTTACCAGTGAC-3' and reverse: 5'-AAAGGATCCTTAAGACTTTATATCTAA-3'), then ligated into the Sall-BamHI cloning site in the pAdLox shuttle vector (27), yielding pAdlox.mIL36 γ . After sequence validation of the plasmid, rAd.mIL36 γ was generated by co-transfection of pAdLox.mIL36 γ and ψ 5 helper virus DNA into the adenoviral packaging cell line CRE8 (27). rAd.mIL36 γ was purified from specific CRE8 lysates by cesium chloride density-gradient centrifugation and subsequent dialysis before storage in 3% threalose at -80°C. Titers of viral particles were determined by optical densitometry. As needed, rAd vectors were further expanded, qualified and supplied by the University of Pittsburgh Cancer Institute's Vector Core Facility (a Shared Resource).

2.5.5 Generation of BM-derived DC and transduction with adenoviral vectors in vitro.

DC were generated from the tibias/femurs of mice, and infected with recombinant adenovirus as previously described (27) for 48h to produce control DC (i.e. DC. ψ 5 or DC.EGFP), DC.Tbet or DC.IL-36 γ . In cases where DC.EGFP was used as the control, DC.Tbet and DC.IL-36 γ were co-transduced with Ad.EGFP to produce DC.Tbet/EGFP and DC.IL-36 γ /EGFP, respectively. Western blotting and qPCR were used to document expression of mTbet in transduced DC as previously reported (27), while the presence of IL-36 γ in transfected DC was detected by Western blotting using a polyclonal rabbit anti-mIL36 γ (IL-1F9) antibody (223) or by qPCR using primers described in **Table S2.1** . For ELISA analyses, cell-free supernatant was harvested 48h following infection. For gene array analyses only, DC.Tbet, DC.IL-36 γ , or uninfected DC (i.e. DC.null) were

activated *in vitro* for 24h in media containing 10 µg/mL LPS (Sigma-Aldrich, part number L4516) and 10 ng/mL rmlFN γ (Peprotech, part number 315-05), or left untreated, prior to mRNA isolation.

2.5.6 In vitro stimulation of DC.

In selected experiments as indicated, DC were generated from the tibias/femurs of mice as previously described (27) and were then stimulated *in vitro* using TLR2 agonist HKLM (10⁸ cells/mL), TLR3 agonist polyI:C (1 µg/mL), TLR7 agonist CLO97 (1 µg/mL) (all from Invitrogen, part number tlr-kit1hw), TLR4 agonist LPS (10 µg/mL) with or without rmlFN γ (10 ng/mL), TLR9 agonist ODN1585 (5 nmol; Invitrogen, part number tlr1585) or anti-CD40 antibody FGK45 (1 µg/mL), in complete media containing 1000 U/mL granulocyte/macrophage colony-stimulating factor (GM-CSF) and 1000 U/mL recombinant murine IL-4 (Peprotech). After 24h of stimulation, cell-free supernatant was harvested for subsequent analysis by ELISA.

2.5.7 ELISA.

Murine IL-36 γ ELISA kit (Aviva Systems Biology Corporation, part number OKEH03002) was used per the manufacturer's instructions.

2.5.8 DC-Based Therapy.

Recipient wild-type, mutant or transgenic (H-2^b) mice received s.c. injections of 5×10^5 MCA205 sarcoma cells or 1×10^5 MC38 colon carcinoma cells in the right flank on day 0. On day 7 post-tumor inoculation, mice were randomized into treatment cohorts of 5 mice, with each cohort exhibiting comparable mean tumor sizes (approximately 40-50 mm²). One million DC (i.e. control DC.ψ5, control DC.EGFP, DC.Tbet, or DC.IL-36γ) developed from wild-type C57BL/6 or syngenic mutant (IL-36R^{-/-} or Tbet^{-/-}) or transgenic Tbet-ZsG mice were then injected i.t. in a total volume of 100 μl (in PBS) on day 7 post-tumor inoculation, and then again 1 week later. In some experiments, where noted, IL-36γ function was blocked by i.t. injection of rmlL-1F5 (an IL-36R antagonist also known as IL-36RA or IL-36RN; purchased from Life Technologies, part number 50213-MNAE) at the time of therapeutic DC delivery (and then daily x 2). In other experiments, where noted, LTβR signaling was blocked by i.t. injection of 100 μg LTβR-Ig or control antibody (Sigma-Aldrich, part number AG714) 3 hours prior to each delivery of DC. Mean tumor size (\pm SEM) was monitored every 3-4 days and recorded in mm² by determining the product of the largest orthogonal diameters measured using vernier calipers. Mice were euthanized when tumors became ulcerated or if they exceeded a size of 400 mm², in accordance with IACUC guidelines.

2.5.9 In vivo depletion of CD4⁺ or CD8⁺ T cells.

In selected experiments, as indicated, mice were injected i.p. with 50 - 100 μg rat isotype control Ab (Sigma-Aldrich), 50 μg anti-CD4 mAb GK1.5 (eBioscience, part number 16-0041) or 100 μg anti-CD8 mAb53-6.7 (Biolegend, part number 100716) on days 6, 13 and 20 after tumor inoculation. Specific cell depletion was > 95% effective *in vivo* based on flow cytometry analysis of peripheral blood mononuclear cells obtained by tail venipuncture from treated mice 24-48h after Ab administration (data not shown).

2.5.10 Imaging of tumor tissues.

Tumor samples were prepared and sectioned as previously reported.⁴⁷ Briefly, tumor tissues were harvested and fixed in 2% paraformaldehyde (Sigma-Aldrich) at 4°C for 2h, then cryoprotected in 30% sucrose for 24 hours. Tumor tissues were then frozen in liquid nitrogen and 6 micron cryosections prepared. Hematoxylin & Eosin (H&E) stains were performed as previously described (276). For immunofluorescence microscopy (IFM) analysis of TLS, sections were stained as previously described using primary and secondary antibodies as indicated in **Table S2.2**. In tumors where a biotinylated primary antibody was used, the following protocol modification was made: after blocking with BSA, slides were treated with Avidin Blocking Buffer for 15 minutes, washed in 0.5% BSA in PBS, and treated with Biotin Blocking Buffer (both from R&D Systems, part number CTS002) for 15 minutes, before the addition of the primary antibody. Cell nuclei were then stained with DAPI as previously described (28). After washing, sections were then covered in Gelvatol (Monsanto) and a coverslip applied. Slide images were acquired using an Olympus 500 scanning confocal microscope or an Olympus Provis AX70 fluorescence microscope (both from Olympus America). Positively stained cells were quantified by analyzing images at a final magnification of x20 using Metamorph Imaging software (Molecular Devices) or NIS-Elements software (Nikon Instruments, Inc.).

2.5.11 Flow cytometric analyses.

Tumors were isolated from C57BL/6 mice 20 days following initial tumor inoculation, mechanically minced, and enzymatically digested with 0.5 mg/mL collagenase IA (Sigma-Aldrich, part number C5894), 0.5 mg/mL collagenase II (Sigma-Aldrich, part number C1764), 0.5 mg/mL collagenase IV (Sigma-Aldrich, part number C1889), and

20 U/mL DNase I (Sigma-Aldrich, part number D5025). The resulting single cell suspensions were labeled using fluorescently labeled antibodies as indicated in **Table S2.2**. Cell staining for cell surface markers was performed in PBS in the presence of anti-CD16/CD32 (i.e. Mouse BD Fc Block; BD Biosciences, part number 553142). To stain for intracellular transcription factors, FoxP3/Transcription factor staining buffer set (eBioscience, part number 00-5523-00) was used with the anti-Tbet APC (Biolegend, part number 644814).

2.5.12 RNA purification and PCR analyses.

Total RNA was isolated from control or rAd-infected DC using Trizol reagents (Invitrogen, part number 15596018) or Buffer RLT (Qiagen, part number 1030963). Total RNA was further purified using the RNeasy Plus Micro Kit (Qiagen, part number 74034) including the gDNA Eliminator spin column. The purity and quantity of the total RNA was assessed using Nanodrop ND-1000 (CelBio SpA). For gene array analyses, gene expression analyses were performed on total RNA using the mouse Clariom D Assay (Affymetrix, part number 902513) according to the manufacturer's instructions by the University of Pittsburgh's Genomics Research Core (a Shared Resource), and data was analyzed using Transcriptome Analysis Console 3.0 (Affymetrix). Otherwise, total RNA (1 μ g) was reversed transcribed into cDNA using the High-Capacity RNA to cDNA Kit (Qiagen, part number 4387406) and the cDNA added to RT2 SYBR Green ROX™ qPCR Mastermix (Qiagen, part number 4385612) and used for quantitative PCR using specific primer pairs (**Table S2.1**). Reactions were performed on a StepOnePlus™ Real-Time PCR thermocycler (Applied Biosystems) using the recommended cycling conditions. mRNA expression levels were normalized to expression of control β -Actin or HPRT mRNA and analyzed using the $2^{-\Delta\Delta CT}$ method.

2.5.13 Statistical analyses.

Comparisons between groups were performed using Student's t-test or one-way Analysis of Variance (ANOVA) with *post-hoc* analysis, as indicated. All data were analyzed using GraphPad software (La Jolla, CA). Differences with a *p*-value < 0.05 were considered significant.

2.6 ADDITIONAL SUPPORTING INFORMATION

2.6.1 Materials and Methods

Female 6-8 week old wild-type C57BL/6 and Rag1^{-/-} mice were purchased from the Jackson Laboratory (Bar Harbor, ME) and maintained under aseptic conditions per an IACUC-approved protocol and in accordance with recommendations for the proper care and use of laboratory animals. Studies were carried out as described in **Section 2.5**. In some experiments, where noted, mice were treated with intravenous injections of 100 ug anti-CD62L (clone: MEL-14) or an isotype control antibody (both from Biolegend) on d7 and d14 post-tumor inoculation (i.e. 4 hours prior to each intratumoral injection of DC).

2.6.2 Adaptive immune cells are required for TLS formation

MC38 tumors were established in Rag1^{-/-} mice and treated on d7 and d14 post-tumor inoculation with i.t. injections of 10⁶ DC.EGFP, DC.Tbet/EGFP, or DC.IL-36γ/EGFP cells and measured 2-3 times per week (**Figure 2.8A**). On d20, tumors were harvested and imaged by immunofluorescence microscopy for the presence of TLS (i.e. based on staining patterns for PNA⁺, CD3⁺ and CD11c⁺ cells; **Figure 2.8B**). Results indicate that despite treatment in these immunodeficient mice, tumors rapidly progress and fail to develop intratumoral TLS.

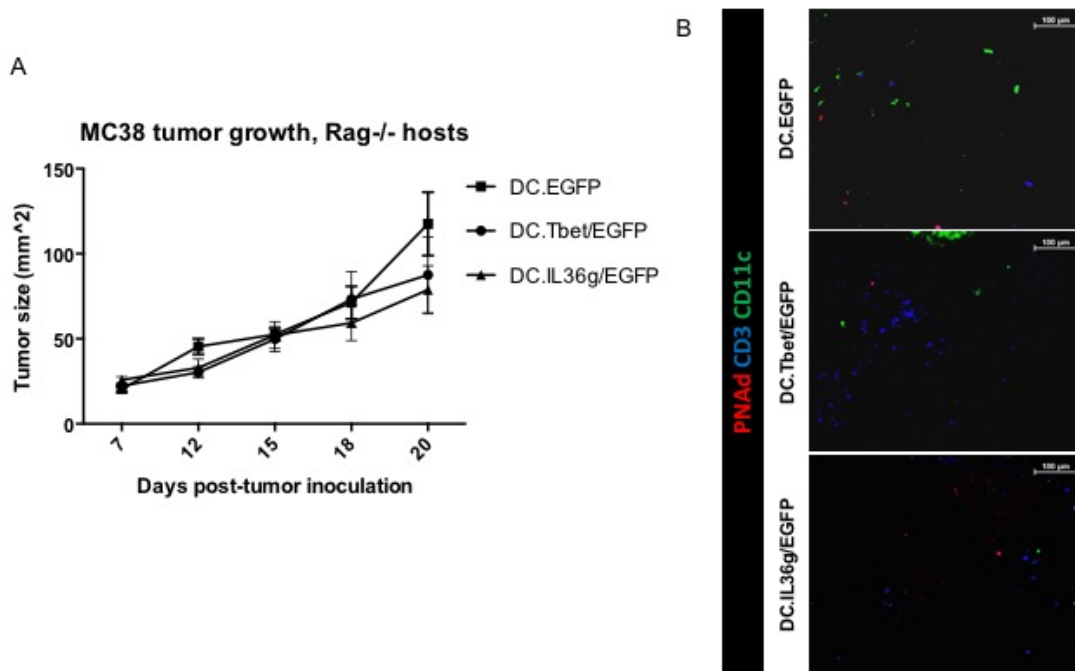


Figure 2.8. The adaptive immune system is required for TLS formation.

Rag1^{-/-} animals were inoculated subcutaneously with 10⁵ MC38 adenocarcinoma cells on d0. On d7 and d14, mice were treated with i.t. injections of 10⁶ DC.EGFP, DC.Tbet/EGFP, or DC.IL-36 γ /EGFP cells. Tumor growth was measured approximately every 3 days (**A**). On d20, tumors were harvested and visualized by immunofluorescence microscopy for PNA α , CD3, and CD11c to assay for the presence of TLS, which were not observed in the TME (**B**). Bars = 100 microns.

2.6.3 Immune cell trafficking via CD62L-PNA α interactions is required for the therapeutic efficacy of DC.IL-36 γ -based therapy

We next sought to understand the mechanism of recruitment of TIL into the TME, and whether PNA α -based recruitment is required for the therapeutic efficacy of DC.IL-36 γ -based treatment. To achieve this, we treated mice as described in **Figure 2.7A**. Additionally, mice treated with DC.IL-36 γ were also treated i.v. with 100 μ g anti-CD62L (MEL-14) or 100 μ g isotype control antibody 4 hours prior to each injection of DC, to block interaction between CD62L expressed on naïve (and central-memory) T cells and PNA α on tumor-associated HEV. While DC.IL-36 γ plus isotype-treated tumors exhibited delayed tumor growth, DC.IL-36 γ plus anti-CD62L-treated tumors progressed at a rate similar to that of DC.EGFP-treated tumors (**Figure 2.9A**). Furthermore, while DC.IL-36 γ plus isotype-treated tumors upregulated transcript expression of *IL36G*, *Tbet*, and biomarkers associated with TLS formation including *LIGHT*, *LTA*, *CCL19*, *CCL21*, *CCR7*, and *CHST4*, DC.IL-36 γ plus anti-CD62L-treated tumors marginally upregulated expression of *IL36G* and failed to upregulate any other TLS-linked transcripts evaluated (**Figure 2.9B**).

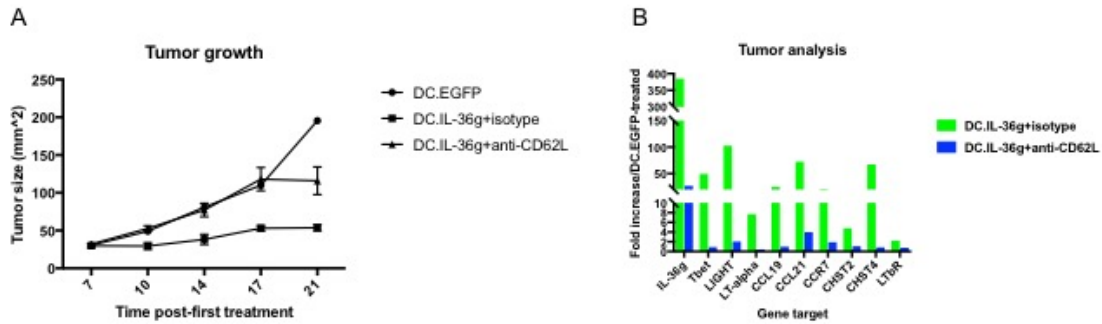


Figure 2.9. CD62L-PNAd interaction is required for the therapeutic efficacy of DC.IL-36 γ treatment.

WT mice were inoculated subcutaneously with 10^5 MC38 adenocarcinoma cells on d0. On d7 and d14, mice were treated with i.t. injections of 10^6 DC.EGFP or DC.IL-36 γ /EGFP cells. Where indicated, some animals were co-treated with i.v. injections of 100 ng anti-CD62L antibody 4h prior to DC injection. Tumor growth was measured approximately every 3 days (**A**). On d20, tumors were harvested and analyzed by qPCR for the expression of indicated TLS-associated genes (**B**).

2.6.4 Interpretation

In these studies, we sought to understand the requirements for T/B cells and for CD62L⁺ immune cell recruitment in delaying tumor progression and forming TLS in DC.IL-36 γ -treated tumors *in vivo*. Previous work from our group determined that CD8⁺ T cells were required for therapeutic efficacy associated with DC.Tbet-based treatment (28). Here, we show that an adaptive immune cell infiltrate is required for the formation of TLS. In Rag1^{-/-} mice that lack mature T and B cells, TLS do not form even after i.t. injection of DC.Tbet or DC.IL-36 γ cells. These results demonstrate that while IL-36 signaling is required for TLS formation (**Figure 2.7D**), its local production may not directly lead to upregulated expression of PNA^d on the tumor vasculature; instead, it likely assists in the early recruitment of lymphocytes into the TME by inducing expression of T cell chemoattractants such as CCL19 and CCL21 produced by DC/VEC within the treated TME; these recruited TIL then drive PNA^d upregulation and the development of HEV. Next, we showed that blockade of CD62L, the ligand for PNA^d, abrogates the efficacy of DC.IL-36 γ treatment. Other work on the DC.Tbet and DC.IL-36 γ therapies showed that these treatment modalities remain effective even when the injected DC (generated from CCR7^{-/-} hosts) are defective in their capacity to traffic to lymph nodes (**Figure 2.3** and ref. (28)), indicating that while anti-CD62L also blocks recirculation of T cells into the lymph nodes, such effects are likely unimportant to the underlying therapeutic biology of our model system. Interestingly, while TIL are recruited into the TME of DC.Tbet- and DC.IL-36 γ -treated tumors at least 72h prior to expression of PNA^d, these results suggest that sustained local therapeutic immunity in the TME requires the presence/function of intratumoral HEV. The mechanism supported by these data is detailed in **Figure 2.10** (updated from (36)).

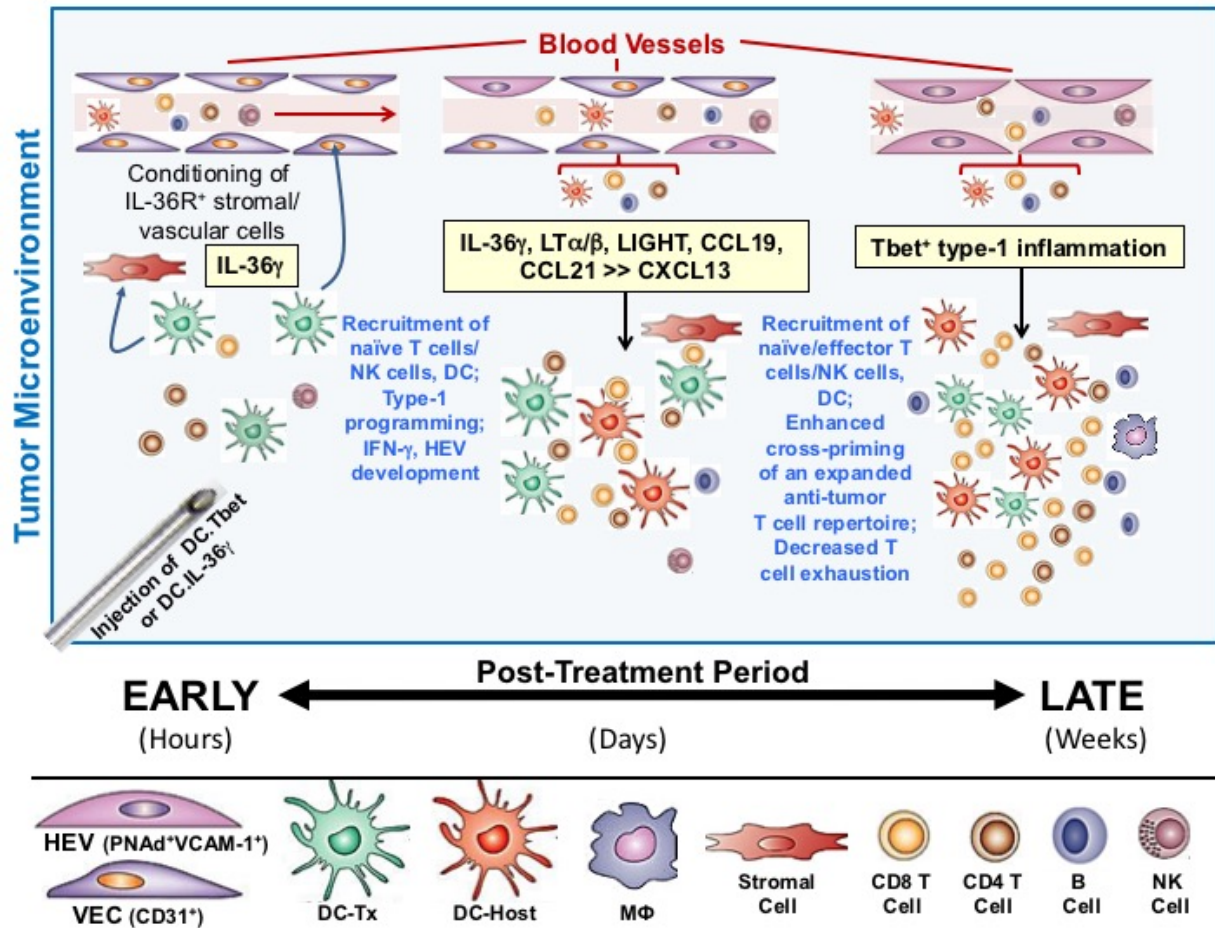


Figure 2.10. Proposed mechanism for the efficacy of DC.Tbet- and DC.IL-36 γ -based therapies.

Following i.t. Injection of DC.Tbet or DC.IL-36 γ cells, a rapid (within 4-10 hour) infiltration of CD4⁺ and CD8⁺ T cells into the TME is observed, likely due to the production of chemokines by the injected DC as well as IL-36 γ interaction with cells of the tumor vasculature to promote further chemokine expression. Within 2 days, NK cell infiltrate is observed. Upregulation of chemokines including CCL19, CCL21, LTA, and LIGHT is observed in the TME beginning at this timepoint. By 4-5 days following treatment, upregulation of PNAAd on the vasculature (i.e formation of HEV) is observed, concurrent with a tightening of TIL and DC to surround these HEV. These TLS persist

for at least 2 weeks post-treatment, at which point a Type-1 T cell response and a decrease in T cell expression of exhaustion markers are noted.

3.0 ASSOCIATION OF IL-36 GAMMA WITH TERTIARY LYMPHOID STRUCTURES AND INFLAMMATORY IMMUNE INFILTRATES IN HUMAN COLORECTAL CANCER

Aliyah M. Weinstein^{1,2,3,6,*}, Nicolas A. Giraldo^{1,2,3}, Florent Petitprez^{1,2,3}, Catherine Julie⁴, Laetitia Lacroix^{1,2,3}, Jean-François Emile⁴, Laetitia Marisa⁵, Wolf H. Fridman^{1,2,3}, Walter J. Storkus^{6,7}, and Catherine Sautès-Fridman^{1,2,3}

From ¹INSERM, UMR_S 1138, Cordeliers Research Center, Team “Cancer, immune control and escape”, F-75006, Paris, France;² University Paris Descartes Paris 5, Sorbonne Paris Cite, UMR_S 1138, Centre de Recherche des Cordeliers, F-75006, Paris, France; ³ Sorbonne University, UMR_S 1138, Centre de Recherche des Cordeliers, F-75006, Paris, France ; ⁴Laboratoire d’anatomie pathologique, Hopital Ambroise Paré, AP-HP, Boulogne, France; ⁵Programme Cartes d’Identite des Tumeurs; Ligue Nationale Contre le Cancer; Paris, France; ⁶University of Pittsburgh School of Medicine, Departments of Dermatology and Immunology, Pittsburgh, PA, 15213 USA; ⁷University of Pittsburgh School of Medicine, Departments of Pathology and Bioengineering, and University of Pittsburgh Cancer Institute, Pittsburgh, PA, 15213 USA.

This chapter is adapted from text that at the time of the submission of this dissertation, is in revision at *Cancer Immunology, Immunotherapy*.

3.1 ABSTRACT

IL-1 family cytokines play a dual role in the gut, with different family members contributing either protective or pathogenic effects. IL-36 γ is an IL-1 family cytokine involved in polarizing Type-1 immune responses. However, its function in the gut, including in colorectal cancer pathogenesis, is not well appreciated. In a murine model of colon carcinoma, IL-36 γ controls tertiary lymphoid structure formation and promotes a Type-1 immune response concurrently with a decrease in expression of immune checkpoint molecules in the tumor microenvironment. Here, we demonstrate that IL-36 γ plays a similar role in driving a pro-inflammatory phenotype in human colorectal cancer. We analyzed a cohort of 33 primary colorectal carcinoma tumors using imaging, flow cytometry, and transcriptomics to determine the pattern and role of IL-36 γ expression in this disease. In the colorectal tumor microenvironment, we observed IL-36 γ to be predominantly expressed by M1 macrophages and cells of the vasculature, including smooth muscle cells and HEV. This pattern of IL-36 γ expression is associated with a CD4⁺ central memory T cell infiltrate and an increased density of B cells in tertiary lymphoid structures, as well as with markers of fibrosis. Conversely, expression of the antagonist to IL-36 signaling, IL-1F5, was associated with intratumoral expression of checkpoint molecules, including PD-1, PD-L1, and CTLA4, which can suppress the immune response. These data support a role for IL-36 γ in the physiologic immune response to colorectal cancer by sustaining inflammation within the tumor microenvironment.

3.2 INTRODUCTION

Colorectal cancer is the third most common form of cancer worldwide (277). In 2017, it is estimated that over 50,000 Americans will die from the disease (278), and in France, approximately 17,500 colorectal cancer-associated deaths are reported each year (279). While the rate of mortality from colorectal cancer is currently decreasing in both countries, only a subset of patients is likely to respond to therapeutic intervention, with most patients having limited or invasive treatment options available (280).

We recently reported the efficacy of an IL-36 γ -based therapy in delaying tumor progression in the MC38 murine model of colon adenocarcinoma (35). The IL-36 cytokines are an IL-1 subfamily (191) consisting of three agonists that signal through a common heterodimeric receptor, IL-36R (232,281). Signaling through the IL-36R can be inhibited by the full receptor antagonist, IL-1F5 (aka IL-36RA), which blocks the recruitment of IL-1RAcP, the IL-1 family receptor accessory protein, required for signaling through the IL-36R (232). IL-36R is expressed on endothelial cells as well as cells of the immune system, including T cells and DCs (220,225,237,282). Through its effects on immune cells, IL-36 γ is involved in polarizing towards Type-1 immune responses (197,222). In particular, it is a downstream target of the Type-1 transactivator Tbet (197) and can induce Tbet expression in target cells (35). The therapeutic introduction of IL-36 γ into the TME using a DC-based vector delayed tumor progression in conjunction with a rapid (within 4-10h) recruitment of T cells into the TME and the formation of tumor-associated tertiary lymphoid structures (TLS). IL-36 γ -overexpressing DC displayed elevated levels of TLS-promoting chemokines, including LT β R agonists LTA and LIGHT, and CCR7 agonist CCL21. When introduced intratumorally, IL-36 γ -based therapy also decreased the level of PD-1, CTLA4, and TIM-3 on CD3⁺ TIL (35).

It has recently been described that in humans, some colorectal cancers also presents with a high immune infiltrate (283), which is sometimes organized into TLS. The presence of TLS within the TME is a positive prognostic marker in colorectal carcinoma and many other solid tumors (60,177,284). TLS form at sites of persistent inflammation, such those found in tissues impacted by chronic viral infections, autoimmune diseases, or cancer. These structures are often marked by a germinal center with dense B cell infiltrate and follicular DCs (15,285). The principal histologic marker used to identify TLS in colorectal cancer is therefore CD20, which identifies these B cells (61,183). In addition, TLS contain follicular DCs and DC-LAMP⁺ mature DCs in a T cell zone, and are surrounded by blood and lymphatic vessels (61,183) including HEV (60) that allow naïve and central memory lymphocytes to be recruited into TLS.

In this study, we attempt to translate our findings from the mouse model of colon carcinoma into human by investigating the pattern of expression of IL-36 γ in colorectal cancer, and whether IL-36 γ expression is associated with TLS components and the infiltration of immune cells into the TME.

3.3 MATERIALS AND METHODS

3.3.1 Public transcriptomic data sets

Transcriptomic data from colorectal cancer tumors (286) was downloaded from Gene Expression Omnibus (accession code GSE39582). The data from Affymetrix Human Genome U133 Plus 2.0 Array was normalized using the frozen RMA method with the R package *frma* (287). Normalized sorted cells transcriptomic data was obtained from Becht et al. (288) (Gene Expression Omnibus accession code GSE86362). The expression fold-change of a gene was computed as the difference between the median log₂ gene expression for the positive samples (defined as all samples from the considered cell population) and all negative samples (defined as all other samples).

3.3.2 Patient cohort

A cohort of 33 primary colorectal tumors was collected between October 2, 2014 and March 3, 2016 from patients operated at the Ambroise Paré hospital (Boulogne Billancourt, France). This research was conducted in accordance with the recommendations outlined in the Helsinki declaration and was approved by the medical ethics board of the hospital. Patient characteristics are summarized in **Table 3.1**.

3.3.3 IHC, immunofluorescence and image quantification

IHC staining was performed as previously described (289). Serial 5-mm formalin-fixed paraffin-embedded tissue sections generated from colorectal cancer were stained using the Dako Autostainer Plus (Agilent). Antigen retrieval and deparaffinization were carried out on a PT-Link (Dako) using the EnVision FLEX Target Retrieval Solutions (Dako). The antibodies used are listed in **Table S3.1** and negative control staining for the IL-36 γ antibody is demonstrated in **Figure S3.1**. Signal intensity was amplified using Envision+ System HRP labelled polymers (Dako) or ImmPRESS HRP Polymer Detection Kit

(Vector). For IHC staining, peroxidase activity was detected using diaminobenzidine (DAB) substrate (Dako), counterstained with hematoxylin (Dako), and mounted with Glycergel Mounting Medium (Dako). The degree of smooth muscle actin (SMA) expression in the tumor stroma was quantified according to the following grading system: (1) scarce fibroblasts; (2) continuous layer of fibroblast between tumor nests with overall thickness inferior to three cells; (3) continuous layer of fibroblast between tumor nests with overall thickness superior to three cells and fibroblast area <50% of tumor area; and (4) continuous layer of fibroblast between tumor nests with overall thickness superior to three cells and fibroblast area >50% of tumor area.

For immunofluorescent staining, signals were detected by Tyramide SuperBoost Signal Amplification (Life Technologies) and slides were counterstained and mounted using ProLong Gold Antifade reagent with DAPI (Molecular Probes). Slides visualized by IHC were digitalized with a NanoZoomer scanner (Hamamatsu) and digitally-quantified with Calopix software (Tribvn). Slides visualized by immunofluorescence were digitalized with an Axioscan scanner (Zeiss) and digitally-quantified with Visiopharm Integration System (VIS) software (Visiopharm).

3.3.4 Tumor processing, surface staining and cell sorting

Flow cytometry staining was performed as previously described (289). Briefly, tumors were dilacerated and incubated for 1 hour at 4°C with Cell Recovery Solution (Fisher Scientific); mixtures were filtrated and TILs separated with Ficoll-Paque PLUS (GE Healthcare Life Science). Cells were then stained with the monoclonal antibodies as listed in **Table S3.2**. Samples were acquired in a FACS Fortessa cytometer with FACSDiva software (BD Bioscience) and data analyzed with FlowJo 7.9.4 software (Tree Star, Inc.). The fraction of cells co-expressing multiple markers was calculated in SPICE 5.3033 (Exon), a data mining software application that normalizes and analyzes large FlowJo datasets (290).

3.3.5 Gene array analyses

Total RNA was isolated from fresh tumor tissue using Quiashredder columns and the RNeasy Mini Kit (both from Qiagen). RNA quality was validated using the RNA 6000 Nano Chip (Agilent) and read on a 2100 Bioanalyzer (Agilent). Transcript analysis was assayed with nCounter (Nanostring). The list of gene targets evaluated in this study is listed in **Table S3.3**.

3.3.6 Statistical analyses

All data was analyzed using R (R Foundation for Statistical Computing). For categorical variables, data was analyzed using the Mann-Whitney test in the case of two groups; for more than two groups, analyses were carried out using the Kruskal-Wallis test for overall comparison and Dunn test for pairwise comparison (with the use of the R package `dunn.test`), with Benjamini-Hochberg (False Discovery Rate) correction method for multiple testing. For comparisons of two continuous variables, data were analyzed by Pearson correlation. Test results were considered significant when $p < 0.05$. For correlations, data were considered biologically meaningful if the absolute value of the correlation value was > 0.5 .

3.4 RESULTS

3.4.1 IL-36 γ is detected in the immune and vascular compartments in the TME

We first used immunohistochemical staining to identify and localize IL-36 γ ⁺ cells within patient colon carcinoma primary tumors. IL-36 γ was detected on a variety of cell types in the TME, including immune cells (**Figure 3.1A**), tumor cells (**Figure 3.1B**) and vascular/perivascular cells (**Figure 3.1C and 3.1D**). We noted that within the vascular compartment, both smooth muscle cells (SMC; **Figure 3.1C**) and vascular endothelial cells (VEC; **Figure 3.1D**, indicated by an arrow and inset) were IL-36 γ positive, though coordinate detection in the same vessel was uncommon. Instead, SMC surrounding large vessels, and VEC of smaller vessels, were found to be IL-36 γ ⁺. We did not observe significant differences in IL-36 γ expression between tumors with MSI versus MSS microsatellite status (data not shown).

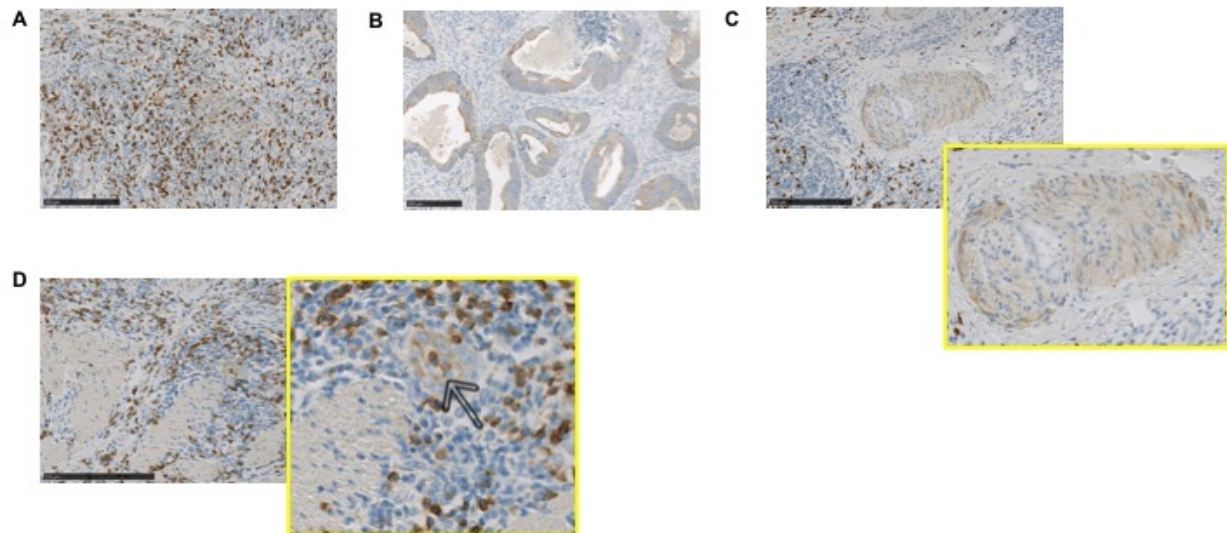


Figure 3.1. IL-36 γ is expressed by a variety of cell populations in the TME.

FFPE tumor sections were stained for IL-36 γ by IHC as described in Materials and Methods for expression of IL-36 γ . Expression of this protein was observed in immune cells (**A**), tumor cells (**B**), and cells of the vasculature (**C**, **D**). Of note, both smooth muscle (**C**) and endothelial cells (**D**) of the vasculature were observed to express IL-36 γ . Bars = 250 microns.

To further investigate the distinct subtypes of immune cells expressing IL-36 γ in the TME, we analyzed transcriptomic data of purified immune cell populations from MCP-transcriptomes of 81 public data sets (**Figure 3.2**). *IL36G* was found to have a higher transcription level in activated macrophages, also referred to as classically-activated or M1 macrophages, than in all other immune cell types, including “alternatively activated”

M2 macrophages (log2-fold change versus other cells 5.35, see Materials and Methods). The two other IL-36 γ transcript positive cell types - dermal DCs and Langerhans cells - are found in other organs than the colon. Immunofluorescence imaging showed that CD68+ macrophages are capable of expressing IL-36 γ protein within the colorectal cancer TME (**Figure 3.3A**). After quantitation, it was determined that 40.4% of CD68+ cells in the TC and 38.7% in the IM of tumors expressed IL-36 γ (**Figure 3.3B**).

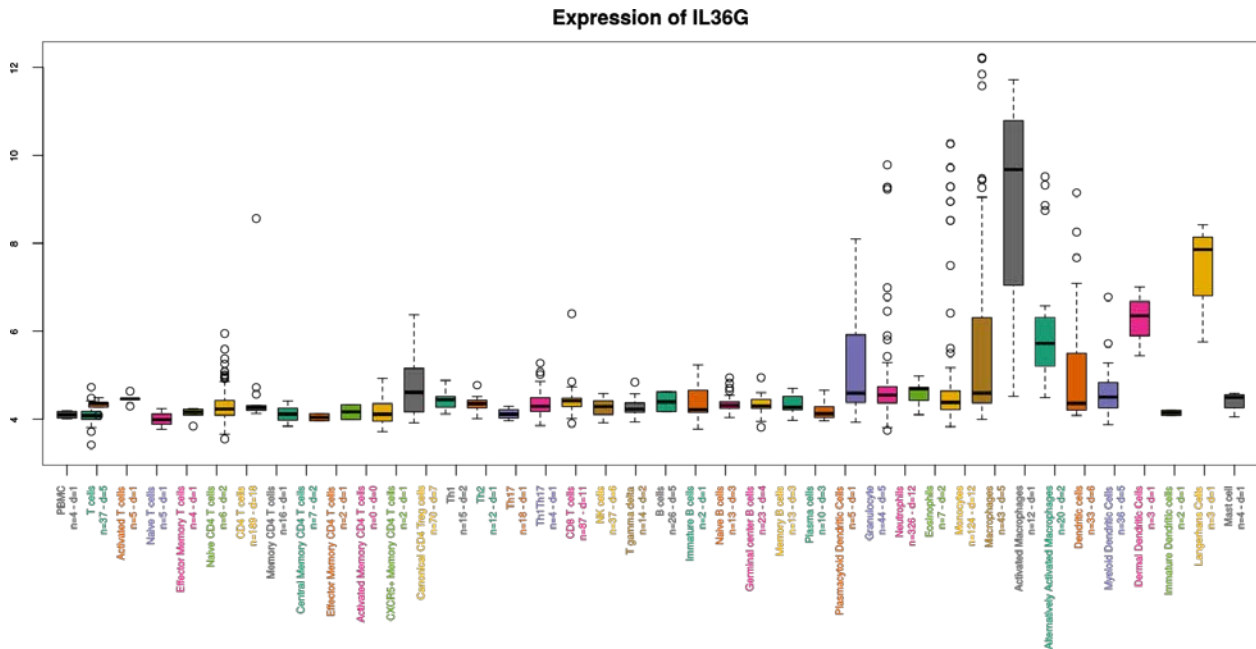


Figure 3.2. M1 macrophages express high levels of IL-36 γ .

Affymetrix microarray data from the Gene Expression Omnibus (GSE39582) was analyzed for expression of *IL36G* in various human immune cell subsets. Data are presented on a log₂ scale. Results indicate an elevated level of *IL36G* expression by activated M1 macrophages compared to the median expression by all other cell types.

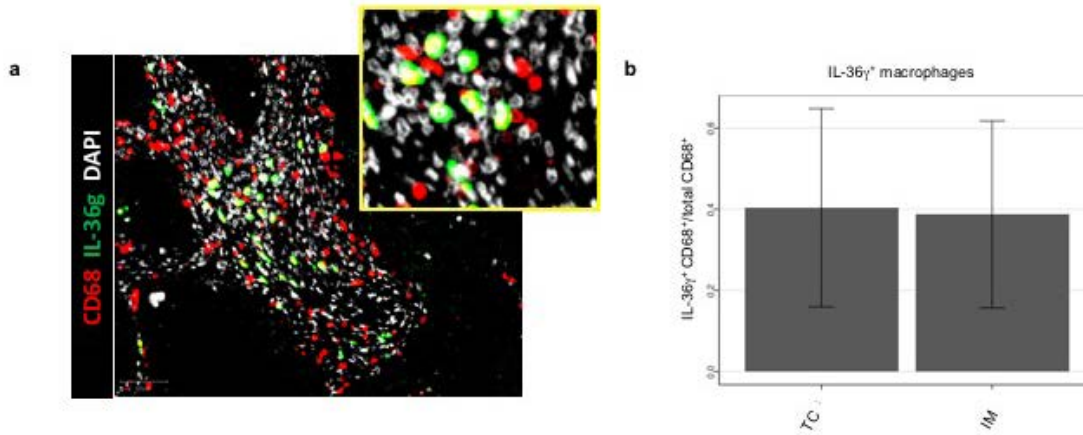


Figure 3.3. Intratumoral macrophages are a source of local IL-36 γ .

IL-36 γ was visualized by immunofluorescence imaging in conjunction CD68⁺ macrophages (A). Bars = 50 microns. Data were analyzed as described in Materials and Methods, and the average frequency of IL-36 γ ⁺ macrophages in both the TC and IM is presented in B.

3.4.2 IL-36 γ expression by macrophages is associated with markers of inflammation

We next investigated whether a correlation could be made between IL-36 γ expression by macrophages and other previously established prognostic markers for patients with

colon cancer, using a prospective cohort of 33 primary tumors. In particular, we were interested in determining whether IL-36 γ ⁺ macrophages were linked to a fibroblastic signature within the TME and/or to a strong intratumoral Type-1 immune response.

Alpha-smooth muscle actin (SMA) was used to detect cancer associated fibroblasts by IHC grading, as described in Materials and Methods (291). In this cohort, 15% (5/33) of tumors were classified as SMA grade 1, 27% (9/33) were grade 2, 42% (14/33) were grade 3, and 15% (5/33) were grade 4. As shown in **Figure 3.4A**, tumor-associated macrophages located in the TC were positively correlated with an increase in SMA grade. When just the IL-36 γ ⁺ macrophage subset was analyzed, this correlation became stronger in the TC, with a similar correlation noted in the IM. IFM imaging suggested a close contact between (IL-36 γ ⁺) macrophages and SMA⁺ cells in the TME (**Figure 3.4B**). TIL subsets were phenotyped by flow cytometric analysis of T cells isolated from fresh tissues. We identified four subsets each of CD4⁺ and CD8⁺ T cells: naïve (CCR7⁺ CD45RA⁺), effector memory (TEM; CCR7⁻ CD45RA⁻), central memory (TCM; CCR7⁺ CD45RA⁻), and effector memory RA (TEMRA; CCR7⁻ CD45RA⁺) (**Table 3.2**) (289). We found a positive correlation between CD4⁺ central memory T cells (**Figure S3.2**) and macrophages in the TC ($r = 0.574$ and $p = 0.000923$; **Figure 3.4C**), but not the IM (data not shown). When just the IL-36 γ ⁺ macrophage subset in the TC was studied, the correlation with CD4⁺ TCM was improved ($r = 0.608$ and $p = 0.000364$; **Figure 3.4D**). We also analyzed the expression of immune genes (**Table S3.3**) in whole tumor samples, and the gene expression studies showing negative correlation between CD4⁺ TCM and the *CSF1R* transcript, a marker of immunosuppressive M2 macrophages ($p = 0.044$; **Figure 3.4E**) confirmed these data. No significant correlations were found between IL-36 γ ⁺ macrophages in the TC and any other naïve or memory CD4⁺ or CD8⁺ TIL subsets (**Figure S3.3**). Thus, it appears that IL-36 γ ⁺ macrophages are associated with both an increased fibroblastic signature – a negative prognostic marker – and a memory/Type-1 immune response – a positive prognostic marker in the setting of colorectal cancer.

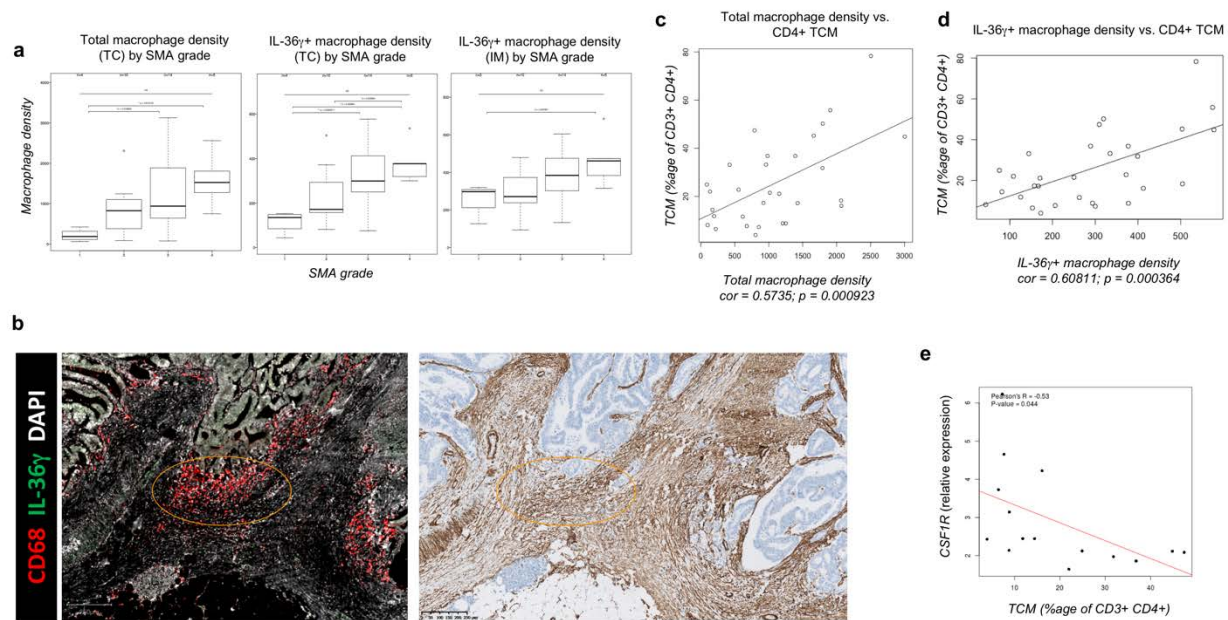


Figure 3.4. IL-36 γ ⁺ macrophages are associated with a proinflammatory TME.

FFPE tumor sections were visualized by IHC for expression of alpha-SMA or by immunofluorescence for IL-36 γ ⁺ CD68⁺ macrophages. A positive correlation between increased alpha-SMA grade and intratumoral density of IL-36 γ ⁺ macrophages is shown in **A**. In **B**, tumors were visualized either by immunofluorescence for CD68 and IL-36 γ (left panel) or by IHC for alpha-SMA (right panel). CD68⁺ macrophages and alpha-SMA⁺ cells were observed in close contact with each other within the TME. Bar = 250 microns. We also investigated the relationship between macrophages and CD4⁺ central memory T cells in tumors. We report that the overall density of macrophages is positively correlated with the presence of CD4⁺ central memory T cells in tumors (**C**), but that the strength of this correlation is increased when just the IL-36 γ ⁺ macrophage subset is analyzed (**D**). Furthermore, the presence of CD4⁺ central memory T cell infiltrate is inversely correlated with the expression of *CSF1R*, a biomarker of M2 macrophages (**E**).

3.4.3 The predominant IL-36 γ -expressing cells in TLS are HEV-associated VEC

CD4⁺ TCM have been reportedly found primarily in TLS (aka tertiary lymphoid organs or ectopic lymphoid-like structures) within the confines of human tumors (45). Since IL-36 γ expression was correlated with CD4⁺ TCM, we next investigated TLS in the colorectal cancer TME, using the B cell marker CD20. Indeed, we found a series of dense CD20⁺ aggregates in tumors from this patient cohort, with most being located in the IM (**Figure 3.5A**). TLS can also be marked by the presence of peripheral node addressin (PNAd)⁺ HEV (**Figure 3.5B**), i.e. specialized CD31⁺ VEC involved in the recruitment of CD62L/L-selectin⁺ naïve or central memory lymphocytes from the peripheral blood circulation. We next investigated the expression of IL-36 γ within these structures. We found that IL-36 γ was principally expressed on HEV themselves, with minimal expression by the constituent immune cells or by “normal” CD31⁺ PNAd⁻ VEC (n = 7; **Figure 3.5B**). Since IL-36 γ has not been reported by other groups to be expressed by the vasculature, we next sought to further investigate this pattern of expression.

3.4.4 IL-36 γ expression on the vasculature is associated with maintenance of TLS structures

To investigate vascular expression of IL-36 γ , we divided our cohort into two groups: patients with IL-36 γ expression on any vessels in the tumor (i.e., including HEV or arteries, n = 21), and those devoid of IL-36 γ expression in vascular structures (n = 12). Within these cohorts, we then analyzed tissues for correlations between vascular expression of IL-36 γ and immune cell infiltrate into the tumors. We observed that in the IM, the density of CD20⁺ B cells in the TLS of patients with IL-36 γ ⁺ blood vessels was

significantly higher than in patients without any IL-36 γ ⁺ vessels ($p=0.00879$; **Figure 3.5C**). We did not discern a significant correlation between IL-36 γ expression on blood vessels and the density of intratumoral B cells outside of TLS ($p=0.829$; **Figure 3.5D**) or absolute numbers of TLS within tumors (data not shown). These data suggest that IL-36 γ expression on the vasculature may be involved in the maintenance of TLS in the TME. A larger cohort of patients presenting with TLS will be required to parse the effects of HEV versus vasculature outside of TLS.

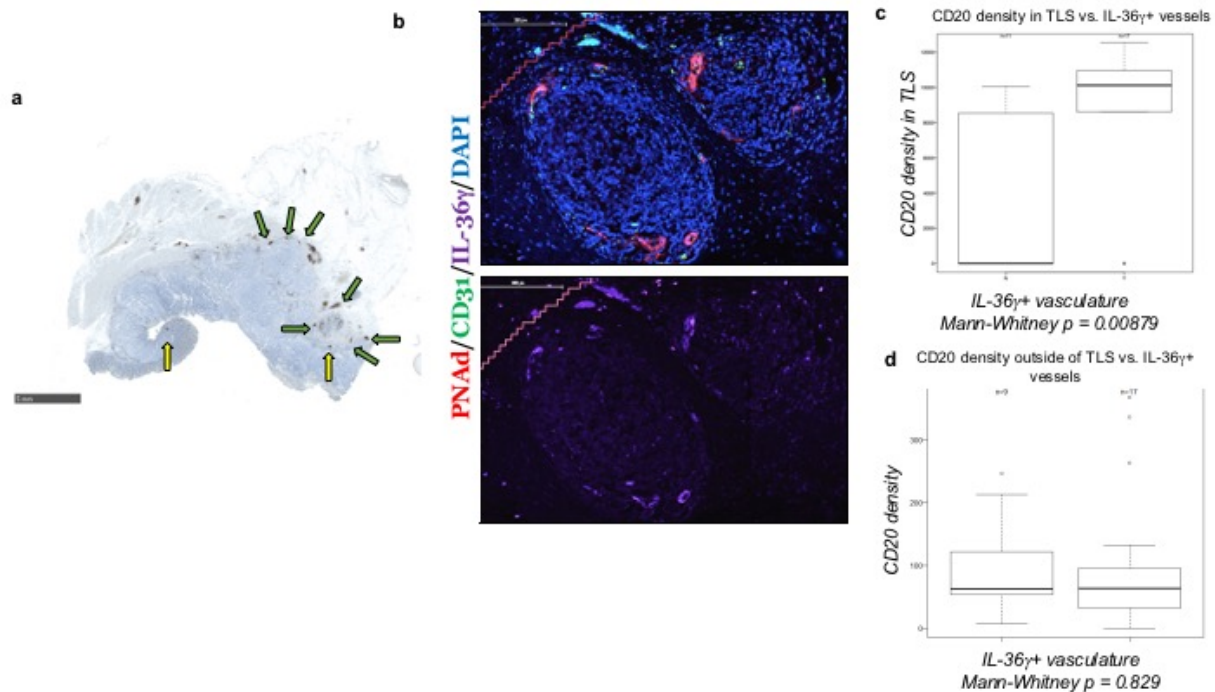


Figure 3.5. Expression of CD20 suggests presence of TLS in colorectal tumors.

FFPE tumors were visualized by IHC for the presence of CD20 (**A**), a B cell marker used to identify TLS. TLS in the IM are annotated with green arrows; TLS in the TC are marked by yellow arrows. Tumor sections were probed with antibodies against CD31

and PNA_d to identify HEV, together with an antibody reactive against IL-36 γ (**B**). Bars = 5 mm in panel A and 200 microns in panel B. Following the observation that HEV were the primary cell type expressing IL-36 γ within TLS, we noted that IL-36 γ expression on the vasculature correlated with an increased density of B cells within TLS (**C**), but not outside of these structures (**D**) within the TME.

3.4.5 IL-1F5 expression in the TME is associated with immunosuppressive markers

Tissue expression of IL-1F5 (aka IL-36RA), the natural antagonist to the IL-36 receptor, was probed using IHC to investigate whether this negative regulatory member of the IL-36R signaling pathway might be associated with suppression of either TIL function or TLS organization in our cohort. IL-1F5 expression was found on the tumor vasculature (**Figure 3.6A**) as well as vasculature in the tonsil, a secondary lymphoid organ (**Figure S3.4**). The density of B cells in IM-localized TLS was not significantly different in tumors whether blood vessels expressed IL-1F5 or not (**Figure 3.6B**). We next investigated whether the presence of intratumoral IL-1F5 correlated with other markers of the TME as detected by transcriptome analysis. IL-1F5 (but not IL-36 γ) expression in the IM of tumors was found to be positively-correlated with local expression of the *PDCD1* (i.e. PD-1), *CTLA4*, and *CD274* (PD-L1) immune checkpoint markers, but not with expression of *LAG3*, *ICOS*, or *ICOSL* (**Figure S3.5**).

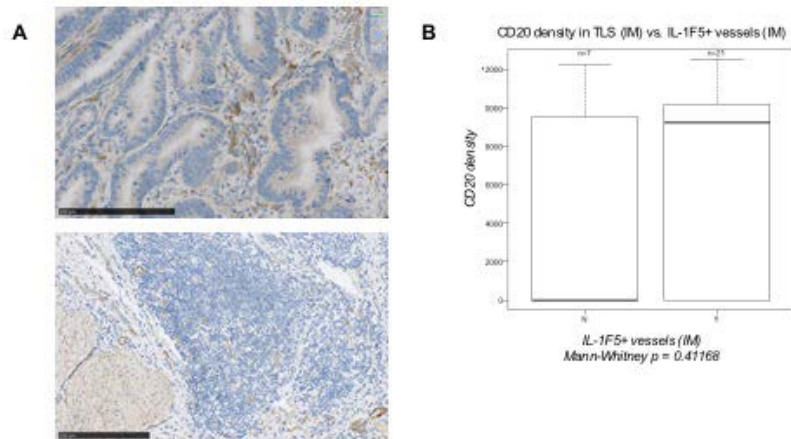


Figure 3.6. Presence of the IL-36 receptor antagonist, IL-1F5, is not correlated with the density of CD20⁺ B cells in TLS.

FFPE tumor sections were visualized by IHC for expression of IL-1F5, the natural antagonist to the IL-36 receptor. Like IL-36 γ , IL-1F5 was observed to be expressed on the tumor vasculature (**A**). Bars = 250 microns. When the intensity of IL-1F5 expression was correlated with the density of B cells in TLS within colon carcinoma lesions, no significant relationship was observed (**B**).

3.5 DISCUSSION

In this study, we report a link between intratumoral expression of IL-36 γ and markers of an ongoing anti-tumor immune response in the TME. IL-36 γ ⁺ macrophage density was

found to correlate with CD4⁺ TCM frequency in TILs. CD4⁺ TCM infiltrate was also associated with a decreased M2 macrophage marker in the TME. In human lung (45) and breast cancer (180) cancers, CD4⁺ TCM have been reported to be found predominantly within tumor-associated TLS. The presence of TLS within the TME has been associated with an ongoing local anti-tumor immune response (284). It has previously been reported as a positive prognostic marker in colorectal cancer (41,177,183), with TLS most commonly identified by dense aggregates of CD20⁺ B cells resembling the germinal centers found in lymph nodes (47).

Our studies also suggest a link between IL-36 γ ⁺ macrophages and SMA grade in our tumors. In colorectal cancer, the grade of SMA is associated with poor progression-free and overall survival rates (283,291). In the setting of esophageal squamous cell carcinoma, expression of fibroblast-associated genes, including SMA, are associated with poor overall and progression-free survival (292). In this latter study, the authors observed that increased prevalence of tumor-infiltrating macrophages was associated with an increased fibroblast signature and poor prognosis. Thus, we would predict that SMA grade 4 patients are most likely to also exhibit robust IL-36 γ ⁺ macrophage infiltrates and Type-1 pro-inflammatory/anti-tumor immune responses. Indeed, it has previously been reported in a murine model of atherosclerosis that M1 macrophages can act indirectly as lymphoid tissue inducer cells that lead to the formation of TLS by the secretion of chemokines and cytokines that act on SMA⁺ vascular smooth muscle cells and convey a lymphoid tissue organizer phenotype onto these cells (293). Further studies should investigate a role for IL-36 γ ⁺ macrophages in TLS organization in the TME, and whether cancer patients with a high IL-36 γ ⁺ macrophage or TLS signature have a better prognostic outcome than their counterparts lacking these specific immune infiltrates.

Release of IL-36 γ in IBD and colitis leads to IL-36R-mediated signaling in colonic fibroblasts and to secondary production of chemokines/cytokines (i.e. GM-CSF, CCL1, CCL2) known to recruit and differentiate monocytes/macrophages (201), and IL-36 γ treatment has been shown in *in vitro* models to lead to the secretion of chemokines

including CXCL1, CXCL2, and CXCL8 by myofibroblasts (294). Furthermore, IL-36R signaling promotes healing of the mucosa following damage. These results are consistent with our current findings suggesting a positive correlation between IL-36 γ ⁺ macrophages and SMA in the TME. Notably, fibrosis is a mechanism involved with the healing of damaged tissues (295), and tumors have long been referred to as “wounds that do not heal” (296). One might therefore anticipate that signaling through the IL-36R on colonic fibroblasts could coordinately promote macrophage recruitment and mucosal healing mechanisms that drive local fibrosis. However, in the context of cancer, fibrosis is classically viewed as a promoter of disease progression (297). In addition to fibroblasts, a common cell type involved with the progression of fibrosis is the myofibroblast (298). Interestingly, IL-36 γ can be intrinsically expressed by colonic myofibroblasts as a consequence of IL-1 β -induced signaling (214). Furthermore, IL-1 β is a key cytokine in the transition of stromal cells including fibroblasts, smooth muscle cells, and pericytes to become myofibroblasts (299). Together, these results suggest that in addition to the IL-36 γ ⁺ SMA⁺ cells within the tumor that were determined by pathologic characterization to be muscle fibers (**Figure 3.2C**), a portion of the IL-36 γ ⁺ SMA⁺ cells may represent mature myofibroblasts. Since myofibroblasts have been reported to facilitate metastasis of colorectal cancer (300), future studies should investigate the relationship between intratumoral patterns of IL-36 γ expression and colon carcinoma progression and metastasis. Such studies should also include analyses of IL-36 α , another agonist of IL-36R, that has been reported to independently predict increased overall survival amongst patients with colorectal cancer (301).

To the best of our knowledge, we are the first to characterize expression of IL-36 γ by cells of the tumor-associated vasculature, with this cytokine found located on vascular endothelial cells in HEV and on SMC surrounding large blood vessels. Signaling through the IL-36R on VEC can result in upregulated expression of VCAM-1 and ICAM-1 and the production of chemokines, such as IL-8, CCL2, and CCL20 (282). Following stimulation of with IL-36 γ , T cells exhibit increased migratory capability towards VEC (282). These data suggest that the vascular endothelial cells of HEV may be able to both produce and respond to IL-36 γ in an autocrine manner, a phenomenon which has

previously been shown to occur in myeloid cells (221,228,302). Thus, a positive feedback signaling mechanism may increase the “recruiting” capacity of IL-36 γ ⁺ HEV for protective/therapeutic immune cell populations into existing TLS, either from the periphery or from elsewhere within colorectal cancer lesions.

In conclusion, our findings support a role for macrophage- and VEC-produced IL-36 γ in recruiting and maintaining intratumoral immune responses, independent of other factors known to promote anti-tumor immunity. The promotion of a memory T cell response and the maintenance of TLS are both predictors of a positive prognosis in colorectal cancer and are both associated with increased IL-36 γ production within the TME. In line with these findings, tumors presenting with elevated levels of the IL-36 receptor antagonist, IL-1F5, generally express less IL-36 γ (data not shown) and were observed to have lower levels of central memory T cell infiltrates and lower densities of intratumoral B cells. IL-1F5 expression also was associated with elevated levels of the immune checkpoint molecules PD-1, PD-L1, and CTLA4 in the TME. In other studies, expression of IL-1F5 has been associated with a poor prognosis in colorectal cancer (303). Because IL-36 γ has a higher binding affinity for the IL-36R than does IL-1F5 (220), administration of an IL-36 γ -based therapy would be expected to at least partially reverse the inhibition mediated by endogenous IL-1F5, leading to enhanced tumor infiltration by beneficial immune cell populations. Because of the correlation between IL-1F5 expression and an upregulation of immune checkpoint molecules, the co-application of an IL-36 γ -based therapy with checkpoint blockade would be expected to also enhance the anti-tumor efficacy of these treatments.

Future studies should determine whether the presence of IL-36 γ in the TME is predictive of superior response to immunotherapeutic intervention. Available data (304) suggests that a high level of expression of IL-36 γ in the tumor microenvironment of several types of human tumors is associated with an increase in overall survival, though this does not reach statistical significance (**Figure S3.6**). Based on the data presented in our studies, we predict that analyzing intratumoral cell type-specific expression of IL-36 γ will prove to be a more robust prognostic marker of survival than expression by bulk tumor.

3.6 ADDITIONAL SUPPORTING INFORMATION

3.6.1 Materials and Methods

Bone marrow cells were collected from the tibias/femurs of C57BL/6 mice and cultured for 7 days in macrophage complete media (DMEM supplemented with 10% FCS, 10% L-929 supernatant (a generous gift from Dr. Bryan Brown, Elizabeth Stahl, and Samuel LoPresti, University of Pittsburgh), 2% MEM non-essential amino acids (Gibco), 1% 1M HEPES buffer (Gibco), 100 mg/mL streptomycin, 100 U/mL penicillin, 10 mmol/L L-glutamine (all from Invitrogen), and 0.615 mM β -mercaptoethanol (Sigma)). On d7, polarization was induced by the addition of either 20 ng/mL rmIFN γ (Peprotech) + 100 ng/mL LPS (Sigma-Aldrich) (M1) or 20 ng/mL IL-4 (Peprotech) (M2) for 24h. To confirm macrophage derivation from bone marrow, cells were profiled by flow cytometry using an antibody against F4/80 (clone: BM8, eBioscience). To check M1 polarization, an IL-12p70 ELISA (BD Biosciences) was performed using cell-free supernatant collected on d8. Additionally, qPCR analysis was performed using primers listed in **Tables S2.1 and S3.4** to both confirm M2 polarization and determine the expression level of pro-inflammatory genes by macrophage subsets.

3.6.2 Murine M1 macrophages exhibit a TLS-promoting phenotype

Bone marrow precursor cells were cultured *in vitro* for 7 days in macrophage complete medium and then stimulated for 24h to induce polarization to an M1 (LPS + IFN γ) or M2 (IL-4) phenotype, or left unstimulated to generate M0. On day 8, macrophages were profiled by flow cytometry to validate F4/80 upregulated expression (**Figure 3.7A**). To confirm M1 polarization, cell-free supernatant from M0, M1, and M2 was analyzed by ELISA for secretion of IL-12p70, and results indicated that M1, but not M0 or M2 macrophages secreted high levels of the cytokine (**Figure 3.7B**). The polarization of M1 macrophages was further supported by qPCR analysis indicating an upregulation of *iNOS/NOS2* specifically in these cells (>10⁵-fold), while M2 polarization was confirmed by qPCR indicating an upregulation of *Arg1* (>500-fold), compared to M0 cells (**Figure 3.7C**). qPCR results also showed that M1, but not M2 macrophages express pro-inflammatory and TLS-inducing cytokines IL-1 β , TNF α , and LTA (but not LIGHT or CCL21, **Figure 3.7C**; or CCL19, data not shown). Concurrently, M1 macrophages also expressed elevated levels of the *IL36G* transcript (>25-fold; **Figure 3.7C**).

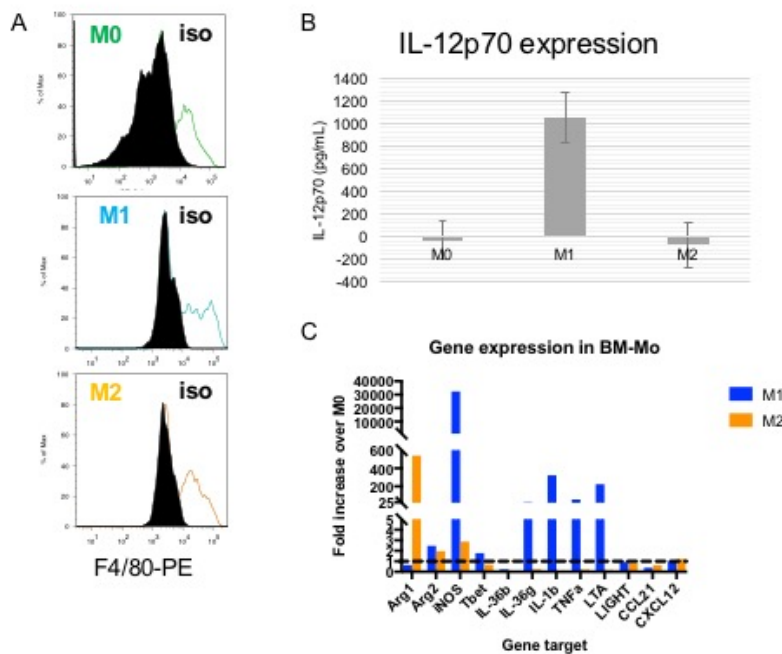


Figure 3.7. M1 macrophages express genes linked to the promotion of tertiary lymphoid organogenesis.

Following 7 days of differentiation and 24h of polarization, M0, M1, and M2 macrophages were profiled by flow cytometric analysis to check for upregulation of the macrophage lineage marker F4/80 (**A**). In **B**, M1 polarization was verified using an ELISA to measure secretion of IL-12p70 by each of the three subsets. M2 polarization was confirmed by qPCR analysis for high expression of *Arg1* and low expression of the M1 marker *iNOS* (**C**). Additionally in **C**, the expression of IL-36 γ , Tbet, and several TLS-associated genes, including TNF α , LTA, LIGHT, and CCL21 was evaluated to determine the potential capacity of M1 versus M2 macrophages to serve as initiators of TLS formation.

3.6.3 Interpretation

These data provide further support for IL-36 γ produced by M1 macrophages as having potential to drive inflammation in the TME, as we observed to be the case in human colorectal cancer. In an *in vitro* model, murine M1 (but not M2) macrophages upregulate numerous molecules known to be involved in tertiary lymphoid organogenesis and immune cell trafficking. Our findings are consistent with a report indicating that M1 macrophages can exhibit a lymphoid tissue organizer phenotype in atherosclerosis (293). Furthermore, these data suggest that therapeutic introduction of M1-polarized macrophages into the TME may confer a therapeutic benefit akin to that observed for intratumorally administered DC.IL-36 γ cells. The attenuation of the M2/tumor-associated macrophage (TAM) phenotype through targeting of *Arg1* (305) is another interventional

strategy by which macrophage skewing towards an M1 phenotype might be achieved for clinical benefit in the cancer setting.

While M1 macrophages exhibit a lymphoid tissue organizer-like phenotype, they also express high levels of iNOS/NOS2. iNOS is known to be immunosuppressive, and can even activate pathways that inhibit further M1 differentiation (306,307). Several groups have proposed that antagonizing iNOS in the TME potentiates the efficacy of existing cancer immunotherapies (308). In the case of iNOS^{hi} macrophages acting as lymphoid tissue inducer cells, however, it remains to be seen whether inhibition of iNOS can further increase the expression level of TLS-inducing genes or if it would adversely impact their expression by negatively affecting M1 polarization. Indeed, one study reports that NO prevents the repolarization of an M1 to M2 phenotype, while inhibition of nitric oxide production by M1 macrophages allows these cells to repolarize towards an M2 phenotype following stimulation with IL-4 (309).

4.0 DISCUSSION AND PERSPECTIVES

4.1 FURTHER DEFINING THE LINK BETWEEN IL-36 γ AND TBET

Previous studies have established Tbet as a driver of IL-36 γ expression in immune cells (197). In this study, we determine that in addition, IL-36 γ can induce expression of Tbet in target cells (**Figure 2.6**). Both (transduced) DC.IL-36 γ cells as well as splenocytes cultured in the presence of cell-free supernatant collected from DC.IL-36 γ cells upregulate expression of Tbet (**Figure 2.6**). These data indicate a positive feedback loop between Tbet and IL-36 γ that can potentiate Type-1 immune responses through the IL-36R. This is further supported by data from our gene array analyses indicating that DC.Tbet cells highly upregulate *IL36G* >100-fold (**Figure 2.1A**) and DC.IL-36 γ cells upregulate *Tbet* to the same magnitude (**Figure 2.6C**). Interestingly, IL-36 γ was shown to be present in the nucleus of DC.IL-36 γ cells (**Figure 2.6H**), similarly observed to occur with other IL-1 family members such as IL-1 α , IL-33, and IL-37 (200,208,310).

4.2 IL-36 γ IS A NOVEL DRIVER OF THE ANTI-TUMOR IMMUNE RESPONSE

The major component of this work investigated the function of IL-36 γ in the anti-tumor immune response. First, we build upon previous work showing the anti-tumor efficacy of DC.Tbet-based therapy (28) by identifying two novel but related roles for IL-36 γ in driving this response (35). IL-36 γ was identified as being highly upregulated in DC.Tbet cells as compared to mock transduced DC, so we generated DC.IL-36 γ cells and determined that production of IL-36 γ by injected DC is sufficient to drive delayed tumor progression, even in the absence of Tbet expression by these cells. Intratumoral injection of either DC.Tbet or DC.IL-36 γ , but not control DC. ψ 5 or DC.EGFP, cells into established MCA205 or MC38 tumors leads to the formation of intratumoral tertiary lymphoid structures by day 4-5 following treatment. Previous work has shown that the efficacy of DC.Tbet therapy is dependent on the presence of CD8⁺ T cells and NK cells (28); here, we elaborate on that requirement by showing that in Rag1^{-/-} animals, not only do tumors rapidly progress, but TLS do not form. This is in line with our data showing that the initial infiltration of immune cells into the TME occurs as early as 4 hours following the injection of DC.Tbet cells into the TME (**Figure 2.2**; i.e. at least 72 hours prior to the upregulation of PNA_d on tumor vasculature), supporting a role for this early T cell infiltrate in the formation of TLS. These data indicate a previously unreported requirement for adaptive immune cells in promoting TLS formation and suggest that the immune cells found within these structures is likely to be a mix of lymphoid tissue inducer-like cells present in the tissue before the formation of TLS, and cells recruited into established after the conversion of the local vasculature to an HEV phenotype. Further supporting the importance of TLS in mediating the anti-tumor immune response downstream of DC.Tbet- or DC.IL-36 γ -based therapy, and building upon previous data showing that injected DC.Tbet cells do not need to migrate to lymph nodes in order for the treatment to be effective (28), MCA205 tumors established in lymph node-deficient, LTA^{-/-} mice and treated with DC.Tbet exhibited delayed tumor progression not

significantly different from the rate of tumor growth observed in WT DC.Tbet-treated animals (**Figure 2.3**).

We also show that the drivers of TLS formation are similar between our model, other reports of TLS formation, and lymph node organogenesis. Indeed, LTA and LIGHT are highly upregulated in both DC.Tbet and DC.IL-36 γ cells and treated tumors, and upregulation of the T cell/DC chemoattractants CCL19 and CCL21 is observed in treated tumors as well (**Figures S2.2, S2.3, S2.6**). It appears likely that locally elevated concentrations of these molecules is specifically required for treatment efficacy and TLS formation, based on the data from tumors established and treated in LTA^{-/-} mice (**Figure 2.3**) and those treated with an LT β R-blocking antibody (**Figure 2.5B**).

Based on these findings, we have proposed a definition for non-classical TLS, which differ from classical TLS due to the lack of a B cell germinal center-like structure. Instead, we define TLS based on the close proximity of CD11c⁺ DC to PNA⁺ (CD31⁺) HEV, a phenotype that has also been observed in human tumors (15,37). These lymphoid aggregates also contain CD3⁺ T cells, in line with reports that TLS function as local sites of immune priming due to the close contact between antigen presenting cells (APC) and lymphocytes at the site of antigen presentation (311). Specifically, we report that the distance of T cells, B cells, and DC from HEV in TLS is consistent with that distance in lymph nodes (**Figure S2.7** and ref. (167)). This further supports the similarities between TLS and SLO in both structure and function. We also show that injected DC persist within TLS in DC.Tbet- and DC.IL-36 γ -treated tumors (**Figure 2.7B**), consistent with the previously reported mechanism of action of DC.Tbet cells requiring close contact with T cells to induce Type-1 immunity (266) and further supporting the definition of non-classical TLS as utilizing DC as the nucleating event.

4.3 ENDOGENOUS EXPRESSION OF IL-36 γ IS LINKED TO A PRO-INFLAMMATORY PROFILE

We next wanted to observe whether the presence of IL-36 γ in human colorectal carcinoma was linked to any of the same immune phenotypes observed in the MC38 murine model of colon carcinoma. Using a cohort of 33 primary colorectal carcinoma patients, we investigated the pattern of expression of IL-36 γ and its relationship to other markers of inflammation, including the memory T cell response, TLS, and fibroblast deposition. Within the immune compartment, IL-36 γ was observed to be primarily expressed by classically activated/M1 macrophages (**Figure 3.2**; something which we also confirmed in murine macrophages; **Figure 3.7**). This pattern of expression was positively correlated with an SMA⁺ fibroblastic signature within the TME as well as the infiltration of CD4⁺ TCM – a cell type linked to TLS presence in human tumors.

We are the first to report that IL-36 γ can also be expressed by cells of the vasculature, including vascular associated smooth muscle and endothelial cells, and HEV (**Figure 3.1C, 3.1D, and 3.5B**). Indeed, within TLS, IL-36 γ is predominantly expressed by the endothelial cells of HEV, and not the constituent immune cells or “normal” CD31⁺ PNA⁻ VEC. The expression of IL-36 γ by the vasculature is associated with an increased density of TLS-associated B cells.

These data link IL-36 γ to a pro-inflammatory and anti-tumoral response in the pathogenesis of human colorectal cancer. Further supporting this, IL-1F5, the antagonist to the IL-36R, is associated with markers of immunosuppression in the TME, including PD-1, CTLA4, and PD-L1. In our murine model, DC.IL-36 γ -based therapy led to decreased the expression of PD-1 and CTLA4 on the surface of intratumoral CD3⁺ T cells. These data suggest that IL-36 γ is dually important for reversing immune suppression in the TME, both by directly downregulating markers of T cell exhaustion and preventing IL-1F5 binding to the IL-36R and blocking agonistic signaling events.

4.4 PERSPECTIVES

4.4.1 The biologic function of IL-36 γ

DC.IL-36 γ cells are engineered to express the truncated, bioactive form of IL-36 γ (192), which is widely thought to be its secreted form. While reports indicate that pyroptotic cell death via a Caspase-1 and 3/7-mediated mechanism, neutrophil elastase, and proteinase-3 are each capable of cleaving this cytokine (195,312) it remains unclear how IL-36 γ is either secreted from or trafficked within a cell as like the other IL-1 family cytokines, IL-36 γ lacks both a defined nuclear localization signal and a canonical cleavage site. Therefore, subsequent work should investigate the regulation of IL-36 γ trafficking and specific roles of intranuclear versus secreted IL-36 γ , in order to better understand the diverse biologic functions of this cytokine. It has also not been investigated whether IL-36 γ is capable of trafficking into the nucleus in immune cell types other than DC, and if so, whether it is involved in the activation of the same or different genes across cell types.

Data from these studies also indicates that signaling through IL-36R on host cells, likely those of the stroma or vasculature, is required for the anti-tumor efficacy of DC.IL-36 γ -based therapy (**Figure 2.7**). Preliminary data suggests that not only is this signaling

event required for therapeutic benefit, but removal of other sources of the IL-36R in the TME, that may act as “sinks” for IL-36 γ , augments the benefit conferred by i.t. delivery of DC.IL-36 γ . Specifically, we noted that DC.IL-36 γ generated from IL-36R-deficient animals and delivered i.t. into MC38 tumor-bearing WT hosts delayed the rate of tumor growth to a greater extent than delivery of WT DC.IL-36 γ (**Figure S4.1**). Thus, it appears that although a feed-forward loop propagating IL-36 γ expression by injected DC is likely to occur in the WT system, this interaction may be at minimum unimportant and at most detrimental to the therapeutic potential of this therapeutic modality. Future studies should specifically investigate which cells in the TME require IL-36R expression for the optimal generation of an anti-tumor immune response.

4.4.2 Tertiary lymphoid structures

Tertiary lymphoid structures were first defined a decade ago in non-small cell lung cancer (15). Since then, they have emerged as a positive prognostic marker in nearly all types of primary human cancer (except for hepatocellular carcinoma; ref. (32)). Several groups have also used murine models to begin to better understand the mechanisms controlling the formation of TLS. Lymphotoxin signaling is known to be important in secondary lymphoid organogenesis; for the formation of TLS, lymphotoxin α_3 was shown to be the crucial signal of this pathway leading to TLS formation in murine models of lung cancer and melanoma (34,313), and this is not contradicted by our data showing an upregulation of LTA in DC.Tbet and DC.IL-36 γ cells and treated sarcomas and colon carcinomas. Subsequent studies should investigate whether there is a mechanistic relationship between IL-36 γ and LTA and/or LIGHT, the other lymphotoxin family member observed to be upregulated in these cells, to determine whether the paradigm mediating DC.Tbet- and DC.IL-36 γ -based therapeutic efficacy is in line with that observed by other groups. This will help to inform the design of future immunotherapies by being able to rationally target the downstream effector molecules

that are directly responsible for tertiary lymphoid organogenesis in different tumor subtypes. Similarly to the advance from using DC.Tbet to using DC.IL-36 γ therapeutically in order to bypass a transcription/translation step before the production of a secreted effector, it may be possible to directly introduce the chemokines/cytokines involved in immune cell recruitment and TLS formation, including the lymphotoxins, CCR7 agonists, or CXCL13, into the TME. This was previously shown to be effective when LIGHT was therapeutically introduced into the TME (94,98,314,315), but has yet to be investigated for other lymphoid tissue-inducing signals.

In human colorectal cancer, we observed that vascular expression of IL-36 γ is positively correlated with the density of CD20+ B cells in TLS. CXCL13 is the B cell homeostatic chemokine that is responsible for the chemotaxis and retention of B cells at lymphoid sites (80). While the precise link between IL-36 γ and CXCL13 has yet to be elucidated, it is possible that in human colorectal cancer, IL-36 γ is driving expression of CXCL13, which is in turn responsible for the observed density of intra-TLS B cells. In the murine MC38 model, ectopic overexpression of IL-36 γ in the TME is associated with a delayed (5 days) but >30-fold upregulation of intratumoral CXCL13 expression (**Figure S2.6**). In several other disease models, signaling via the CXCR5-CXCL13 axis is required for classical tertiary lymphoid organogenesis (316,317), such as what is observed in human colorectal cancer. Alternatively, LPS has been shown to drive expression of both IL-36 γ (e.g. **Figure 2.6F**) and CXCL13 (318); in the colon microenvironment, it is possible that bacterial LPS is stimulating the expression of these two molecules in parallel. However, LPS stimulation in colorectal cancer appears to drive a metastatic phenotype (319,320), and expression of CXCL13 has been associated with a poor prognosis and metastatic disease (136,321). The apparent dual functions of CXCL13 in colorectal cancer, and their link to IL-36 γ , should be reconciled in future studies.

4.4.3 Combination immunotherapy

Because of the relationship between signaling through the IL-36R and a decrease in immunosuppressive markers in the TME, there is also the potential for IL-36 γ -based therapy to be used in combination with established immunotherapies for cancer that also block the PD-1/PD-L1 and CTLA4 signaling pathways. Checkpoint blockade immunotherapies have shown clinical success over the past decade, with FDA approval for several of these drugs being awarded in recent years (322,323). In colorectal cancer, a subset of patients that bears a high mutational burden responds favorably to this kind of therapy (324), and several clinical trials are in progress to test the efficacy of anti-PD-(L)1 therapies in this disease (325); however, CRC overall remains extremely difficult to treat with checkpoint blockade therapies (326). The combination of an anti-PD-1, anti-PD-L1, or anti-CTLA4 antibody with an IL-36 γ -based therapy could confer a benefit to patients that currently do not respond to checkpoint blockade, as the addition of exogenous IL-36 γ should decrease the expression of immunosuppressive receptors on TIL while increasing the overall number of TIL within the TME (*i.e.* **Figure S2.5**) and promoting the formation of TLS. Conversely, one can think of combining an IL-36 γ -based therapy with checkpoint blockade immunotherapy as a means of shifting from a delay in the rate of tumor progression, as observed following treatment with DC:IL-36 γ (**Figure 2.7A**), to tumor regression by changing the phenotype of TIL recruited into the TME following the therapeutic introduction of IL-36 γ to a more effector-like and less exhausted phenotype.

However, in several immunotherapy trials, the prevalence of immune-related adverse events affecting the colon, as well as a lack of efficacy of checkpoint blockade immunotherapies in colon cancer, have been reported. One meta-analysis indicated that while the incidence of death following immune checkpoint blockade therapy across a variety of tumor types was low, colon-associated adverse events, including colitis, diarrhea, and bowel perforation, were often linked to mortality (327). In a Phase II study of the anti-CTLA4 antibody tremelimumab in colorectal cancer, the study results indicated no significant improvement of patient outcome following treatment, with 11% of patients presenting with grade 3/4 diarrhea, and 2% with grade 3/4 ulcerative colitis (328). Anti-PD-1 therapy has, as well, not conferred an objective response to colorectal

cancer patients in the clinic, despite the expression of PD-L1 by tumor cells (329). Thus, it will remain important to strike a balance between developing combinatorial strategies to improve the efficacy of checkpoint blockade therapies and preventing serious immune-related adverse events, especially when treating disease burden in the colon.

4.4.4 Alternative means of therapeutically introducing IL-36 γ into the TME

In these studies, we therapeutically introduce IL-36 γ into the TME using DC engineered to ectopically overexpress IL-36 γ . While this model has some advantages, including the delivery of additional DC into the TME which can then serve as the nucleating event leading to the formation of TLS, other delivery mechanisms may be more advantageous for clinical use. Indeed, we have observed that introducing IL-36 γ into the TME of established MC38 tumors either via direct injection of IL-36 γ protein into tumor lesions (data not shown) or by transducing the tumor cells themselves to ectopically overexpress IL-36 γ can also delay the growth of the tumor (223). Thus, cell-free delivery of IL-36 γ into the TME is a mechanism that warrants further investigation.

Additionally, several signaling pathways can induce IL-36 γ expression by APC. The most well-characterized signals leading to IL-36 γ expression are the agonists to TLR3, TLR4, TLR7, and TLR9 (213,330–332); in our studies, the highest level of IL-36 γ secretion was observed following TLR7 stimulation (**Figure 2.6F**). Several TLR agonists have been tested therapeutically in animal models of tumors. Imiquimod, a TLR7/8 agonist that has been shown to induce IL-36 γ expression by keratinocytes (229), can also activate plasmacytoid DC to destroy melanoma tumors (333,334). A TLR2/4 agonist has been shown in a murine model of lymphoma to polarize DC towards a Type-1 phenotype and function as an adjuvant in combination with autologous DC and antigen to delay tumor progression (335).

STING agonism also leads to IL-36 γ expression by target cells. Ongoing work in our laboratory seeks to investigate whether therapeutic introduction of STING agonists (e.g. dsDNA or analogues) into the TME causes tumor regression by the same TLS-inducing mechanism as does DC.IL-36 γ treatment. Our preliminary data suggests that treatment of BMDC with STING agonists leads to production of IL-36 γ by target cells that is comparable to DC.IL-36 γ cells (data not shown). Therapeutic STING agonism has been shown in the preclinical MC38 and B16 models to cause the regression of established tumors (336,337). Tumors themselves can also agonize STING in the local milieu via the release of dsDNA that activates DC in the TME, and this is required for the control of tumor growth (338).

Multiple TLR and STING agonists are currently in clinical trials (reviewed in (339,340)). In the context of the data presented in our studies, it would be beneficial to evaluate whether IL-36 γ is upregulated in tumors treated with these therapies, as well as whether TLS formation might serve as a prognostic biomarker for the therapeutic efficacy of these agents.

Expression of IL-36 γ can also be induced by the cathelicidins LL-37 (in humans) and CRAMP (in mice) (198). In cancer, LL-37 appears to play a dual role as it can support tumor progression, metastasis, or apoptosis depending on the tissue type and magnitude of expression (341). In colon cancer, LL-37 may play an anti-tumorigenic role, by targeting cancer-associated fibroblasts and interrupting epithelial to mesenchymal transition (342), or a pro-tumorigenic role by activating the Wnt/ β -catenin pathway in tumor cells (343). While no clinical trials are currently in progress evaluating cathelicidin treatment in colon cancer, it is being studied in melanoma (344,345) Of note to this study, colonic fibroblasts can be IL-36R⁺, and signaling through the IL-36R promotes intestinal inflammation in a mouse model (201), suggesting that a possible secondary method of action for the anti-tumoral properties of cathelicidin treatment in colon cancer warrants further investigation.

4.4.5 Clinically relevant murine models

The murine studies described in this work used transplantable models of sarcoma and colon adenocarcinoma to evaluate the efficacy of DC.Tbet- and DC.IL-36 γ -based therapies. Using inducible or spontaneous tumor models can provide a more translational understanding of the benefit of (immuno)therapeutic interventions. These models can more closely mimic characteristics of human disease than transplantable models that take less time to establish (346), and the immunosuppressive microenvironment that develops over time in inducible or spontaneous models may be a useful trait for predicting the clinical efficacy of novel therapeutics; for example, *in vitro* studies of anti-CTLA4 antibodies show that this intervention appears to act at least in part by blocking the function of Tregs (347). Proteins expressed by tumors can also impact the immune microenvironment; for example, the addition of transgenic MUC1 expression to a spontaneous murine model of adenocarcinoma is associated with fibrosis and an increased CD4⁺ T cell infiltrate in the TME – more closely mimicking the phenotype of human adenocarcinomas – compared to MUC1⁻ models (348).

Modeling primary versus metastatic tumors in mice is another facet in better recapitulating the biology of progressive human tumors. In this regard, the success rate for anti-angiogenic therapies differs dramatically when comparing treatments applied to spontaneous versus experimental lung metastases of breast and colon cancers in murine models (349). Notably, bilateral tumor models or tumor rechallenge models following initial treatment can also be used to evaluate the ability of a therapeutic intervention to generate robust systemic effects that are durable (27,55).

APPENDIX A

SUPPLEMENTARY FIGURES

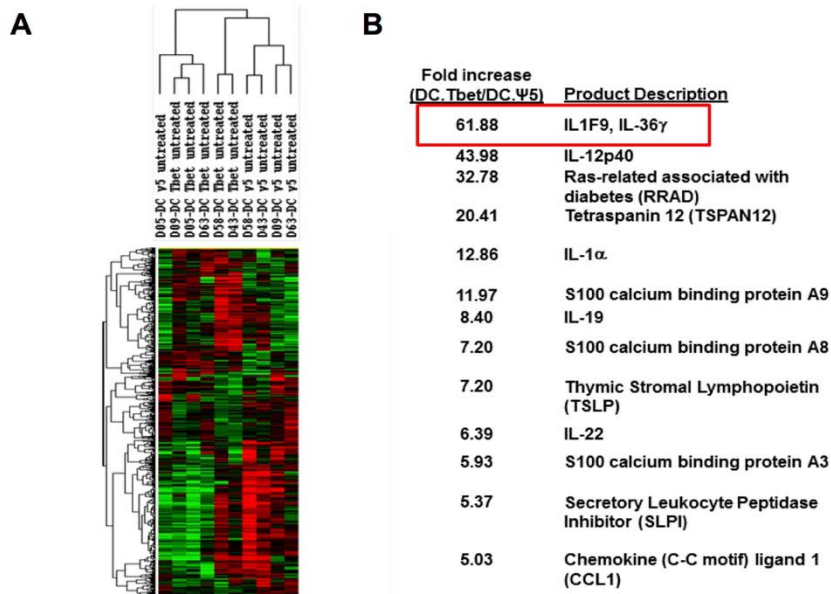


Figure S2.1. Human DC.Tbet cells upregulate expression of IL-36γ.

DC were isolated from human PBMC by lymphocyte depletion and infected for 48h with

rAd.hTbet or empty (control) vector rAd.ψ5 for 48h. Transduced DC (i.e. DC.ψ5 or DC.Tbet) were treated with 250 ng/mL IFN-γ and 10 μg/mL LPS, or left untreated, for an additional 24h. DC.ψ5 and DC.Tbet were then analyzed as described in Supplemental Methods. In **A**, a hierarchical clustering analysis of the 903 genes differentially expressed ($p < 0.01$) between DC.Tbet and DC.ψ5 depicted. In **B**, transcripts up-regulated > 5 fold in DC.Tbet versus DC.ψ5 are reported.

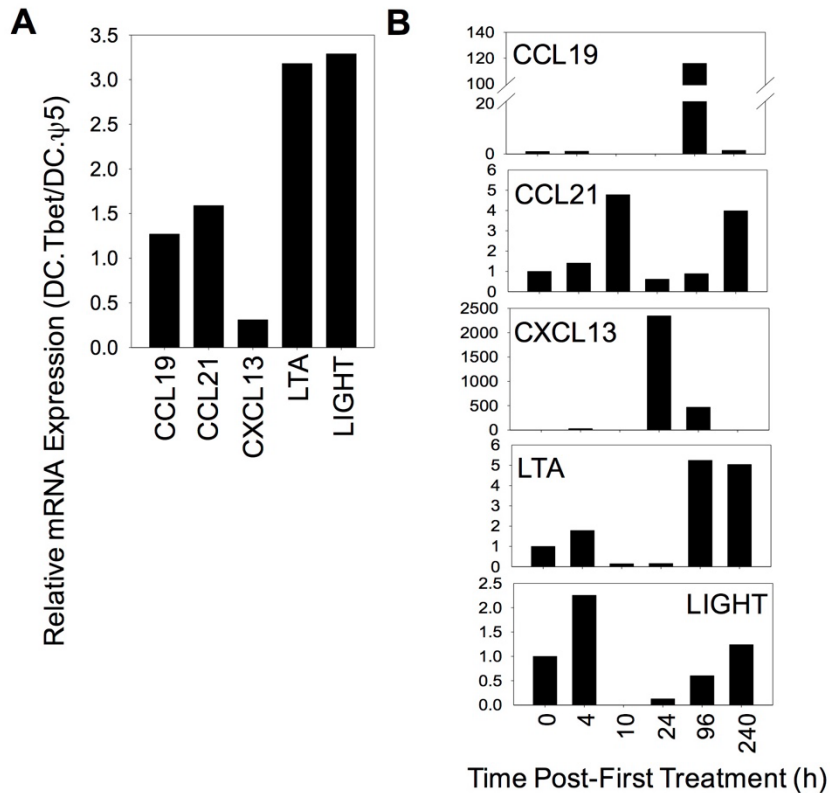


Figure S2.2. DC.mTbet express TLS-associated cytokines/chemokines and further potentiate their expression in the therapeutic TME.

In **A**, mRNA was extracted from DC.Tbet or control DC.ψ5 (48h after DC infection with rAd) and analyzed by real-time PCR for the indicated TLS-associated transcripts. In **B**, DC.Tbet or control DC.ψ5 were injected i.t. into established day 7 s.c. MCA205 sarcomas. At various time points after treatment, animals were euthanized and tumors isolated, with total mRNA extracted for subsequent real-time PCR analyses of TLS-associated transcript levels. Data are presented as the ratio of mRNA transcript levels between the DC.Tbet and control treated cohorts for each time point analyzed.

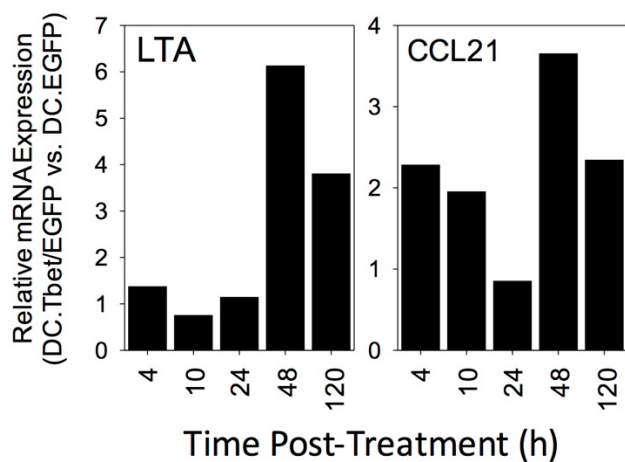


Figure S2.3. LTA and CCL21 are upregulated in DC.Tbet/EGFP- vs. DC.EGFP-treated tumors.

DC.Tbet/EGFP or control DC.EGFP were injected i.t. into established day 7 s.c. MC38 carcinomas. At various time points after treatment, animals were euthanized and tumors isolated, with total mRNA extracted for subsequent real-time PCR analyses of LTA and CCL21 transcript levels. Data are representative of those obtained in 2 independent experiments performed.

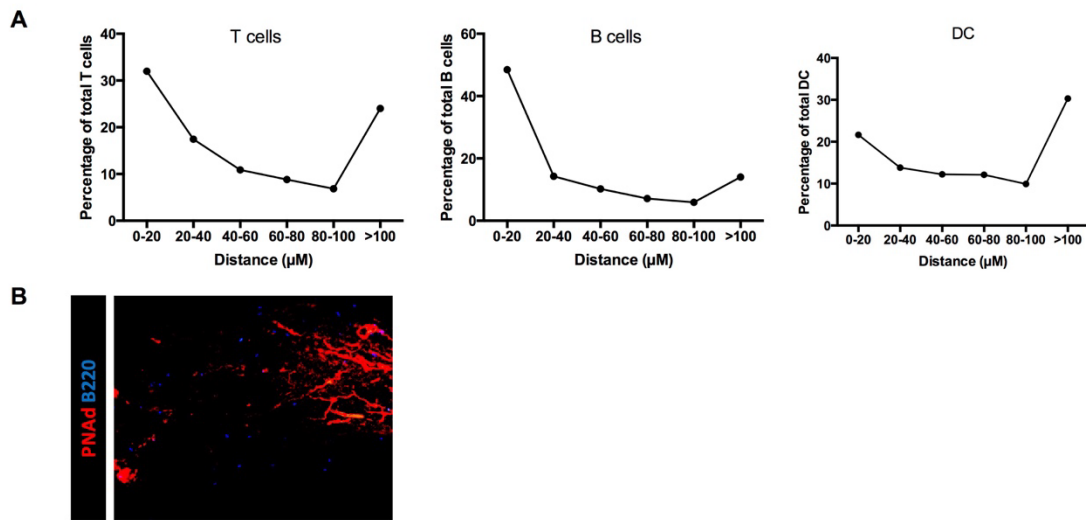


Figure S2.4. Lymphocytes in TLS functionally resemble HEV in SLO.

10^5 MC38 colon carcinoma cells were injected into the flanks of syngenic wild-type C57BL/6 mice and allowed to establish. Tumor-bearing mice were randomized into groups of 5 animals/cohort on day 7 post-implantation, with all cohorts exhibiting comparable mean tumor sizes. These animals were then treated on days 7 and 14 by i.t. injection of 10^6 control DC.EGFP or DC.Tbet/EGFP ($n = 5$ mice/group). Tumors were isolated on day 20 (i.e. 6 days post- 2^{nd} injection of DC) and analyzed for PNA $^+$ and T cells, DC, (A) or B cells (A, B). In A, the distance between each lymphocyte and the nearest PNA $^+$ HEV was measured using Euclidian distance analysis. In B, a representative immunofluorescence microscopy image showing B cells (B220) and HEV (PNA $^+$) is shown.

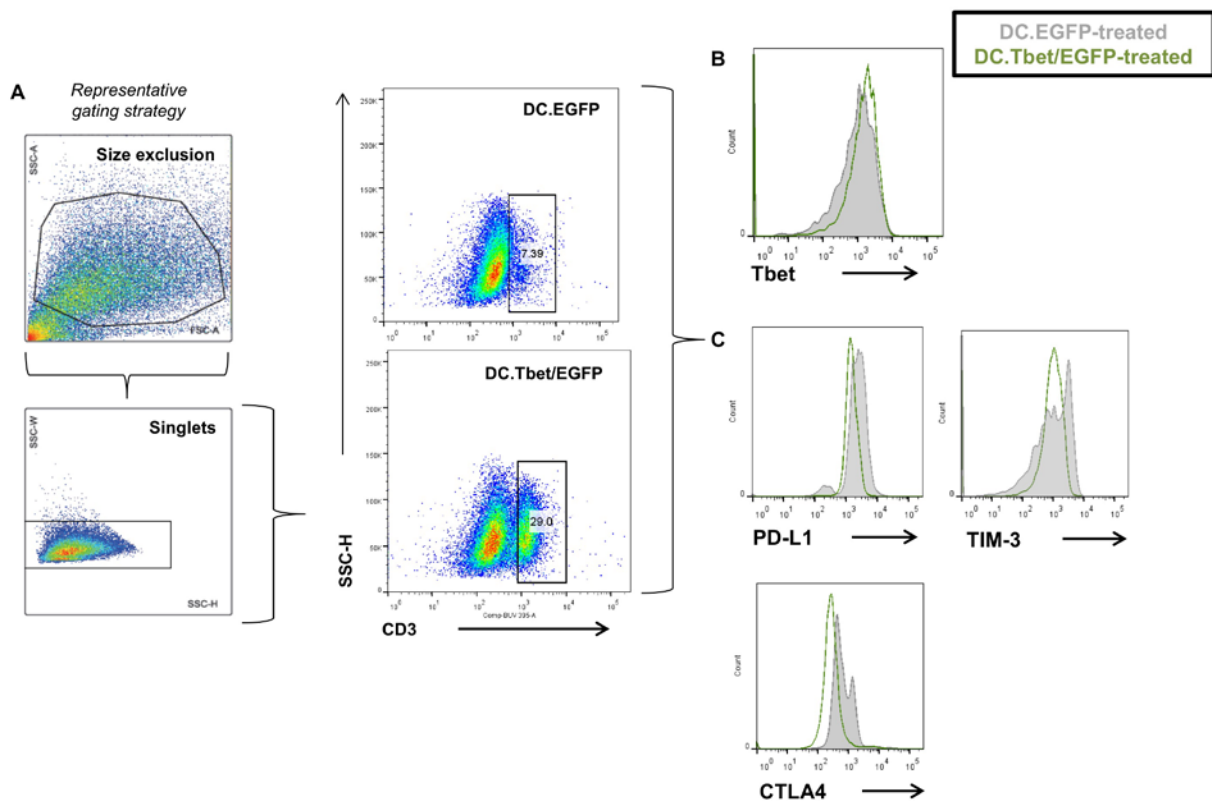


Figure S2.5. Phenotype of TIL from DC.Tbet/EGFP- versus DC.EGFP-treated tumors shows increased Type-1 functional polarity and decreased expression of exhaustion/nergic markers.

10^5 MC38 colon carcinoma cells were injected into the flanks of syngenic wild-type C57BL/6 mice and allowed to establish. Tumor-bearing mice were randomized into groups of 5 animals/cohort on day 7 post-implantation, with all cohorts exhibiting comparable mean tumor size. These animals were then treated on days 7 and 14 by i.t. injection of 10^6 control DC.EGFP or DC.Tbet/EGFP ($n = 5$ mice/group). On day 5 post-2nd injection of DC, tumors were isolated and subject to collagenase and DNase digestion, with single-cells analyzed by flow cytometry for expression of the indicated markers. In **A**, tumors were gated by FSC, SSC-A, SSC-H, and SSC-W, as shown. In **B** and **C**, plots were additionally gated on CD3+ T cells, as represented in **A**.

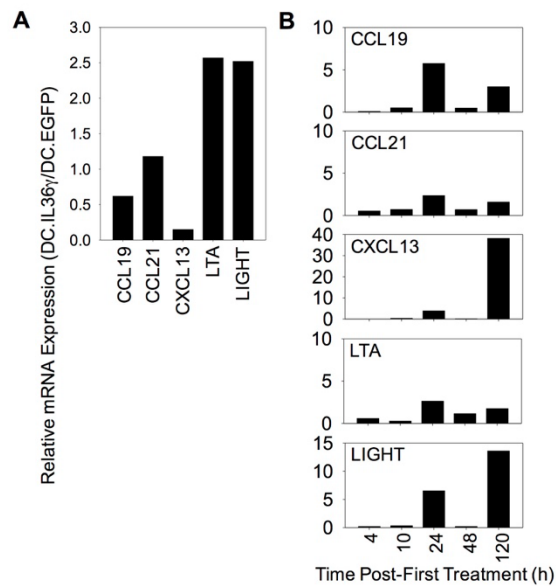


Figure S2.6. DC.IL-36 γ express TLS-associated cytokines/chemokines and further potentiate their expression in the therapeutic TME.

In **A**, mRNA was extracted from DC.IL-36 γ /EGFP or control DC.EGFP (48h after DC infection with rAd) and analyzed by real-time PCR for the indicated TLS-associated transcripts. In **B**, DC.IL-36 γ /EGFP or control DC.EGFP were injected i.t. into established day 7 s.c. MC38 colon carcinomas. At various time points after treatment, animals were euthanized and tumors isolated, with total mRNA extracted for subsequent real-time PCR analyses of TLS-associated transcript levels. Data are presented as the ratio of mRNA transcript levels between the DC.Tbet and control treated cohorts for each time point analyzed.

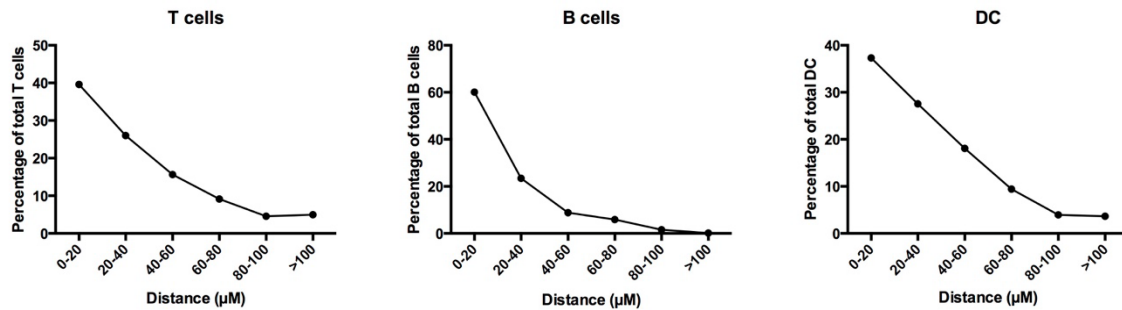


Figure S2.7. Lymphocytes in TLS functionally resemble HEV in SLO.

10^5 MC38 colon carcinoma cells were injected into the flanks of syngenic wild-type C57BL/6 mice and allowed to establish. Tumor-bearing mice were randomized into groups of 5 animals/cohort on day 7 post-implantation, with all cohorts exhibiting comparable mean tumor sizes. These animals were then treated on days 7 and 14 by i.t. injection of 10^6 control DC.EGFP or DC.IL-36 γ /EGFP (n = 5 mice/group). Tumors were isolated on day 20 (i.e. 6 days post-2nd injection of DC) and analyzed for PNA⁺ and T cells (left) or B cells (right). The distance between each lymphocyte and the nearest PNA⁺ HEV was measured using Euclidian distance analysis.

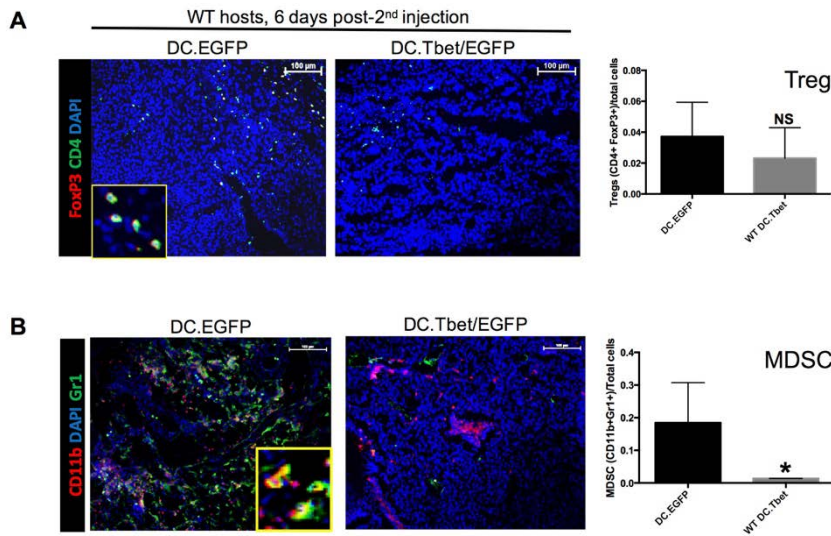


Figure S2.8. MDSC, but not Tregs, are reduced in the TME after treatment with DC.Tbet/EGFP versus DC.EGFP.

10^5 MC38 colon carcinoma cells were injected into the flanks of syngenic wild-type C57BL/6 mice and allowed to establish. Tumor-bearing mice were randomized into groups of 5 animals/cohort on day 7 post-implantation, with all cohorts exhibiting comparable mean tumor sizes. These animals were then treated on days 7 and 14 by i.t. injection of 10^6 control DC.EGFP or DC.Tbet/EGFP ($n = 5$ mice/group). Tumors were isolated on day 20 (i.e. 6 days post-2nd injection of DC) and analyzed for Tregs (CD4⁺ FoxP3⁺; **A**) or MDSC (CD11b⁺ Gr1⁺; **B**) by immunofluorescence microscopy. Data were digitally-quantitated and are reported as mean \pm SEM; * $p < 0.05$ (t-test).

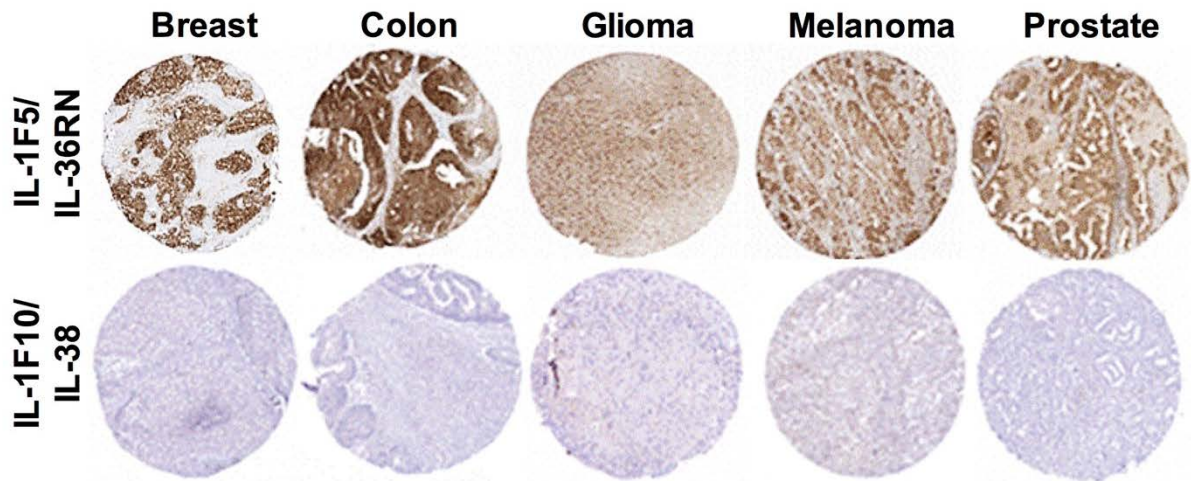


Figure S2.9. Expression of IL-1F5/IL-36RN and IL-1F10/IL-38 across human cancer types.

Representative images of specific IHC-stained tissues from human breast carcinoma, colon carcinoma, glioma, melanoma and prostate carcinoma were downloaded from the Human Protein Atlas (<http://www.proteinatlas.org/>). Consensus staining for IL-1F5 is summarized as: “Most of the malignant tissues exhibited moderate to strong cytoplasmic positivity” (<http://www.proteinatlas.org/ENSG00000136695-IL36RN/cancer>). Consensus staining for IL-1F10/IL-38 is summarized as “a single case of glioma exhibited moderate cytoplasmic staining. Fraction of cells in rare squamous cell carcinomas of cervix showed moderate, granular staining. Remaining cancer tissues were negative” (<http://www.proteinatlas.org/ENSG00000136697-IL1F10/cancer>).

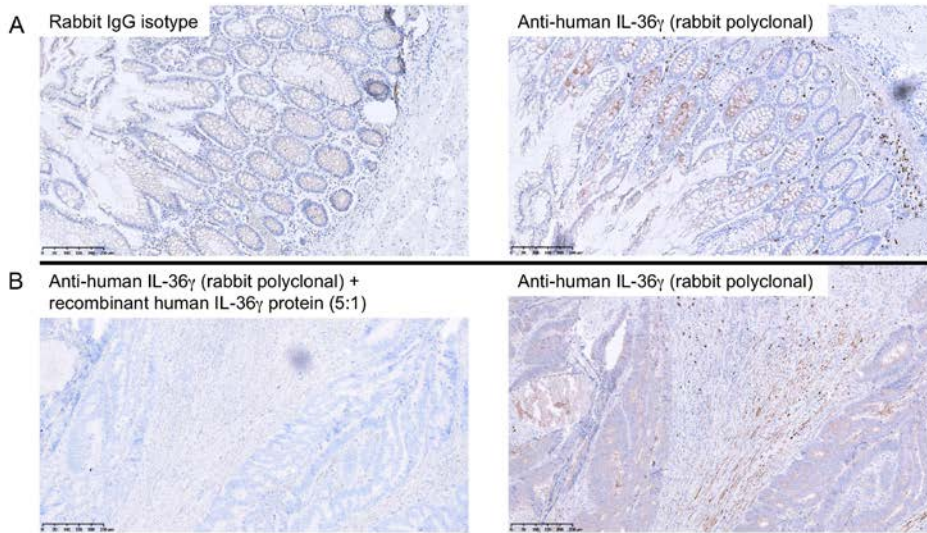


Figure S3.1. Negative control staining.

Colon sections were stained as described in Materials and Methods with a rabbit polyclonal anti-human IL-36 γ antibody (**A** and **B**, right). To confirm antibody specificity, staining on serial sections was performed using either a rabbit IgG isotype control antibody (**A**) or by a mixture of the rabbit polyclonal anti-human IL-36 γ antibody with 5-times molar excess recombinant human IL-36 γ protein (R&D Systems). Scale bars = 250 microns.

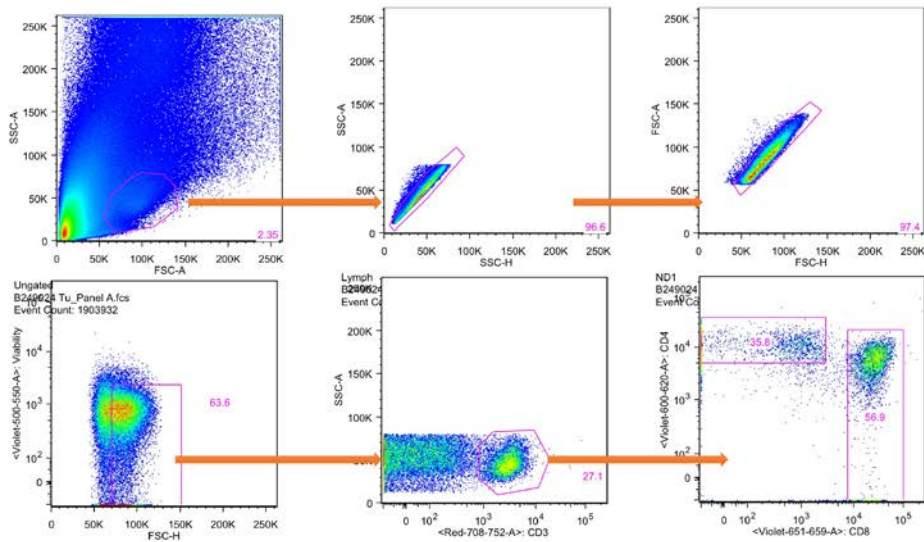


Figure S3.2. Representative gating strategy to identify T cells.

After digestion and staining as described in Materials and Methods, cells were gated by size and by expression of CD3 T cells were then gated on expression of CD4 and CD8. To identify memory and naïve subsets, central memory T cells were considered CD45RA⁻ CCR7⁺; effector memory RA (EMRA) T cells were CD45RA⁺ CCR7⁻; effector memory T cells were CD45RA⁻ CCR7⁻; and naïve T cells were CD45RA⁺ CCR7⁺.

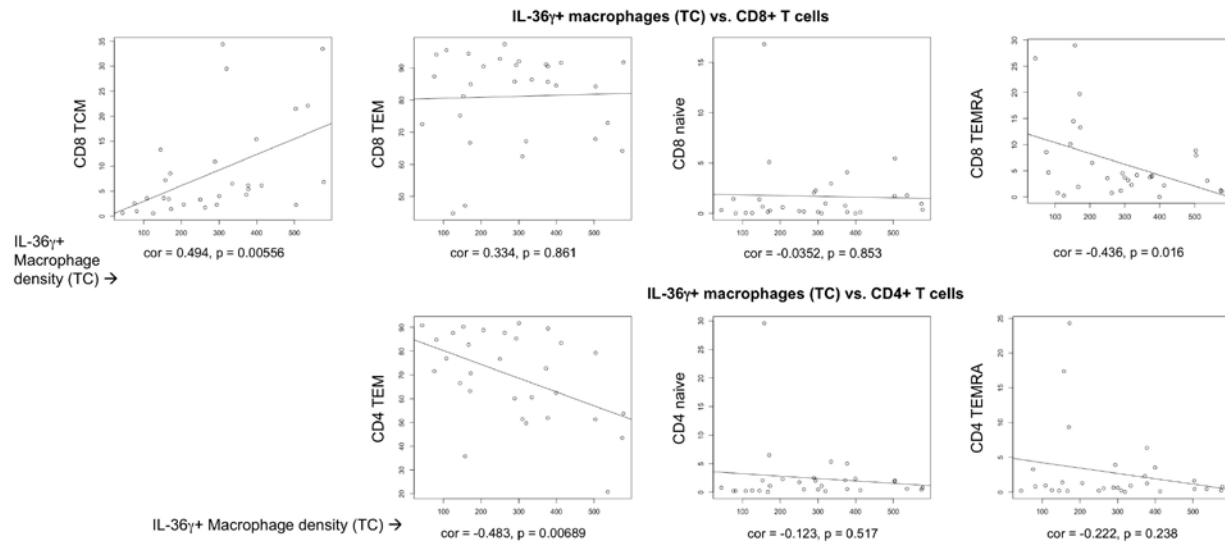


Figure S3.3. IL-36 γ ⁺ macrophages are not strongly correlated with most naïve and memory TIL subsets.

FFPE tumor sections were visualized by immunofluorescence for CD68 and IL-36 γ or fresh tumor lysate was analyzed by flow cytometry for naïve and memory TIL populations. The correlation between IL-36 γ ⁺ macrophages and all CD4⁺ and CD8⁺ naïve and memory cell populations (including naïve, central memory, effector memory, and EMRA, except for CD4⁺ TCM as shown in **Fig. 4**) was either not statistically significant or did not meet our threshold for correlation value of 0.5.

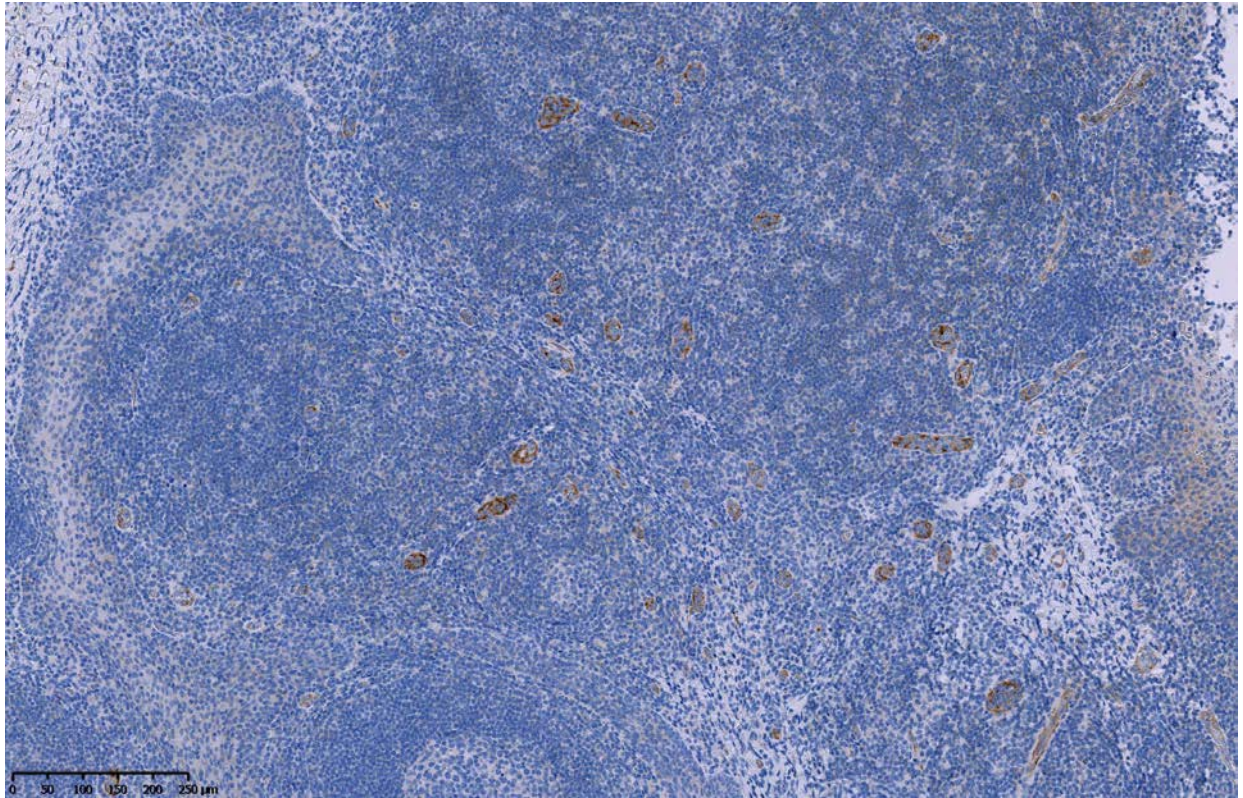


Figure S3.4. Vasculature of secondary lymphoid organs express IL-1F5.

FFPE sections of tonsil (a secondary lymphoid organ used as a control in this set of experiments) were visualized by IHC for expression of IL-1F5, which was observed to be expressed on the vasculature, especially surrounding germinal centers. Bar = 250 microns.

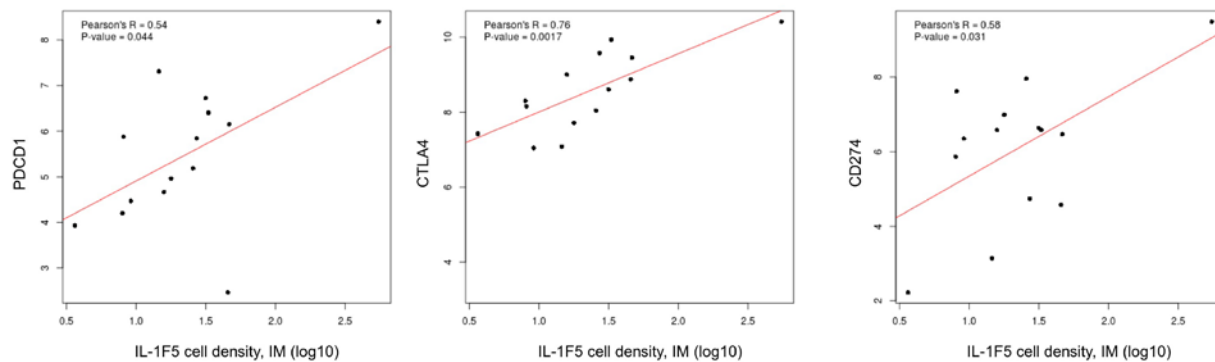


Figure S3.5. IL-1F5 expression positively-correlates with expression of immunosuppressive genes in the TME.

IL-1F5 expression was visualized by IHC as described in **Fig. 7**, and transcript expression of *PDCD1* (PD1), *CTLA4*, *CD274* (PD-L1), *LAG3*, *ICOS*, and *ICOSL* was quantified by nCounter (Nanostring). Only expression of *PDCD1* (PD1), *CTLA4*, and *CD274* (PD-L1) was directly correlated with IL-1F5 expression in the IM of tumors.

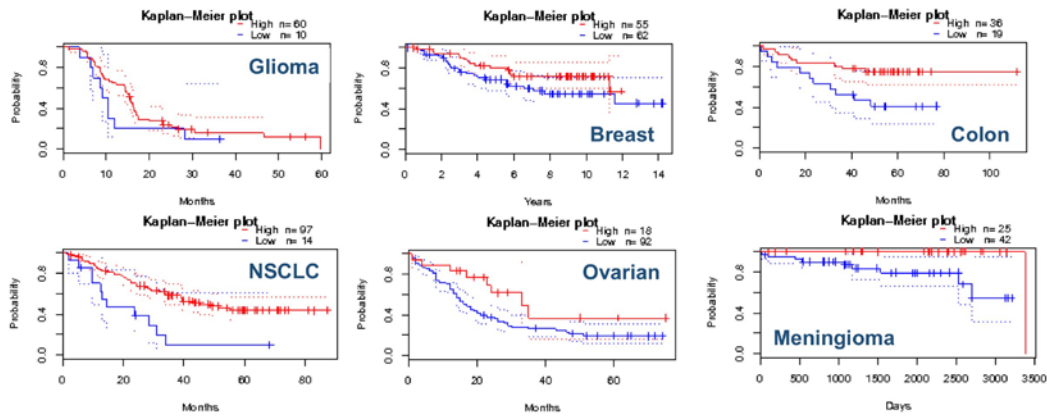


Figure S3.6. Intratumoral expression of IL-36 γ is associated with a trend towards increased overall survival in several human cancers.

Kaplan-Meier plots showing the association of intratumoral *IL36G* expression and overall survival were retrieved from PrognoScan (<http://www.abren.net/PrognoScan/cgi/PrognoScan.cgi>). Results indicate a trend towards an increase in overall survival of patients expressing high versus low levels of IL-36 γ , though the data did not reach statistical significance.

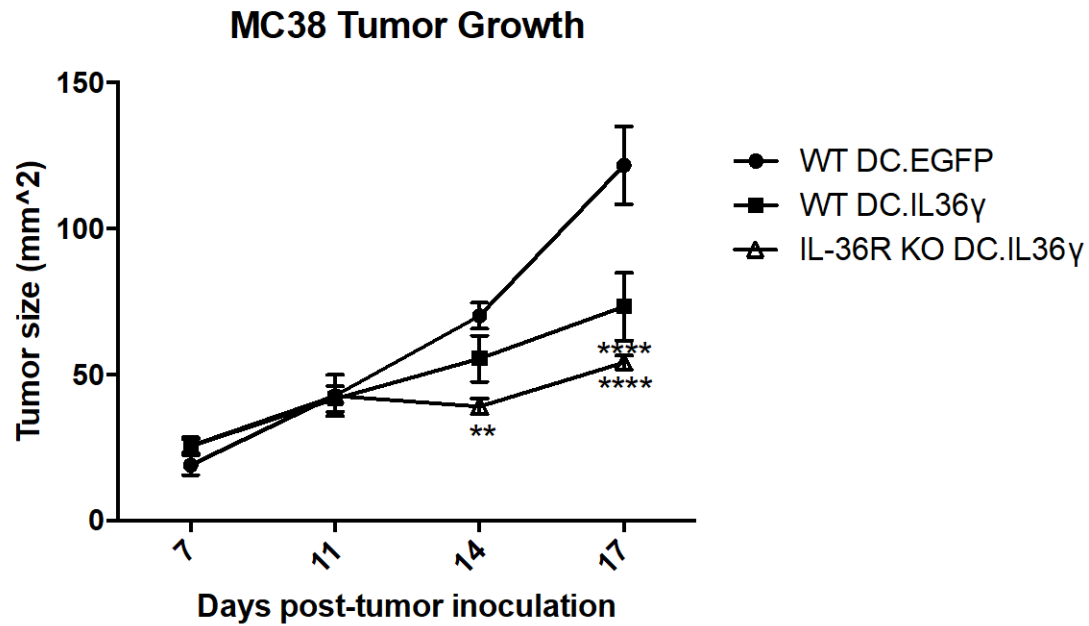


Figure S4.1. IL-36R-deficient DC.IL-36 γ confer superior therapeutic benefit versus WT DC.IL-36 γ .

10^5 MC38 colon carcinoma cells were injected into the flanks of syngenic wild-type C57BL/6 mice and allowed to establish. Tumor-bearing mice were randomized into groups of 5 animals/cohort on day 7 post-implantation, with all cohorts exhibiting comparable mean tumor sizes. These animals were then treated on days 7 and 14 by i.t. injection of 10^6 control DC.EGFP, WT DC.IL-36 γ /EGFP, or DC.IL-36 γ /EGFP generated from IL-36R-deficient cells. Tumor growth was measured every 3-4 days.

APPENDIX B

SUPPLEMENTARY TABLES

Table S2.1. Real-time PCR primers used in this study.

| Target | Primer direction | 5' → 3' Sequence |
|----------------|------------------|-----------------------|
| mCCL19 | Forward | TGTTCACCACACTAAGGGGC |
| | Reverse | TGTTGCCTTTGTTCTTGGCAG |
| mCCL21 | Forward | AGGCAGTGATGGAGGGGGA |
| | Reverse | GCTTAGAGTGCTTCCGGGGTA |
| mCXCL13 | Forward | TCTCCAGGCCACGGTATTCT |
| | Reverse | GGGGCGTAACTTGAATCCGA |
| mIL36 γ | Forward | ACTCCTGACTTTGGGGAGGT |
| | Reverse | CACGCTGACTGGGGTTACTC |
| mLIGHT | Forward | ATCTTACAGGAGCCAACGCC |
| | Reverse | ACGTCAAGCCCCTCAAGAAG |
| mLT α | Forward | GCCCATCCACTCCCTCAGAA |
| | Reverse | TGCTGGGGTACCCAACAAGG |

Table S2.2. Antibodies used in this study.

| Primary-Secondary Antibody Pairs | | | | | | | |
|---|---------|-------------|--------------------------|--------------------|--------------|--------------------------|----------|
| Primary Antibody | | | | Secondary Antibody | | | Assay |
| Target | Host | Clone | Company | Host | Conjugate | Company | |
| β-Actin | rabbit | polyclonal | Abcam | goat | HRP | Santa Cruz Biotechnology | WB |
| Tbet | rabbit | polyclonal | Santa Cruz Biotechnology | goat | HRP | Santa Cruz Biotechnology | WB |
| IL-36γ | rabbit | polyclonal | Denning laboratory | goat | HRP | Santa Cruz Biotechnology | WB |
| IL-36γ | rabbit | polyclonal | Denning laboratory | donkey | Cy3 | Jackson ImmunoResearch | IFM |
| CD4 | rat | RM4-5 | BD Pharmingen | goat | Cy3 | Jackson ImmunoResearch | IFM |
| CD4 | rat | RM4-5 | eBioscience | N/A | Streptavidin | Jackson ImmunoResearch | IFM |
| CD8a | rat | 53-6.7 | BD Pharmingen | goat | Cy3 | Jackson ImmunoResearch | IFM |
| CD19 | rat | 1D3 | BD Pharmingen | goat | Cy3 | Jackson ImmunoResearch | IFM |
| PNAd | rat | MECA-79 | BD Pharmingen | goat | Cy3 | Jackson ImmunoResearch | IFM |
| CD11c | hamster | N418 | eBioscience | donkey | AF-488 | Life Technologies | IFM |
| CD11c | hamster | N418 | eBioscience | goat | Cy3 | Jackson ImmunoResearch | IFM |
| CD11c | hamster | N418 | eBioscience | goat | Cy5 | Jackson ImmunoResearch | IFM |
| CD45R/B220 | rat | RA3-6B2 | BD Pharmingen | goat | AF-647 | Life Technologies | IFM |
| CD3 | rat | 17A2 | BD Pharmingen | goat | AF-647 | Life Technologies | IFM |
| rat IgG2a (Control) | rat | KLH/G2a-1-1 | eBioscience | N/A | N/A | N/A | blocking |
| CD11b | rat | M1/70 | Biolegend | N/A | Streptavidin | Jackson ImmunoResearch | IFM |
| Gr1 | rat | RB6-8C5 | BD Pharmingen | goat | AF-647 | Life Technologies | IFM |
| CD4 | rat | RM4-5 | BD Pharmingen | goat | AF-647 | Life Technologies | IFM |
| FoxP3 | rat | FJK-16s | eBioscience | N/A | Streptavidin | Jackson ImmunoResearch | IFM |
| CD16/CD32 | rat | 2.4G2 | BD Biosciences | N/A | N/A | N/A | blocking |
| Fluorescently Conjugated Primary Antibodies | | | | | | | |
| Target | Host | Clone | Company | Conjugate | Assay | | |

| | | | | | |
|-------|---------|----------|---------------|--------|----|
| CD3 | hamster | 145-2C11 | BD Pharmingen | BUV395 | FC |
| Tbet | mouse | 4B10 | Biolegend | APC | FC |
| PD-1 | hamster | J43 | eBioscience | FITC | FC |
| Tim3 | rat | B8.2C12 | Biolegend | APC | FC |
| CTLA4 | hamster | UC10-4B9 | eBioscience | PE | FC |

Table S3.1. Antibodies used for immunohistochemical and immunofluorescent imaging.

| Target | Company | Clone |
|--------------------|------------------------|--------------|
| α SMA | Dako | 1A4 |
| CD20 | Dako | L26 |
| CD31 | Leica | 1A10 |
| CD68 | Dako | PG-M1 |
| DC-LAMP | Dendritics | 1010E1.01 |
| IL-1F5 | Novus | polyclonal |
| IL-36 γ | Novus | polyclonal |
| PNA _d | BD | MECA-79 |
| Rabbit IgG isotype | Jackson ImmunoResearch | polyclonal |

Table S3.2. Antibodies used for flow cytometric analyses.

| Target | Company | Clone | Conjugate |
|---------------|-----------------|--------------|------------------|
| CCR7 | Biolegend | G043H7 | PE-Cy7 |
| CD3 | BD | UCHT1 | AF700 |
| CD4 | Biolegend | OKT4 | BV 605 |
| CD45RA | Beckman Coulter | 2H4 | ECD |
| CD8 | Biolegend | RPA-T8 | BV 650 |

Table S3.3. mRNA expression analysis of immune genes.

| Gene target | |
|--------------------|-----------------|
| <i>CCL19</i> | <i>IL12A</i> |
| <i>CCL2</i> | <i>IL17A</i> |
| <i>CCL20</i> | <i>IL23</i> |
| <i>CCL21</i> | <i>IL6</i> |
| <i>CD19</i> | <i>LAG3</i> |
| <i>CD274</i> | <i>PDCD1</i> |
| <i>CD68</i> | <i>PDCD1LG2</i> |
| <i>CSF1R</i> | <i>TGFB1</i> |
| <i>CTLA4</i> | <i>TGFB2</i> |
| <i>CXCL10</i> | <i>TGFB3</i> |
| <i>CXCL13</i> | <i>TIE1</i> |
| <i>EOMES</i> | <i>TNF</i> |
| <i>FLT3</i> | <i>VEGFA</i> |
| <i>ICOS</i> | <i>VEGFB</i> |
| <i>ICOSLG</i> | <i>VEGFC</i> |
| <i>IFNG</i> | |

Table S3.4. Additional real-time PCR primers used in this study.

| Target | Primer direction | 5' → 3' Sequence |
|---------------|------------------|---------------------------|
| mArg1 | Forward | TTGGGTGGATGCTCACA CTG |
| | Reverse | TTGCCCATGCAGATTCCC |
| mArg2 | Forward | GGGCCCTGAAGGCTGTAG |
| | Reverse | AATGGAGCCACTGCCATC |
| miNOS | Forward | CAGGACCACACCCCCTCGGA |
| | Reverse | CCTGACCATCTCGGGTGCGG |
| mIL36 β | Forward | TGCATGGATCCTCACAATCTCC |
| | Reverse | TCAGTCAGGACCCATACCA |
| mTbet | Forward | GTTCCATTCTGTCTTC |
| | Reverse | CCTTGTTGTTGGTGAGCTT |
| mIL1 β | Forward | GGAGAACCAAGCAACGACAAAATA |
| | Reverse | TGGGGA ACTCTGCAGACTCAAAC |
| mTNF α | Forward | CATCTTCTCAAAATTCGAGTGACAA |
| | Reverse | TGGGAGTAGACAAGGTACAACCC |
| mCXCL12 | Forward | GCCCTTCAGATTGTTGCACGGC |
| | Reverse | GCGCCCCTTGTTAAAGCTTTCTC |

BIBLIOGRAPHY

1. Mittal D, Gubin MM, Schreiber RD, Smyth MJ. New insights into cancer immunoediting and its three component phases--elimination, equilibrium and escape. *Curr Opin Immunol*. NIH Public Access; 2014;27:16–25.
2. Ikeda H, Chamoto K, Tsuji T, Suzuki Y, Wakita D, Takeshima T, et al. The critical role of type-1 innate and acquired immunity in tumor immunotherapy. *Cancer Sci*. Blackwell Publishing Ltd; 2004;95:697–703.
3. Lazarevic V, Glimcher LH, Lord GM. T-bet: a bridge between innate and adaptive immunity. *Nat Rev Immunol*. Nature Publishing Group, a division of Macmillan Publishers Limited. All Rights Reserved.; 2013;13:777–89.
4. Lugo-Villarino G, Maldonado-Lopez R, Possemato R, Penaranda C, Glimcher LH. T-bet is required for optimal production of IFN-gamma and antigen-specific T cell activation by dendritic cells. *Proc Natl Acad Sci U S A*. 2003;100:7749–54.
5. Szabo SJ, Sullivan BM, Stemmann C, Satoskar AR, Sleckman BP, Glimcher LH. Distinct Effects of T-bet in TH1 Lineage Commitment and IFN- γ Production in CD4 and CD8 T Cells. *Science (80-)*. 2002;295.
6. Usui T, Preiss JC, Kanno Y, Yao ZJ, Bream JH, O'Shea JJ, et al. T-bet regulates Th1 responses through essential effects on GATA-3 function rather than on IFNG gene acetylation and transcription. *J Exp Med*. The Rockefeller University Press;

- 2006;203:755–66.
7. Szabo SJ, Kim ST, Costa GL, Zhang X, Fathman CG, Glimcher LH. A novel transcription factor, T-bet, directs Th1 lineage commitment. *Cell*. Elsevier; 2000;100:655–69.
 8. Villarino A V, Gallo E, Abbas AK. STAT1-activating cytokines limit Th17 responses through both T-bet-dependent and -independent mechanisms. *J Immunol*. American Association of Immunologists; 2010;185:6461–71.
 9. Sullivan BM, Juedes A, Szabo SJ, von Herrath M, Glimcher LH. Antigen-driven effector CD8 T cell function regulated by T-bet. *Proc Natl Acad Sci U S A*. National Academy of Sciences; 2003;100:15818–23.
 10. Li G, Yang Q, Zhu Y, Wang H-R, Chen X, Zhang X, et al. T-Bet and Eomes Regulate the Balance between the Effector/Central Memory T Cells versus Memory Stem Like T Cells. Matloubian M, editor. *PLoS One*. Public Library of Science; 2013;8:e67401.
 11. Lugo-Villarino G, Ito S-I, Klinman DM, Glimcher LH. The adjuvant activity of CpG DNA requires T-bet expression in dendritic cells. *Proc Natl Acad Sci U S A*. 2005;102:13248–53.
 12. Peng SL, Szabo SJ, Glimcher LH, Glimcher LH. T-bet regulates IgG class switching and pathogenic autoantibody production. *Proc Natl Acad Sci U S A*. National Academy of Sciences; 2002;99:5545–50.
 13. Serre K, Cunningham AF, Coughlan RE, Lino AC, Rot A, Hub E, et al. CD8 T cells induce T-bet-dependent migration toward CXCR3 ligands by differentiated B cells produced during responses to alum-protein vaccines. *Blood*. 2012;120:4552–9.
 14. Knox JJ, Cosma GL, Betts MR, McLane LM. Characterization of T-bet and eomes in peripheral human immune cells. *Front Immunol*. Frontiers Media SA;

2014;5:217.

15. Dieu-Nosjean M-C, Antoine M, Danel C, Heudes D, Wislez M, Poulot V, et al. Long-Term Survival for Patients With Non–Small-Cell Lung Cancer With Intratumoral Lymphoid Structures. *J Clin Oncol*. 2008;26:4410–7.
16. Pagès F, Galon J, Dieu-Nosjean M-C, Tartour E, Sautès-Fridman C, Fridman W-H. Immune infiltration in human tumors: a prognostic factor that should not be ignored. *Oncogene*. Nature Publishing Group; 2010;29:1093–102.
17. Martinet L, Filleron T, Le Guellec S, Rochaix P, Garrido I, Girard J-PJ-P. High endothelial venule blood vessels for tumor-infiltrating lymphocytes are associated with lymphotoxin β -producing dendritic cells in human breast cancer. *J Immunol*. American Association of Immunologists; 2013;191:2001–8.
18. Martinet L, Le Guellec S, Filleron T, Lamant L, Meyer N, Rochaix P, et al. High endothelial venules (HEVs) in human melanoma lesions: Major gateways for tumor-infiltrating lymphocytes. *Oncoimmunology*. Taylor & Francis; 2012;1:829–39.
19. Mailliard RB, Wankowicz-Kalinska A, Cai Q, Wesa A, Hilkens CM, Kapsenberg ML, et al. α -Type-1 Polarized Dendritic Cells. *Cancer Res*. 2004;64.
20. Wierecky J, Müller MR, Wirths S, Halder-Oehler E, Dörfel D, Schmidt SM, et al. Immunologic and Clinical Responses after Vaccinations with Peptide-Pulsed Dendritic Cells in Metastatic Renal Cancer Patients. *Cancer Res*. 2006;66.
21. Fong L, Brockstedt D, Benike C, Wu L, Engleman EG. Dendritic Cells Injected Via Different Routes Induce Immunity in Cancer Patients. *J Immunol*. American Association of Immunologists; 2001;166:4254–9.
22. Zhao X, Bose A, Komita H, Taylor JL, Chi N, Lowe DB, et al. Vaccines Targeting Tumor Blood Vessel Antigens Promote CD8+ T Cell-Dependent Tumor Eradication or Dormancy in HLA-A2 Transgenic Mice. *J Immunol*. 2012;188.

23. Chi Sabins N, Taylor JL, Fabian KP, Appleman LJ, Maranchie JK, Stolz DB, et al. DLK1: A Novel Target for Immunotherapeutic Remodeling of the Tumor Blood Vasculature. *Mol Ther.* 2013;21:1958–68.
24. Fabian KPL, Chi-Sabins N, Taylor JL, Fecek R, Weinstein A, Storkus WJ. Therapeutic efficacy of combined vaccination against tumor pericyte-associated antigens DLK1 and DLK2 in mice. *Oncoimmunology.* Taylor & Francis; 2017;6:e1290035.
25. Watchmaker PB, Berk E, Muthuswamy R, Mailliard RB, Urban JA, Kirkwood JM, et al. Independent regulation of chemokine responsiveness and cytolytic function versus CD8+ T cell expansion by dendritic cells. *J Immunol.* American Association of Immunologists; 2010;184:591–7.
26. Ribas A, Timmerman JM, Butterfield LH, Economou JS. Determinant spreading and tumor responses after peptide-based cancer immunotherapy. *Trends Immunol.* Elsevier; 2003;24:58–61.
27. Qu Y, Chen L, Lowe DB, Storkus WJ, Taylor JL. Combined Tbet and IL12 gene therapy elicits and recruits superior antitumor immunity in vivo. *Mol Ther.* The American Society of Gene & Cell Therapy; 2012;20:644–51.
28. Chen L, Taylor JL, Sabins NC, Lowe DB, Qu Y, You Z, et al. Extranodal induction of therapeutic immunity in the tumor microenvironment after intratumoral delivery of Tbet gene-modified dendritic cells. *Cancer Gene Ther.* Nature America, Inc.; 2013;20:469–77.
29. Butterfield LH. Dendritic Cells in Cancer Immunotherapy Clinical Trials: Are We Making Progress? *Front Immunol.* Frontiers; 2013;4:454.
30. Aloisi F, Pujol-Borrell R. Lymphoid neogenesis in chronic inflammatory diseases. *Nat Rev Immunol.* Nature Publishing Group; 2006;6:205–17.
31. Pimenta EM, Barnes BJ. Role of Tertiary Lymphoid Structures (TLS) in Anti-

- Tumor Immunity: Potential Tumor-Induced Cytokines/Chemokines that Regulate TLS Formation in Epithelial-Derived Cancers. *Cancers (Basel)*. Multidisciplinary Digital Publishing Institute; 2014;6:969–97.
32. Fridman WH, Pagès F, Sautès-Fridman C, Galon J. The immune contexture in human tumours: impact on clinical outcome. *Nat Rev Cancer*. Nature Publishing Group, a division of Macmillan Publishers Limited. All Rights Reserved.; 2012;12:298–306.
 33. Pitzalis C, Jones GW, Bombardieri M, Jones SA. Ectopic lymphoid-like structures in infection, cancer and autoimmunity. *Nat Rev Immunol*. Nature Publishing Group, a division of Macmillan Publishers Limited. All Rights Reserved.; 2014;14:447–62.
 34. Peske JD, Thompson ED, Gemta L, Baylis RA, Fu Y-X, Engelhard VH. Effector lymphocyte-induced lymph node-like vasculature enables naive T-cell entry into tumours and enhanced anti-tumour immunity. *Nat Commun*. Nature Publishing Group; 2015;6:7114.
 35. Weinstein AM, Chen L, Brzana EA, Patil PR, Taylor JL, Fabian KL, et al. Tbet and IL-36 γ cooperate in therapeutic DC-mediated promotion of ectopic lymphoid organogenesis in the tumor microenvironment. *Oncoimmunology*. 2017;
 36. Chen L, Fabian KL, Taylor JL, Storkus WJ. Therapeutic use of dendritic cells to promote the extranodal priming of anti-tumor immunity. *Front Immunol*. Frontiers; 2013;4:388.
 37. Wirsing AM, Rikardsen OG, Steigen SE, Uhlin-Hansen L, Hadler-Olsen E. Characterisation and prognostic value of tertiary lymphoid structures in oral squamous cell carcinoma. *BMC Clin Pathol*. 2014;14:38.
 38. Behr DS, Peitsch WK, Hametner C, Lasitschka F, Houben R, Schönhaar K, et al. Prognostic value of immune cell infiltration, tertiary lymphoid structures and PD-L1

- expression in Merkel cell carcinomas. *Int J Clin Exp Pathol*. e-Century Publishing Corporation; 2014;7:7610–21.
39. Gu-Trantien C, Loi S, Garaud S, Equeter C, Libin M, de Wind A, et al. CD4⁺ follicular helper T cell infiltration predicts breast cancer survival. *J Clin Invest*. American Society for Clinical Investigation; 2013;123:2873–92.
 40. Mahmoud SMA, Lee AHS, Paish EC, Macmillan RD, Ellis IO, Green AR. The prognostic significance of B lymphocytes in invasive carcinoma of the breast. *Breast Cancer Res Treat*. Springer US; 2012;132:545–53.
 41. Meshcheryakova A, Tamandl D, Bajna E, Stift J, Mittlboeck M, Svoboda M, et al. B cells and ectopic follicular structures: novel players in anti-tumor programming with prognostic power for patients with metastatic colorectal cancer. *PLoS One*. Public Library of Science; 2014;9:e99008.
 42. Pickens SR, Chamberlain ND, Volin M V, Pope RM, Talarico NE, Mandelin AM, et al. Role of the CCL21 and CCR7 pathways in rheumatoid arthritis angiogenesis. *Arthritis Rheum*. NIH Public Access; 2012;64:2471–81.
 43. Cheng S, Han L, Guo J, Yang Q, Zhou J, Yang X. The essential roles of CCR7 in epithelial-to-mesenchymal transition induced by hypoxia in epithelial ovarian carcinomas. *Tumour Biol*. 2014;35:12293–8.
 44. Kossenkov A V, Dawany N, Evans TL, Kucharczuk JC, Albelda SM, Showe LC, et al. Peripheral immune cell gene expression predicts survival of patients with non-small cell lung cancer. *PLoS One*. 2012;7:e34392.
 45. de Chaisemartin L, Goc J, Damotte D, Validire P, Magdeleinat P, Alifano M, et al. Characterization of chemokines and adhesion molecules associated with T cell presence in tertiary lymphoid structures in human lung cancer. *Cancer Res*. American Association for Cancer Research; 2011;71:6391–9.
 46. Messina JL, Fenstermacher DA, Eschrich S, Qu X, Berglund AE, Lloyd MC, et al.

- 12-Chemokine gene signature identifies lymph node-like structures in melanoma: potential for patient selection for immunotherapy? *Sci Rep*. Nature Publishing Group; 2012;2:765.
47. Germain C, Gnjatic S, Tamzalit F, Knockaert S, Remark R, Goc J, et al. Presence of B cells in tertiary lymphoid structures is associated with a protective immunity in patients with lung cancer. *Am J Respir Crit Care Med*. American Thoracic Society; 2014;189:832–44.
 48. Goc J, Germain C, Vo-Bourgais TKD, Lupo A, Klein C, Knockaert S, et al. Dendritic cells in tumor-associated tertiary lymphoid structures signal a Th1 cytotoxic immune contexture and license the positive prognostic value of infiltrating CD8+ T cells. *Cancer Res*. 2014;74:705–15.
 49. Goc J, Fridman W-H, Hammond SA, Sautès-Fridman C, Dieu-Nosjean M-C. Tertiary lymphoid structures in human lung cancers, a new driver of antitumor immune responses. *Oncoimmunology*. 2014;3:e28976.
 50. Alexe G, Dalgin GS, Scandfeld D, Tamayo P, Mesirov JP, DeLisi C, et al. High expression of lymphocyte-associated genes in node-negative HER2+ breast cancers correlates with lower recurrence rates. *Cancer Res*. American Association for Cancer Research; 2007;67:10669–76.
 51. Nzula S, Going JJ, Stott DI. Antigen-driven clonal proliferation, somatic hypermutation, and selection of B lymphocytes infiltrating human ductal breast carcinomas. *Cancer Res*. American Association for Cancer Research; 2003;63:3275–80.
 52. DiLillo DJ, Yanaba K, Tedder TF. B cells are required for optimal CD4+ and CD8+ T cell tumor immunity: therapeutic B cell depletion enhances B16 melanoma growth in mice. *J Immunol*. American Association of Immunologists; 2010;184:4006–16.

53. Fridman WH, Galon J, Dieu-Nosjean M-C, Cremer I, Fisson S, Damotte D, et al. Immune infiltration in human cancer: prognostic significance and disease control. *Curr Top Microbiol Immunol*. Springer Berlin Heidelberg; 2011;344:1–24.
54. Salama P, Phillips M, Grieu F, Morris M, Zeps N, Joseph D, et al. Tumor-Infiltrating FOXP3+ T Regulatory Cells Show Strong Prognostic Significance in Colorectal Cancer. *J Clin Oncol*. American Society of Clinical Oncology; 2008;27:186–92.
55. Spranger S, Koblish HK, Horton B, Scherle PA, Newton R, Gajewski TF. Mechanism of tumor rejection with doublets of CTLA-4, PD-1/PD-L1, or IDO blockade involves restored IL-2 production and proliferation of CD8(+) T cells directly within the tumor microenvironment. *J Immunother cancer*. 2014;2:3.
56. Denkert C, Loibl S, Noske A, Roller M, Müller BM, Komor M, et al. Tumor-associated lymphocytes as an independent predictor of response to neoadjuvant chemotherapy in breast cancer. *J Clin Oncol*. American Society of Clinical Oncology; 2010;28:105–13.
57. Taga M, Hoshino H, Low S, Imamura Y, Ito H, Yokoyama O, et al. A potential role for 6-sulfo sialyl Lewis X in metastasis of bladder urothelial carcinoma. *Urol Oncol*. 2015;33:496.e1-9.
58. Koti M, Xu AS, Ren KYM, Visram K, Ren R, Berman DM, et al. Tertiary Lymphoid Structures Associate with Tumour Stage in Urothelial Bladder Cancer. *Bl cancer (Amsterdam, Netherlands)*. IOS Press; 2017;3:259–67.
59. Gu-Trantien C, Migliori E, Buisseret L, de Wind A, Brohée S, Garaud S, et al. CXCL13-producing TFH cells link immune suppression and adaptive memory in human breast cancer. *JCI insight*. American Society for Clinical Investigation; 2017;2.
60. Di Caro G, Bergomas F, Grizzi F, Doni A, Bianchi P, Malesci A, et al. Occurrence

of tertiary lymphoid tissue is associated with T-cell infiltration and predicts better prognosis in early-stage colorectal cancers. *Clin Cancer Res. Clinical Cancer Research*; 2014;20:2147–58.

61. Bergomas F, Grizzi F, Doni A, Pesce S, Laghi L, Allavena P, et al. Tertiary intratumor lymphoid tissue in colo-rectal cancer. *Cancers (Basel)*. 2011;4:1–10.
62. Hennequin A, Derangère V, Boidot R, Apetoh L, Vincent J, Orry D, et al. Tumor infiltration by Tbet+ effector T cells and CD20+ B cells is associated with survival in gastric cancer patients. *Oncoimmunology*. Taylor & Francis; 2016;5:e1054598.
63. Sakimura C, Tanaka H, Okuno T, Hiramatsu S, Mugeruma K, Hirakawa K, et al. B cells in tertiary lymphoid structures are associated with favorable prognosis in gastric cancer. *J Surg Res. Elsevier*; 2017;215:74–82.
64. Balermipas P, Michel Y, Wagenblast J, Seitz O, Weiss C, Rödel F, et al. Tumour-infiltrating lymphocytes predict response to definitive chemoradiotherapy in head and neck cancer. *Br J Cancer. Cancer Research UK*; 2013;110:501–9.
65. Finkin S, Yuan D, Stein I, Taniguchi K, Weber A, Unger K, et al. Ectopic lymphoid structures function as microniches for tumor progenitor cells in hepatocellular carcinoma. *Nat Immunol*. Nature Publishing Group, a division of Macmillan Publishers Limited. All Rights Reserved.; 2015;16:1235–44.
66. Lutz ER, Wu AA, Bigelow E, Sharma R, Mo G, Soares K, et al. Immunotherapy converts nonimmunogenic pancreatic tumors into immunogenic foci of immune regulation. *Cancer Immunol Res. American Association for Cancer Research*; 2014;2:616–31.
67. Hiraoka N, Ino Y, Yamazaki-Itoh R, Kanai Y, Kosuge T, Shimada K. Intratumoral tertiary lymphoid organ is a favourable prognosticator in patients with pancreatic cancer. *Br J Cancer. Nature Publishing Group*; 2015;112:1782–90.
68. Poschke I, Faryna M, Bergmann F, Flossdorf M, Lauenstein C, Hermes J, et al.

- Identification of a tumor-reactive T-cell repertoire in the immune infiltrate of patients with resectable pancreatic ductal adenocarcinoma. *Oncoimmunology*. Taylor & Francis; 2016;5:e1240859.
69. Giraldo NA, Becht E, Pagès F, Skliris G, Verkarre V, Vano Y, et al. Orchestration and Prognostic Significance of Immune Checkpoints in the Microenvironment of Primary and Metastatic Renal Cell Cancer. *Clin Cancer Res*. American Association for Cancer Research; 2015;21:3031–40.
 70. Schneider K, Potter KG, Ware CF. Lymphotoxin and LIGHT signaling pathways and target genes. *Immunol Rev*. 2004;202:49–66.
 71. Mauri DN, Ebner R, Montgomery RI, Kochel KD, Cheung TC, Yu G-L, et al. LIGHT, a New Member of the TNF Superfamily, and Lymphotoxin α Are Ligands for Herpesvirus Entry Mediator. *Immunity*. 1998;8:21–30.
 72. Zhu M, Fu Y-X. The role of core TNF/LIGHT family members in lymph node homeostasis and remodeling. *Immunol Rev*. 2011;244:75–84.
 73. Browning JL, Allaire N, Ngam-Ek A, Notidis E, Hunt J, Perrin S, et al. Lymphotoxin-beta receptor signaling is required for the homeostatic control of HEV differentiation and function. *Immunity*. 2005;23:539–50.
 74. Dohi T, Rennert PD, Fujihashi K, Kiyono H, Shirai Y, Kawamura YI, et al. Elimination of Colonic Patches with Lymphotoxin Receptor-Ig Prevents Th2 Cell-Type Colitis. *J Immunol*. American Association of Immunologists; 2001;167:2781–90.
 75. Gonzalez M, Mackay F, Browning JL, Kosco-Vilbois MH, Noelle RJ. The sequential role of lymphotoxin and B cells in the development of splenic follicles. *J Exp Med*. 1998;187:997–1007.
 76. Drayton DL, Ying X, Lee J, Lesslauer W, Ruddle NH. Ectopic LT alpha beta directs lymphoid organ neogenesis with concomitant expression of peripheral

- node addressin and a HEV-restricted sulfotransferase. *J Exp Med*. Rockefeller University Press; 2003;197:1153–63.
77. Bradley LM, Watson SR, Swain SL. Entry of naive CD4 T cells into peripheral lymph nodes requires L-selectin. *J Exp Med*. The Rockefeller University Press; 1994;180:2401–6.
78. Gunn MD, Tangemann K, Tam C, Cyster JG, Rosen SD, Williams LT. A chemokine expressed in lymphoid high endothelial venules promotes the adhesion and chemotaxis of naive T lymphocytes. *Proc Natl Acad Sci U S A*. 1998;95:258–63.
79. Jung YW, Rutishauser RL, Joshi NS, Haberman AM, Kaech SM. Differential localization of effector and memory CD8 T cell subsets in lymphoid organs during acute viral infection. *J Immunol*. 2010;185:5315–25.
80. Ansel KM, Ngo VN, Hyman PL, Luther SA, Förster R, Sedgwick JD, et al. A chemokine-driven positive feedback loop organizes lymphoid follicles. *Nature*. Nature Publishing Group; 2000;406:309–14.
81. Wang J, Foster A, Chin R, Yu P, Sun Y, Wang Y, et al. The complementation of lymphotoxin deficiency with LIGHT, a newly discovered TNF family member, for the restoration of secondary lymphoid structure and function. *Eur J Immunol*. 2002;32:1969–79.
82. Luther SA, Bidgol A, Hargreaves DC, Schmidt A, Xu Y, Paniyadi J, et al. Differing Activities of Homeostatic Chemokines CCL19, CCL21, and CXCL12 in Lymphocyte and Dendritic Cell Recruitment and Lymphoid Neogenesis. *J Immunol*. American Association of Immunologists; 2002;169:424–33.
83. Bossen C, Ingold K, Tardivel A, Bodmer J-L, Gaide O, Hertig S, et al. Interactions of tumor necrosis factor (TNF) and TNF receptor family members in the mouse and human. *J Biol Chem*. American Society for Biochemistry and Molecular

- Biology; 2006;281:13964–71.
84. Yu KY, Kwon B, Ni J, Zhai Y, Ebner R, Kwon BS. A newly identified member of tumor necrosis factor receptor superfamily (TR6) suppresses LIGHT-mediated apoptosis. *J Biol Chem. American Society for Biochemistry and Molecular Biology*; 1999;274:13733–6.
 85. Degli-Esposti MA, Davis-Smith T, Din WS, Smolak PJ, Goodwin RG, Smith CA. Activation of the lymphotoxin beta receptor by cross-linking induces chemokine production and growth arrest in A375 melanoma cells. *J Immunol. American Association of Immunologists*; 1997;158:1756–62.
 86. Tamada K, Ni J, Zhu G, Fiscella M, Teng B, van Deursen JMA, et al. Cutting Edge: Selective Impairment of CD8+ T Cell Function in Mice Lacking the TNF Superfamily Member LIGHT. *J Immunol. American Association of Immunologists*; 2002;168:4832–5.
 87. Miyagaki T, Sugaya M, Suga H, Morimura S, Ohmatsu H, Fujita H, et al. Low herpesvirus entry mediator (HVEM) expression on dermal fibroblasts contributes to a Th2-dominant microenvironment in advanced cutaneous T-cell lymphoma. *J Invest Dermatol. The Society for Investigative Dermatology, Inc*; 2012;132:1280–9.
 88. Gantsev SK, Umezawa K, Islamgulov D V, Khusnutdinova EK, Ishmuratova RS, Frolova VY, et al. The role of inflammatory chemokines in lymphoid neoorganogenesis in breast cancer. *Biomed Pharmacother.* 2013;67:363–6.
 89. Yu P, Lee Y, Liu W, Chin RK, Wang J, Wang Y, et al. Priming of naive T cells inside tumors leads to eradication of established tumors. *Nat Immunol.* 2004;5:141–9.
 90. Yu P, Lee Y, Wang Y, Liu X, Auh S, Gajewski TF, et al. Targeting the primary tumor to generate CTL for the effective eradication of spontaneous metastases. *J*

- Immunol. 2007;179:1960–8.
91. Hu G, Liu Y, Li H, Zhao D, Yang L, Shen J, et al. Adenovirus-mediated LIGHT gene modification in murine B-cell lymphoma elicits a potent antitumor effect. *Cell Mol Immunol.* 2010;7:296–305.
 92. Kanodia S, Da Silva DM, Karamanukyan T, Bogaert L, Fu Y-X, Kast WM. Expression of LIGHT/TNFSF14 combined with vaccination against human papillomavirus Type 16 E7 induces significant tumor regression. *Cancer Res.* 2010;70:3955–64.
 93. Zhu X, Su D, Xuan S, Ma G, Dai Z, Liu T, et al. Gene therapy of gastric cancer using LIGHT-secreting human umbilical cord blood-derived mesenchymal stem cells. *Gastric Cancer.* 2013;16:155–66.
 94. Zou W, Zheng H, He T-C, Chang J, Fu Y-X, Fan W. LIGHT delivery to tumors by mesenchymal stem cells mobilizes an effective antitumor immune response. *Cancer Res.* 2012;72:2980–9.
 95. Heo S-K, Ju S-A, Kim GY, Park S-M, Back SH, Park N-H, et al. The presence of high level soluble herpes virus entry mediator in sera of gastric cancer patients. *Exp Mol Med.* 2012;44:149–58.
 96. Jung HW, La SJ, Kim JY, Heo SK, Kim JY, Wang S, et al. High levels of soluble herpes virus entry mediator in sera of patients with allergic and autoimmune diseases. *Exp Mol Med. Korean Society of Medical Biochemistry and Molecular Biology;* 2003;35:501–8.
 97. Qin JZ, Upadhyay V, Prabhakar B, Maker A V. Shedding LIGHT (TNFSF14) on the tumor microenvironment of colorectal cancer liver metastases. *J Transl Med.* 2013;11:70.
 98. Yan L, Silva DM Da, Verma B, Gray A, Brand HE, Skeate JG, et al. Forced LIGHT expression in prostate tumors overcomes Treg mediated immunosuppression and

- synergizes with a prostate tumor therapeutic vaccine by recruiting effector T lymphocytes. *Prostate*. 2015;75:280–91.
99. Tao R, Wang L, Murphy KM, Fraser CC, Hancock WW. Regulatory T Cell Expression of Herpesvirus Entry Mediator Suppresses the Function of B and T Lymphocyte Attenuator-Positive Effector T Cells. *J Immunol. American Association of Immunologists*; 2008;180:6649–55.
 100. Lin W-W, Hsieh S-L. Decoy receptor 3: a pleiotropic immunomodulator and biomarker for inflammatory diseases, autoimmune diseases and cancer. *Biochem Pharmacol*. 2011;81:838–47.
 101. Morishige T, Yoshioka Y, Inakura H, Tanabe A, Yao X, Tsunoda S, et al. Creation of a LIGHT mutant with the capacity to evade the decoy receptor for cancer therapy. *Biomaterials*. 2010;31:3357–63.
 102. Haybaeck J, Zeller N, Wolf MJ, Weber A, Wagner U, Kurrer MO, et al. A lymphotoxin-driven pathway to hepatocellular carcinoma. *Cancer Cell*. 2009;16:295–308.
 103. Fan Z, Yu P, Wang Y, Wang Y, Fu ML, Liu W, et al. NK-cell activation by LIGHT triggers tumor-specific CD8+ T-cell immunity to reject established tumors. *Blood*. 2006;107:1342–51.
 104. Holmes TD, Wilson EB, Black EVI, Benest A V, Vaz C, Tan B, et al. Licensed human natural killer cells aid dendritic cell maturation via TNFSF14/LIGHT. *Proc Natl Acad Sci U S A*. 2014;111:E5688-96.
 105. Legler DF, Uetz-von Allmen E, Hauser MA. CCR7: roles in cancer cell dissemination, migration and metastasis formation. *Int J Biochem Cell Biol*. 2014;54:78–82.
 106. Ohmatsu H, Sugaya M, Kadono T, Tamaki K. CXCL13 and CCL21 are expressed in ectopic lymphoid follicles in cutaneous lymphoproliferative disorders. *J Invest*

- Dermatol. Nature Publishing Group; 2007;127:2466–8.
107. Badr G, Borhis G, Treton D, Richard Y. IFN α enhances human B-cell chemotaxis by modulating ligand-induced chemokine receptor signaling and internalization. *Int Immunol.* 2005;17:459–67.
 108. Chen S-C, Vassileva G, Kinsley D, Holzmann S, Manfra D, Wiekowski MT, et al. Ectopic Expression of the Murine Chemokines CCL21a and CCL21b Induces the Formation of Lymph Node-Like Structures in Pancreas, But Not Skin, of Transgenic Mice. *J Immunol. American Association of Immunologists;* 2002;168:1001–8.
 109. Chen S-C, Leach MW, Chen Y, Cai X-Y, Sullivan L, Wiekowski M, et al. Central Nervous System Inflammation and Neurological Disease in Transgenic Mice Expressing the CC Chemokine CCL21 in Oligodendrocytes. *J Immunol. American Association of Immunologists;* 2002;168:1009–17.
 110. Pahne-Zeppenfeld J, Schröder N, Walch-Rückheim B, Oldak M, Gorter A, Hegde S, et al. Cervical cancer cell-derived interleukin-6 impairs CCR7-dependent migration of MMP-9-expressing dendritic cells. *Int J Cancer.* 2014;134:2061–73.
 111. Shi J-Y, Yang L-X, Wang Z-C, Wang L-Y, Zhou J, Wang X-Y, et al. CC chemokine receptor-like 1 functions as a tumour suppressor by impairing CCR7-related chemotaxis in hepatocellular carcinoma. *J Pathol.* 2015;235:546–58.
 112. Comerford I, Milasta S, Morrow V, Milligan G, Nibbs R. The chemokine receptor CCX-CKR mediates effective scavenging of CCL19 in vitro. *Eur J Immunol.* 2006;36:1904–16.
 113. Dobner BC, Riechardt AI, Jousen AM, Englert S, Bechrakis NE. Expression of haematogenous and lymphogenous chemokine receptors and their ligands on uveal melanoma in association with liver metastasis. *Acta Ophthalmol. Blackwell Publishing Ltd;* 2012;90:e638-44.

114. Nakano H, Gunn MD. Gene Duplications at the Chemokine Locus on Mouse Chromosome 4: Multiple Strain-Specific Haplotypes and the Deletion of Secondary Lymphoid-Organ Chemokine and EBI-1 Ligand Chemokine Genes in the plt Mutation. *J Immunol. American Association of Immunologists*; 2001;166:361–9.
115. Hedrick JA, Zlotnik A. Identification and characterization of a novel beta chemokine containing six conserved cysteines. *J Immunol. American Association of Immunologists*; 1997;159:1589–93.
116. Ashour AE, Turnquist HR, Singh RK, Talmadge JE, Solheim JC. CCL21-induced immune cell infiltration. *Int Immunopharmacol.* 2007;7:272–6.
117. Mulé JJ. Dendritic cell-based vaccines for pancreatic cancer and melanoma. *Ann N Y Acad Sci. Blackwell Publishing Inc*; 2009;1174:33–40.
118. Schneider MA, Meingassner JG, Lipp M, Moore HD, Rot A. CCR7 is required for the in vivo function of CD4+ CD25+ regulatory T cells. *J Exp Med.* 2007;204:735–45.
119. Zlotnik A, Burkhardt AM, Homey B. Homeostatic chemokine receptors and organ-specific metastasis. *Nat Rev Immunol. Nature Publishing Group, a division of Macmillan Publishers Limited. All Rights Reserved.*; 2011;11:597–606.
120. Shields JD, Kourtis IC, Tomei AA, Roberts JM, Swartz MA. Induction of lymphoidlike stroma and immune escape by tumors that express the chemokine CCL21. *Science. American Association for the Advancement of Science*; 2010;328:749–52.
121. Sanchez-Sanchez N, Riol-Blanco L, Rodriguez-Fernandez JL. The Multiple Personalities of the Chemokine Receptor CCR7 in Dendritic Cells. *J Immunol. American Association of Immunologists*; 2006;176:5153–9.
122. Pietila TE, Veckman V, Lehtonen A, Lin R, Hiscott J, Julkunen I. Multiple NF- B

- and IFN Regulatory Factor Family Transcription Factors Regulate CCL19 Gene Expression in Human Monocyte-Derived Dendritic Cells. *J Immunol. American Association of Immunologists*; 2006;178:253–61.
123. Su M-L, Chang T-M, Chiang C-H, Chang H-C, Hou M-F, Li W-S, et al. Inhibition of chemokine (C-C motif) receptor 7 sialylation suppresses CCL19-stimulated proliferation, invasion and anti-apoptosis. *PLoS One*. 2014;9:e98823.
 124. Peng C, Zhou K, An S, Yang J. The effect of CCL19/CCR7 on the proliferation and migration of cell in prostate cancer. *Tumour Biol*. 2015;36:329–35.
 125. Cheng S, Guo J, Yang Q, Yang X. Crk-like adapter protein regulates CCL19/CCR7-mediated epithelial-to-mesenchymal transition via ERK signaling pathway in epithelial ovarian carcinomas. *Med Oncol*. 2015;32:494.
 126. Clatworthy MR, Aronin CEP, Mathews RJ, Morgan NY, Smith KGC, Germain RN. Immune complexes stimulate CCR7-dependent dendritic cell migration to lymph nodes. *Nat Med. Nature Publishing Group, a division of Macmillan Publishers Limited. All Rights Reserved.*; 2014;20:1458–63.
 127. Hong CY, Lee H-J, Kim H-J, Lee J-J. The lymphoid chemokine CCL21 enhances the cytotoxic T lymphocyte-inducing functions of dendritic cells. *Scand J Immunol*. 2014;79:173–80.
 128. Thanarajasingam U, Sanz L, Diaz R, Qiao J, Sanchez-Perez L, Kottke T, et al. Delivery of CCL21 to metastatic disease improves the efficacy of adoptive T-cell therapy. *Cancer Res*. 2007;67:300–8.
 129. Sharma S, Stolina M, Luo J, Strieter RM, Burdick M, Zhu LX, et al. Secondary Lymphoid Tissue Chemokine Mediates T Cell-Dependent Antitumor Responses In Vivo. *J Immunol. American Association of Immunologists*; 2000;164:4558–63.
 130. Sharma S, Yang S-C, Hillinger S, Zhu LX, Huang M, Batra RK, et al. SLC/CCL21-mediated anti-tumor responses require IFN γ , MIG/CXCL9 and IP-

- 10/CXCL10. *Mol Cancer*. 2003;2:22.
131. Lu J, Ma J, Cai W, Wangpu X, Feng H, Zhao J, et al. CC motif chemokine ligand 19 suppressed colorectal cancer in vivo accompanied by an increase in IL-12 and IFN- γ . *Biomed Pharmacother*. 2015;69:374–9.
 132. Flanagan K, Moroziewicz D, Kwak H, Hörig H, Kaufman HL. The lymphoid chemokine CCL21 costimulates naive T cell expansion and Th1 polarization of non-regulatory CD4+ T cells. *Cell Immunol*. 2004;231:75–84.
 133. León B, Ballesteros-Tato A, Browning JL, Dunn R, Randall TD, Lund FE. Regulation of T(H)2 development by CXCR5+ dendritic cells and lymphotoxin-expressing B cells. *Nat Immunol*. Nature Publishing Group; 2012;13:681–90.
 134. Luther SA, Lopez T, Bai W, Hanahan D, Cyster JG. BLC Expression in Pancreatic Islets Causes B Cell Recruitment and Lymphotoxin-Dependent Lymphoid Neogenesis. *Immunity*. 2000;12:471–81.
 135. Coelho FM, Natale D, Soriano SF, Hons M, Swoger J, Mayer J, et al. Naive B-cell trafficking is shaped by local chemokine availability and LFA-1-independent stromal interactions. *Blood*. American Society of Hematology; 2013;121:4101–9.
 136. Zhu Z, Zhang X, Guo H, Fu L, Pan G, Sun Y. CXCL13-CXCR5 axis promotes the growth and invasion of colon cancer cells via PI3K/AKT pathway. *Mol Cell Biochem*. 2015;400:287–95.
 137. Zucker S, Vacirca J. Role of matrix metalloproteinases (MMPs) in colorectal cancer. *Cancer Metastasis Rev*. 2004;23:101–17.
 138. Singh S, Singh R, Singh UP, Rai SN, Novakovic KR, Chung LWK, et al. Clinical and biological significance of CXCR5 expressed by prostate cancer specimens and cell lines. *Int J Cancer*. 2009;125:2288–95.
 139. Ammirante M, Shalapour S, Kang Y, Jamieson CAM, Karin M. Tissue injury and

- hypoxia promote malignant progression of prostate cancer by inducing CXCL13 expression in tumor myofibroblasts. *Proc Natl Acad Sci U S A*. 2014;111:14776–81.
140. Singh R, Gupta P, Kloecker GH, Singh S, Lillard JW. Expression and clinical significance of CXCR5/CXCL13 in human non-small cell lung carcinoma. *Int J Oncol*. 2014;45:2232–40.
 141. Panse J, Friedrichs K, Marx A, Hildebrandt Y, Luetkens T, Barrels K, et al. Chemokine CXCL13 is overexpressed in the tumour tissue and in the peripheral blood of breast cancer patients. *Br J Cancer*. 2008;99:930–8.
 142. Biswas S, Sengupta S, Roy Chowdhury S, Jana S, Mandal G, Mandal PK, et al. CXCL13-CXCR5 co-expression regulates epithelial to mesenchymal transition of breast cancer cells during lymph node metastasis. *Breast Cancer Res Treat*. 2014;143:265–76.
 143. Qi X-W, Xia S-H, Yin Y, Jin L-F, Pu Y, Hua D, et al. Expression features of CXCR5 and its ligand, CXCL13 associated with poor prognosis of advanced colorectal cancer [Internet]. *Eur Rev Med Pharmacol Sci*. 2014 [cited 2015 Feb 21]. page 1916–24. Available from: <http://www.ncbi.nlm.nih.gov/pubmed/25010623>
 144. Denkert C, von Minckwitz G, Brase JC, Sinn B V, Gade S, Kronenwett R, et al. Tumor-Infiltrating Lymphocytes and Response to Neoadjuvant Chemotherapy With or Without Carboplatin in Human Epidermal Growth Factor Receptor 2-Positive and Triple-Negative Primary Breast Cancers. *J Clin Oncol*. 2014;JCO.2014.58.1967-.
 145. Razis E, Kalogeras KT, Kotoula V, Eleftheraki AG, Nikitas N, Kronenwett R, et al. Improved outcome of high-risk early HER2 positive breast cancer with high CXCL13-CXCR5 messenger RNA expression. *Clin Breast Cancer*. 2012;12:183–93.

146. Pimenta EM, De S, Weiss R, Feng D, Hall K, Kilic S, et al. IRF5 is a novel regulator of CXCL13 expression in breast cancer that regulates CXCR5(+) B- and T-cell trafficking to tumor-conditioned media. *Immunol Cell Biol.* Australasian Society for Immunology Inc.; 2014;
147. Onder L, Danuser R, Scandella E, Firner S, Chai Q, Hehlgans T, et al. Endothelial cell-specific lymphotoxin- β receptor signaling is critical for lymph node and high endothelial venule formation. *J Exp Med.* Rockefeller Univ Press; 2013;210:465–73.
148. Moussion C, Girard J-P. Dendritic cells control lymphocyte entry to lymph nodes through high endothelial venules. *Nature.* Nature Publishing Group, a division of Macmillan Publishers Limited. All Rights Reserved.; 2011;479:542–6.
149. Marinkovic T, Garin A, Yokota Y, Fu Y-X, Ruddle NH, Furtado GC, et al. Interaction of mature CD3+CD4+ T cells with dendritic cells triggers the development of tertiary lymphoid structures in the thyroid. *J Clin Invest.* American Society for Clinical Investigation; 2006;116:2622–32.
150. Liao S, Ruddle NH. Synchrony of High Endothelial Venules and Lymphatic Vessels Revealed by Immunization. *J Immunol.* 2006;177:3369–79.
151. Sperandio M, Gleissner CA, Ley K. Glycosylation in immune cell trafficking. *Immunol Rev.* 2009;230:97–113.
152. Umemoto E, Tanaka T, Kanda H, Jin S, Tohya K, Otani K, et al. Nepmucin, a novel HEV sialomucin, mediates L-selectin–dependent lymphocyte rolling and promotes lymphocyte adhesion under flow. *J Exp Med.* Rockefeller University Press; 2006;203:1603–14.
153. Suzuki A, Andrew DP, Gonzalo JA, Fukumoto M, Spellberg J, Hashiyama M, et al. CD34-deficient mice have reduced eosinophil accumulation after allergen exposure and show a novel crossreactive 90-kD protein. *Blood.* American Society

- of Hematology; 1996;87:3550–62.
154. Rosen SD. Ligands for L-selectin: homing, inflammation, and beyond. *Annu Rev Immunol. Annual Reviews*; 2004;22:129–56.
 155. Arata-Kawai H, Singer MS, Bistrup A, Zante A van, Wang Y-Q, Ito Y, et al. Functional contributions of N- and O-glycans to L-selectin ligands in murine and human lymphoid organs. *Am J Pathol.* 2011;178:423–33.
 156. Hemmerich S. Sulfation-dependent recognition of high endothelial venules (HEV)-ligands by L-selectin and MECA 79, and adhesion-blocking monoclonal antibody. *J Exp Med.* 1994;180:2219–26.
 157. Lowe JB. Glycosylation, Immunity, and Autoimmunity. *Cell.* 2001;104:809–12.
 158. Kobayashi M, Fukuda M, Nakayama J. Role of sulfated O-glycans expressed by high endothelial venule-like vessels in pathogenesis of chronic inflammatory gastrointestinal diseases. *Biol Pharm Bull.* 2009;32:774–9.
 159. Grunwell JR, Bertozzi CR. Carbohydrate Sulfotransferases of the GalNAc/Gal/GlcNAc6ST Family †. *Biochemistry. American Chemical Society*; 2002;41:13117–26.
 160. Hemmerich S, Bistrup A, Singer MS, van Zante A, Lee JK, Tsay D, et al. Sulfation of L-Selectin Ligands by an HEV-Restricted Sulfotransferase Regulates Lymphocyte Homing to Lymph Nodes. *Immunity. Elsevier*; 2001;15:237–47.
 161. Uchimura K, Kadomatsu K, El-Fasakhany FM, Singer MS, Izawa M, Kannagi R, et al. N-acetylglucosamine 6-O-sulfotransferase-1 regulates expression of L-selectin ligands and lymphocyte homing. *J Biol Chem.* 2004;279:35001–8.
 162. Kawashima H, Hirakawa J, Tobisawa Y, Fukuda M, Saga Y. Conditional gene targeting in mouse high endothelial venules. *J Immunol. American Association of Immunologists*; 2009;182:5461–8.

163. Uchimura K, Gauguier J-M, Singer MS, Tsay D, Kannagi R, Muramatsu T, et al. A major class of L-selectin ligands is eliminated in mice deficient in two sulfotransferases expressed in high endothelial venules. *Nat Immunol.* 2005;6:1105–13.
164. Malý P, Thall AD, Petryniak B, Rogers CE, Smith PL, Marks RM, et al. The $\alpha(1,3)$ Fucosyltransferase Fuc-TVII Controls Leukocyte Trafficking through an Essential Role in L-, E-, and P-selectin Ligand Biosynthesis. *Cell.* 1996;86:643–53.
165. Homeister JW, Thall AD, Petryniak B, Malý P, Rogers CE, Smith PL, et al. The $\alpha(1,3)$ fucosyltransferases FucT-IV and FucT-VII Exert Collaborative Control over Selectin-Dependent Leukocyte Recruitment and Lymphocyte Homing. *Immunity.* 2001;15:115–26.
166. Miyasaka M, Tanaka T. Lymphocyte trafficking across high endothelial venules: dogmas and enigmas. *Nat Rev Immunol.* 2004;4:360–70.
167. Tsuboi K, Hirakawa J, Seki E, Imai Y, Yamaguchi Y, Fukuda M, et al. Role of high endothelial venule-expressed heparan sulfate in chemokine presentation and lymphocyte homing. *J Immunol.* 2013;191:448–55.
168. Berg EL, Robinson MK, Warnock RA, Butcher EC. The human peripheral lymph node vascular addressin is a ligand for LECAM-1, the peripheral lymph node homing receptor. *J Cell Biol.* Rockefeller University Press; 1991;114:343–9.
169. Förster R, Schubel A, Breitfeld D, Kremmer E, Renner-Müller I, Wolf E, et al. CCR7 Coordinates the Primary Immune Response by Establishing Functional Microenvironments in Secondary Lymphoid Organs. *Cell.* 1999;99:23–33.
170. Nelson RM, Cecconi O, Roberts WG, Aruffo A, Linhardt RJ, Bevilacqua MP. Heparin oligosaccharides bind L- and P-selectin and inhibit acute inflammation. *Blood.* American Society of Hematology; 1993;82:3253–8.

171. Michie SA, Streeter PR, Bolt PA, Butcher EC, Picker LJ. The human peripheral lymph node vascular addressin. An inducible endothelial antigen involved in lymphocyte homing. *Am J Pathol.* 1993;143:1688–98.
172. Yang J, Rosen SD, Bendele P, Hemmerich S. Induction of PNA^d and N-acetylglucosamine 6-O-sulfotransferases 1 and 2 in mouse collagen-induced arthritis. *BMC Immunol.* 2006;7:12.
173. Kobayashi M, Hoshino H, Masumoto J, Fukushima M, Suzawa K, Kageyama S, et al. GlcNAc6ST-1-mediated decoration of MAdCAM-1 protein with L-selectin ligand carbohydrates directs disease activity of ulcerative colitis. *Inflamm Bowel Dis.* 2009;15:697–706.
174. Hu D, Mohanta SK, Yin C, Peng L, Ma Z, Srikakulapu P, et al. Artery Tertiary Lymphoid Organs Control Aorta Immunity and Protect against Atherosclerosis via Vascular Smooth Muscle Cell Lymphotoxin β Receptors. *Immunity.* 2015;42:1100–15.
175. Neyt K, Perros F, GeurtsvanKessel CH, Hammad H, Lambrecht BN. Tertiary lymphoid organs in infection and autoimmunity. *Trends Immunol.* 2012;33:297–305.
176. Enarsson K, Johnsson E, Lindholm C, Lundgren A, Pan-Hammarström Q, Strömberg E, et al. Differential mechanisms for T lymphocyte recruitment in normal and neoplastic human gastric mucosa. *Clin Immunol.* 2006;118:24–34.
177. Remark R, Alifano M, Cremer I, Lupo A, Dieu-Nosjean M-C, Riquet M, et al. Characteristics and clinical impacts of the immune environments in colorectal and renal cell carcinoma lung metastases: influence of tumor origin. *Clin Cancer Res.* 2013;19:4079–91.
178. Bento DC, Jones E, Junaid S, Tull J, Williams GT, Godkin A, et al. High endothelial venules are rare in colorectal cancers but accumulate in extra-tumoral

- areas with disease progression. *Oncoimmunology*. Taylor & Francis; 2015;4:e974374.
179. Cipponi A, Mercier M, Seremet T, Baurain J-F, Théate I, van den Oord J, et al. Neogenesis of lymphoid structures and antibody responses occur in human melanoma metastases. *Cancer Res*. 2012;72:3997–4007.
 180. Martinet L, Garrido I, Filleron T, Le Guellec S, Bellard E, Fournie J-J, et al. Human solid tumors contain high endothelial venules: association with T- and B-lymphocyte infiltration and favorable prognosis in breast cancer. *Cancer Res*. 2011;71:5678–87.
 181. van Baren N, Baurain J-F, Coulie PG. Lymphoid neogenesis in melanoma: What does it tell us? *Oncoimmunology*. 2013;2:e22505.
 182. Avram G, Sánchez-Sendra B, Martín JM, Terrádez L, Ramos D, Monteagudo C. The density and type of MECA-79-positive high endothelial venules correlate with lymphocytic infiltration and tumour regression in primary cutaneous melanoma. *Histopathology*. 2013;63:852–61.
 183. Coppola D, Nebozhyn M, Khalil F, Dai H, Yeatman T, Loboda A, et al. Unique ectopic lymph node-like structures present in human primary colorectal carcinoma are identified by immune gene array profiling. *Am J Pathol*. Elsevier; 2011;179:37–45.
 184. Sautès-Fridman C, Lawand M, Giraldo NA, Kaplon H, Germain C, Fridman WH, et al. Tertiary Lymphoid Structures in Cancers: Prognostic Value, Regulation, and Manipulation for Therapeutic Intervention. *Front Immunol*. Frontiers Media SA; 2016;7:407.
 185. Shen H, Wang X, Shao Z, Liu K, Xia X-Y, Zhang H-Z, et al. Alterations of high endothelial venules in primary and metastatic tumors are correlated with lymph node metastasis of oral and pharyngeal carcinoma. *Cancer Biol Ther*. Landes

- Bioscience; 2014;15:342–9.
186. Kobayashi M, Mitoma J, Hoshino H, Yu S-Y, Shimojo Y, Suzawa K, et al. Prominent expression of sialyl Lewis X-capped core 2-branched O-glycans on high endothelial venule-like vessels in gastric MALT lymphoma. *J Pathol.* 2011;224:67–77.
 187. Weinstein AMAM, Storkus WJWJ. Therapeutic Lymphoid Organogenesis in the Tumor Microenvironment. *Adv Cancer Res.* 2015;128:197–233.
 188. Fridman WH, Zitvogel L, Sautès–Fridman C, Kroemer G. The immune contexture in cancer prognosis and treatment. *Nat Rev Clin Oncol.* Nature Publishing Group; 2017;14:717–34.
 189. Stoll G, Enot D, Mlecnik B, Galon J, Zitvogel L, Kroemer G. Immune-related gene signatures predict the outcome of neoadjuvant chemotherapy. *Oncoimmunology.* Taylor & Francis; 2014;3:e27884.
 190. Barton JLL, Herbst R, Bosisio D, Higgins L, Nicklin MJHJ. A tissue specific IL-1 receptor antagonist homolog from the IL-1 cluster lacks IL-1, IL-1ra, IL-18 and IL-18 antagonist activities. *Eur J Immunol.* WILEY-VCH Verlag GmbH; 2000;30:3299–308.
 191. Busfield SJ, Comrack CA, Yu G, Chickering TW, Smutko JS, Zhou H, et al. Identification and gene organization of three novel members of the IL-1 family on human chromosome 2. *Genomics.* 2000;66:213–6.
 192. Towne JE, Renshaw BR, Douangpanya J, Lipsky BP, Shen M, Gabel CA, et al. Interleukin-36 (IL-36) ligands require processing for full agonist (IL-36 α , IL-36 β , and IL-36 γ) or antagonist (IL-36Ra) activity. *J Biol Chem.* 2011;286:42594–602.
 193. van de Veerdonk FL, Stoeckman AK, Wu G, Boeckermann AN, Azam T, Netea MG, et al. IL-38 binds to the IL-36 receptor and has biological effects on immune cells similar to IL-36 receptor antagonist. *Proc Natl Acad Sci U S A.* National

- Academy of Sciences; 2012;109:3001–5.
194. van de Veerdonk FL, Netea MG, Dinarello CA, Joosten LAB. Inflammasome activation and IL-1 β and IL-18 processing during infection. *Trends Immunol.* 2011;32:110–6.
 195. Lian L-H, Milora KA, Manupipatpong KK, Jensen LE. The double-stranded RNA analogue polyinosinic-polycytidylic acid induces keratinocyte pyroptosis and release of IL-36 γ . *J Invest Dermatol. The Society for Investigative Dermatology, Inc;* 2012;132:1346–53.
 196. Bergsbaken T, Fink SL, Cookson BT. Pyroptosis: host cell death and inflammation. *Nat Rev Microbiol. Nature Publishing Group;* 2009;7:99–109.
 197. Bachmann M, Scheiermann P, Härdle L, Pfeilschifter J, Mühl H. IL-36 γ /IL-1F9, an innate T-bet target in myeloid cells. *J Biol Chem.* 2012;287:41684–96.
 198. Li N, Yamasaki K, Saito R, Fukushi-Takahashi S, Shimada-Omori R, Asano M, et al. Alarmin function of cathelicidin antimicrobial peptide LL37 through IL-36 γ induction in human epidermal keratinocytes. *J Immunol. American Association of Immunologists;* 2014;193:5140–8.
 199. Ross R, Grimm J, Goedicke S, Möbus AM, Bulau A-M, Bufler P, et al. Analysis of nuclear localization of interleukin-1 family cytokines by flow cytometry. *J Immunol Methods. Elsevier;* 2013;387:219–27.
 200. Luheshi NM, Rothwell NJ, Brough D. Dual functionality of interleukin-1 family cytokines: implications for anti-interleukin-1 therapy. *Br J Pharmacol. Wiley-Blackwell;* 2009;157:1318–29.
 201. Scheibe K, Backert I, Wirtz S, Hueber A, Schett G, Vieth M, et al. IL-36R signalling activates intestinal epithelial cells and fibroblasts and promotes mucosal healing in vivo. *Gut. BMJ Publishing Group;* 2016;66:823–38.

202. Werman A, Werman-Venkert R, White R, Lee J-K, Werman B, Krelin Y, et al. The precursor form of IL-1alpha is an intracrine proinflammatory activator of transcription. *Proc Natl Acad Sci U S A. National Academy of Sciences*; 2004;101:2434–9.
203. Curtis BM, Widmer MB, deRoos P, Qvarnstrom EE. IL-1 and its receptor are translocated to the nucleus. *J Immunol. American Association of Immunologists*; 1990;144:1295–303.
204. Stevenson FT, Torrano F, Locksley RM, Lovett DH. Interleukin 1: The patterns of translation and intracellular distribution support alternative secretory mechanisms. *J Cell Physiol.* 1992;152:223–31.
205. Qvarnstrom EE, Page RC, Gillis S, Dower SK. Binding, internalization, and intracellular localization of interleukin-1 beta in human diploid fibroblasts. *J Biol Chem.* 1988;263:8261–9.
206. Moussion C, Ortega N, Girard J-P. The IL-1-Like Cytokine IL-33 Is Constitutively Expressed in the Nucleus of Endothelial Cells and Epithelial Cells In Vivo: A Novel “Alarmin”? Unutmaz D, editor. *PLoS One. Public Library of Science*; 2008;3:e3331.
207. Carriere V, Roussel L, Ortega N, Lacorre D-A, Americh L, Aguilar L, et al. IL-33, the IL-1-like cytokine ligand for ST2 receptor, is a chromatin-associated nuclear factor in vivo. *Proc Natl Acad Sci.* 2007;104:282–7.
208. Sharma S, Kulk N, Nold MF, Gräf R, Kim S-H, Reinhardt D, et al. The IL-1 family member 7b translocates to the nucleus and down-regulates proinflammatory cytokines. *J Immunol. American Association of Immunologists*; 2008;180:5477–82.
209. POLLOCK AS, TURCK J, LOVETT DH. The prodomain of interleukin 1 α interacts with elements of the RNA processing apparatus and induces apoptosis in

- malignant cells. *FASEB J.* 2003;17:203–13.
210. Gresnigt MS, van de Veerdonk FL. Biology of IL-36 cytokines and their role in disease. *Semin Immunol.* 2013;25:458–65.
211. Blumberg H, Dinh H, Trueblood ES, Pretorius J, Kugler D, Weng N, et al. Opposing activities of two novel members of the IL-1 ligand family regulate skin inflammation. *J Exp Med.* Rockefeller University Press; 2007;204:2603–14.
212. Bochkov YA, Hanson KM, Keles S, Brockman-Schneider RA, Jarjour NN, Gern JE. Rhinovirus-induced modulation of gene expression in bronchial epithelial cells from subjects with asthma. *Mucosal Immunol.* NIH Public Access; 2010;3:69–80.
213. Vos JB, van Sterkenburg MA, Rabe KF, Schalkwijk J, Hiemstra PS, Datson NA. Transcriptional response of bronchial epithelial cells to *Pseudomonas aeruginosa*: identification of early mediators of host defense. *Physiol Genomics.* American Physiological Society; 2005;21:324–36.
214. Takahashi K, Nishida A, Shioya M, Imaeda H, Bamba S, Inatomi O, et al. Interleukin (IL)-1 β Is a Strong Inducer of IL-36 γ Expression in Human Colonic Myofibroblasts. Hu W, editor. *Public Library of Science*; 2015;10:e0138423.
215. Boutet M-A, Bart G, Penhoat M, Amiaud J, Brulin B, Charrier C, et al. Distinct expression of interleukin (IL)-36 α , β and γ , their antagonist IL-36Ra and IL-38 in psoriasis, rheumatoid arthritis and Crohn's disease. *Clin Exp Immunol.* 2016;184:159–73.
216. Lamacchia C, Palmer G, Rodriguez E, Martin P, Vigne S, Seemayer CA, et al. The severity of experimental arthritis is independent of IL-36 receptor signaling. *Arthritis Res Ther.* 2013;15:R38.
217. Chustz RT, Nagarkar DR, Poposki JA, Favoreto S, Avila PC, Schleimer RP, et al. Regulation and function of the IL-1 family cytokine IL-1F9 in human bronchial epithelial cells. *Am J Respir Cell Mol Biol.* 2011;45:145–53.

218. Russell SE, Horan RM, Stefanska AM, Carey A, Leon G, Aguilera M, et al. IL-36 α expression is elevated in ulcerative colitis and promotes colonic inflammation. *Mucosal Immunol*. Nature Publishing Group; 2016;9:1193–204.
219. Barnes SE, Wang Y, Chen L, Molinero LL, Gajewski TF, Evaristo C, et al. T cell-NF- κ B activation is required for tumor control in vivo. *J Immunother Cancer*. BioMed Central Ltd; 2015;3:1.
220. Vigne S, Palmer G, Lamacchia C, Martin P, Talabot-Ayer D, Rodriguez E, et al. IL-36R ligands are potent regulators of dendritic and T cells. *Blood*. American Society of Hematology; 2011;118:5813–23.
221. Foster AM, Baliwag J, Chen CS, Guzman AM, Stoll SW, Gudjonsson JE, et al. IL-36 promotes myeloid cell infiltration, activation, and inflammatory activity in skin. *J Immunol*. American Association of Immunologists; 2014;192:6053–61.
222. Vigne S, Palmer G, Martin P, Lamacchia C, Strebel D, Rodriguez E, et al. IL-36 signaling amplifies Th1 responses by enhancing proliferation and Th1 polarization of naive CD4⁺ T cells. *Blood*. American Society of Hematology; 2012;120:3478–87.
223. Wang X, Zhao X, Feng C, Weinstein A, Xia R, Wen W, et al. IL-36 γ transforms the tumor microenvironment and promotes type 1 lymphocyte-mediated antitumor immune responses. *Cancer Cell*. 2015;28.
224. Tsurutani N, Mittal P, St. Rose M-C, Ngoi SM, Svedova J, Menoret A, et al. Costimulation Endows Immunotherapeutic CD8 T Cells with IL-36 Responsiveness during Aerobic Glycolysis. *J Immunol*. American Association of Immunologists; 2016;196:124–34.
225. Mutamba S, Allison A, Mahida Y, Barrow P, Foster N. Expression of IL-1Rrp2 by human myelomonocytic cells is unique to DCs and facilitates DC maturation by IL-1F8 and IL-1F9. *Eur J Immunol*. 2012;42:607–17.

226. Arakawa A, Vollmer S, Besgen P, Summer B, Ruzicka T, Thomas P, et al. 310 Unopposed IL-36 activity promotes clonal CD4 + T-cell responses with IL-17A production in generalized pustular psoriasis. *J Invest Dermatol*. Elsevier; 2017;137:S246.
227. Bozoyan L, Dumas A, Patenaude A, Vallières L. Interleukin-36 γ is expressed by neutrophils and can activate microglia, but has no role in experimental autoimmune encephalomyelitis. *J Neuroinflammation*. BioMed Central; 2015;12:173.
228. Dietrich D, Martin P, Flacher V, Sun Y, Jarrossay D, Brembilla N, et al. Interleukin-36 potently stimulates human M2 macrophages, Langerhans cells and keratinocytes to produce pro-inflammatory cytokines. *Cytokine*. Academic Press; 2016;84:88–98.
229. Tortola L, Rosenwald E, Abel B, Blumberg H, Schäfer M, Coyle AJ, et al. Psoriasiform dermatitis is driven by IL-36-mediated DC-keratinocyte crosstalk. *J Clin Invest*. American Society for Clinical Investigation; 2012;122:3965–76.
230. Kovach MA, Singer BH, Newstead MW, Zeng X, Moore TA, White ES, et al. IL-36 γ is secreted in microparticles and exosomes by lung macrophages in response to bacteria and bacterial components. *J Leukoc Biol*. 2016;100:413–21.
231. Aoyagi T, Newstead MW, Zeng X, Nanjo Y, Peters-Golden M, Kaku M, et al. Interleukin-36 γ and IL-36 receptor signaling mediate impaired host immunity and lung injury in cytotoxic *Pseudomonas aeruginosa* pulmonary infection: Role of prostaglandin E2. Zamboni DS, editor. *PLOS Pathog*. Public Library of Science; 2017;13:e1006737.
232. Debets R, Timans JC, Homey B, Zurawski S, Sana TR, Lo S, et al. Two Novel IL-1 Family Members, IL-1 β and IL-1 δ , Function as an Antagonist and Agonist of NF- κ B Activation Through the Orphan IL-1 Receptor-Related Protein 2. *J Immunol*. American Association of Immunologists; 2001;167:1440–6.

233. Garzorz-Stark N, Lauffer F, Krause L, Thomas J, Atenhan A, Franz R, et al. Toll-like receptor 7/8 agonists stimulate plasmacytoid dendritic cells to initiate T H 17-deviated acute contact dermatitis in human subjects. *J Allergy Clin Immunol*. 2017;
234. Wang H, Li Z-Y, Jiang W-X, Liao B, Zhai G-T, Wang N, et al. The activation and function of IL-36 γ in neutrophilic inflammation in chronic rhinosinusitis. *J Allergy Clin Immunol*. Elsevier; 2017;0.
235. Harusato A, Abo H, Ngo VL, Yi SW, Mitsutake K, Osuka S, et al. IL-36 γ signaling controls the induced regulatory T cell–Th9 cell balance via NF κ B activation and STAT transcription factors. *Mucosal Immunol*. 2017;10:1455–67.
236. Chu M, Tam LS, Zhu J, Jiao D, Liu DH, Cai Z, et al. In vivo anti-inflammatory activities of novel cytokine IL-38 in Murphy Roths Large (MRL)/lpr mice. *Immunobiology*. 2017;222:483–93.
237. Penha R, Higgins J, Mutamba S, Barrow P, Mahida Y, Foster N. IL-36 receptor is expressed by human blood and intestinal T lymphocytes and is dose-dependently activated via IL-36 β and induces CD4 $^{+}$ lymphocyte proliferation. *Cytokine*. Academic Press; 2016;85:18–25.
238. Gresnigt MS, Rösler B, Jacobs CWM, Becker KL, Joosten LAB, van der Meer JWM, et al. The IL-36 receptor pathway regulates *Aspergillus fumigatus*-induced Th1 and Th17 responses. *Eur J Immunol*. 2013;43:416–26.
239. Turtoi A, Brown I, Schläger M, Schneeweiss FHA. Gene Expression Profile of Human Lymphocytes Exposed to 211 At α Particles. *Radiat Res*. The Radiation Research Society ; 2010;174:125–36.
240. Tsurutani N, Mittal P, St. Rose M-C, Ngoi SM, Svedova J, Menoret A, et al. Costimulation Endows Immunotherapeutic CD8 T Cells with IL-36 Responsiveness during Aerobic Glycolysis. *J Immunol*. 2015;

241. Ciccia F, Accardo-Palumbo A, Alessandro R, Alessandri C, Priori R, Guggino G, et al. Interleukin-36 α axis is modulated in patients with primary Sjögren's syndrome. *Clin Exp Immunol*. Wiley-Blackwell; 2015;181:230–8.
242. Renert-Yuval Y, Horev L, Babay S, Tams S, Ramot Y, Zlotogorski A, et al. IL36RN mutation causing generalized pustular psoriasis in a Palestinian patient. *Int J Dermatol*. 2014;53:866–8.
243. Navarini AA, Valeyrie-Allanore L, Setta-Kaffetzi N, Barker JN, Capon F, Creamer D, et al. Rare variations in IL36RN in severe adverse drug reactions manifesting as acute generalized exanthematous pustulosis. *J Invest Dermatol*. The Society for Investigative Dermatology, Inc; 2013;133:1904–7.
244. Nakai N, Sugiura K, Akiyama M, Katoh N. Acute Generalized Exanthematous Pustulosis Caused by Dihydrocodeine Phosphate in a Patient With Psoriasis Vulgaris and a Heterozygous IL36RN Mutation. *JAMA dermatology*. 2014;
245. He Q, Chen H, Li W, Wu Y, Chen S, Yue Q, et al. IL-36 cytokine expression and its relationship with p38 MAPK and NF- κ B pathways in psoriasis vulgaris skin lesions. *J Huazhong Univ Sci Technolog Med Sci*. 2013;33:594–9.
246. Johnston A, Xing X, Guzman AM, Riblett M, Loyd CM, Ward NL, et al. IL-1F5, -F6, -F8, and -F9: a novel IL-1 family signaling system that is active in psoriasis and promotes keratinocyte antimicrobial peptide expression. *J Immunol*. 2011;186:2613–22.
247. Medina-Contreras O, Harusato A, Nishio H, Flannigan KL, Ngo V, Leoni G, et al. Cutting Edge: IL-36 Receptor Promotes Resolution of Intestinal Damage. *J Immunol*. American Association of Immunologists; 2016;196:34–8.
248. Frey S, Derer A, Messbacher M-E, Baeten DLP, Bugatti S, Montecucco C, et al. The novel cytokine interleukin-36 α is expressed in psoriatic and rheumatoid arthritis synovium. *Ann Rheum Dis*. 2013;72:1569–74.

249. Derer A, Groetsch B, Harre U, Böhm C, Towne J, Schett G, et al. Blockade of IL-36 receptor signaling does not prevent from TNF-induced arthritis. *PLoS One*. 2014;9:e101954.
250. Roychoudhuri R, Eil RL, Restifo NP. The interplay of effector and regulatory T cells in cancer. *Curr Opin Immunol*. 2015;33:101–11.
251. Parker KH, Beury DW, Ostrand-Rosenberg S. Myeloid-Derived Suppressor Cells: Critical Cells Driving Immune Suppression in the Tumor Microenvironment. *Adv Cancer Res*. NIH Public Access; 2015;128:95–139.
252. Whiteside TL. Clinical Impact of Regulatory T cells (Treg) in Cancer and HIV. *Cancer Microenviron*. Springer; 2015;8:201–7.
253. Teng MWL, Ngiow SF, Ribas A, Smyth MJ. Classifying Cancers Based on T-cell Infiltration and PD-L1. *Cancer Res*. 2015;75.
254. Bruno TC, French JD, Jordan KR, Ramirez O, Sippel TR, Borges VF, et al. Influence of human immune cells on cancer: studies at the University of Colorado. *Immunol Res*. NIH Public Access; 2013;55:22–33.
255. Nosho K, Baba Y, Tanaka N, Shima K, Hayashi M, Meyerhardt JA, et al. Tumour-infiltrating T-cell subsets, molecular changes in colorectal cancer, and prognosis: cohort study and literature review. *J Pathol*. NIH Public Access; 2010;222:350–66.
256. Josien R, Li H-L, Ingulli E, Sarma S, R.Wong B, Vologodskaja M, et al. Trance, a Tumor Necrosis Factor Family Member, Enhances the Longevity and Adjuvant Properties of Dendritic Cells in Vivo. *J Exp Med*. 2000;191.
257. Angeli V, Randolph GJ. Inflammation, Lymphatic Function, And Dendritic Cell Migration. *Lymphat Res Biol*. 2006;4:217–28.
258. Knight SC. Dendritic cells in contact sensitivity. *Res Immunol*. 140:907-10-26.

259. Fridman W-H, Dieu-Nosjean M-C, Pagès F, Cremer I, Damotte D, Sautès-Fridman C, et al. The immune microenvironment of human tumors: general significance and clinical impact. *Cancer Microenviron.* Springer; 2013;6:117–22.
260. Tseng WW, Malu S, Zhang M, Chen J, Sim GC, Wei W, et al. Analysis of the Intratumoral Adaptive Immune Response in Well Differentiated and Dedifferentiated Retroperitoneal Liposarcoma. *Sarcoma.* Hindawi Publishing Corporation; 2015;2015:1–9.
261. Ruddle NH. Lymphatic vessels and tertiary lymphoid organs. *J Clin Invest.* American Society for Clinical Investigation; 2014;124:953–9.
262. Dieu-Nosjean M-C, Goc J, Giraldo NA, Sautès-Fridman C, Fridman WH. Tertiary lymphoid structures in cancer and beyond. *Trends Immunol.* Elsevier; 2014;35:571–80.
263. Astorri E, Bombardieri M, Gabba S, Peakman M, Pozzilli P, Pitzalis C. Evolution of Ectopic Lymphoid Neogenesis and In Situ Autoantibody Production in Autoimmune Nonobese Diabetic Mice: Cellular and Molecular Characterization of Tertiary Lymphoid Structures in Pancreatic Islets. *J Immunol.* 2010;185:3359–68.
264. Noort AR, van Zoest KPM, van Baarsen LG, Maracle CX, Helder B, Papazian N, et al. Tertiary Lymphoid Structures in Rheumatoid Arthritis: NF- κ B–Inducing Kinase–Positive Endothelial Cells as Central Players. *Am J Pathol.* 2015;185:1935–43.
265. Warnock RA, Askari S, Butcher EC, Andrian UH von. Molecular Mechanisms of Lymphocyte Homing to Peripheral Lymph Nodes. *J Exp Med.* 1998;187.
266. Lipscomb MW, Chen L, Taylor JL, Goldbach C, Watkins SC, Kalinski P, et al. Ectopic T-bet expression licenses dendritic cells for IL-12-independent priming of type 1 T cells in vitro. *J Immunol.* American Association of Immunologists; 2009;183:7250–8.

267. Carrier Y, Ma H-L, Ramon HE, Napierata L, Small C, O'Toole M, et al. Inter-regulation of Th17 cytokines and the IL-36 cytokines in vitro and in vivo: implications in psoriasis pathogenesis. *J Invest Dermatol. The Society for Investigative Dermatology, Inc*; 2011;131:2428–37.
268. Cañete JD, Santiago B, Cantaert T, Sanmartí R, Palacin A, Celis R, et al. Ectopic lymphoid neogenesis in psoriatic arthritis. *Ann Rheum Dis. BMJ Publishing Group*; 2007;66:720–6.
269. Banks TA, Rouse BT, Kerley MK, Blair PJ, Godfrey VL, Kuklin NA, et al. Lymphotoxin-alpha-deficient mice. Effects on secondary lymphoid organ development and humoral immune responsiveness. *J Immunol.* 1995;155.
270. Joshi NS, Akama-Garren EH, Lu Y, Lee D-Y, Chang GP, Li A, et al. Regulatory T Cells in Tumor-Associated Tertiary Lymphoid Structures Suppress Anti-tumor T Cell Responses. *Immunity.* 2015;43:579–90.
271. Crotty S. T follicular helper cell differentiation, function, and roles in disease. *Immunity. NIH Public Access*; 2014;41:529–42.
272. Cook KD, Kline HC, Whitmire JK. NK cells inhibit humoral immunity by reducing the abundance of CD4+ T follicular helper cells during a chronic virus infection. *J Leukoc Biol. The Society for Leukocyte Biology*; 2015;98:153–62.
273. Lande R, Chamilos G, Ganguly D, Demaria O, Frasca L, Durr S, et al. Cationic antimicrobial peptides in psoriatic skin cooperate to break innate tolerance to self-DNA. *Eur J Immunol.* 2015;45:203–13.
274. Towne J, Sims J. IL-36 in psoriasis. *Curr Opin Pharmacol.* 2012;12:486–90.
275. Zhu J, Jankovic D, Oler AJ, Wei G, Sharma S, Hu G, et al. The Transcription Factor T-bet Is Induced by Multiple Pathways and Prevents an Endogenous Th2 Cell Program during Th1 Cell Responses. *Immunity. Elsevier*; 2012;37:660–73.

276. Cardiff RD, Miller CH, Munn RJ. Manual Hematoxylin and Eosin Staining of Mouse Tissue Sections. *Cold Spring Harb Protoc.* 2014;2014:pdb.prot073411-prot073411.
277. Jorgensen ML, Young JM, Solomon MJ. Optimal delivery of colorectal cancer follow-up care: improving patient outcomes. *Patient Relat Outcome Meas.* Dove Press; 2015;6:127–38.
278. Siegel RL, Miller KD, Fedewa SA, Ahnen DJ, Meester RGS, Barzi A, et al. Colorectal cancer statistics, 2017. *CA Cancer J Clin.* 2017;67:177–93.
279. Ribassin-Majed L, Le Teuff G, Hill C. La fréquence des cancers en 2016 et leur évolution. *Bull Cancer.* Elsevier Masson; 2017;104:20–9.
280. Iqbal A, George TJ. Randomized Clinical Trials in Colon and Rectal Cancer. *Surg Oncol Clin N Am.* Elsevier; 2017;26:689–704.
281. Towne JE, Garka KE, Renshaw BR, Virca GD, Sims JE. Interleukin (IL)-1F6, IL-1F8, and IL-1F9 signal through IL-1Rrp2 and IL-1RAcP to activate the pathway leading to NF-kappaB and MAPKs. *J Biol Chem.* 2004;279:13677–88.
282. Bridgewood C, Stacey M, Alase A, Lagos D, Graham A, Wittmann M. IL-36 γ has proinflammatory effects on human endothelial cells. *Exp Dermatol.* 2017;26:402–8.
283. Guinney J, Dienstmann R, Wang X, de Reyniès A, Schlicker A, Soneson C, et al. The consensus molecular subtypes of colorectal cancer. *Nat Med. Nature Research;* 2015;21:1350–6.
284. Dieu-Nosjean M-C, Giraldo NA, Kaplon H, Germain C, Fridman WH, Sautès-Fridman C. Tertiary lymphoid structures, drivers of the anti-tumor responses in human cancers. *Immunol Rev.* 2016;271:260–75.
285. Gatto D, Brink R. The germinal center reaction. *J Allergy Clin Immunol.* Elsevier;

2010;126:898-907-9.

286. Marisa L, de Reyniès A, Duval A, Selves J, Gaub MP, Vescovo L, et al. Gene expression classification of colon cancer into molecular subtypes: characterization, validation, and prognostic value. *PLoS Med. Public Library of Science*; 2013;10:e1001453.
287. McCall MN, Bolstad BM, Irizarry RA. *Frozen robust multiarray analysis (fRMA)*. *Biostatistics*. Oxford University Press; 2010;11:242–53.
288. Becht E, Giraldo NA, Lacroix L, Buttard B, Elarouci N, Petitprez F, et al. Estimating the population abundance of tissue-infiltrating immune and stromal cell populations using gene expression. *Genome Biol. BioMed Central*; 2016;17:218.
289. Giraldo NA, Becht E, Vano Y, Petitprez F, Lacroix L, Validire P, et al. Tumor-Infiltrating and Peripheral Blood T-cell Immunophenotypes Predict Early Relapse in Localized Clear Cell Renal Cell Carcinoma. *Clin Cancer Res*. 2017;23:4416–28.
290. Roederer M, Nozzi JL, Nason MC. SPICE: exploration and analysis of post-cytometric complex multivariate datasets. *Cytometry A. NIH Public Access*; 2011;79:167–74.
291. Becht E, de Reyniès A, Giraldo NA, Pilati C, Buttard B, Lacroix L, et al. Immune and Stromal Classification of Colorectal Cancer Is Associated with Molecular Subtypes and Relevant for Precision Immunotherapy. *Clin Cancer Res. American Association for Cancer Research*; 2016;22:4057–66.
292. Ha SY, Yeo S-Y, Xuan Y, Kim S-H. The prognostic significance of cancer-associated fibroblasts in esophageal squamous cell carcinoma. *PLoS One. Public Library of Science*; 2014;9:e99955.
293. Guedj K, Khallou-Laschet J, Clement M, Morvan M, Gaston A-T, Fornasa G, et al. M1 macrophages act as LT β R-independent lymphoid tissue inducer cells during

- atherosclerosis-related lymphoid neogenesis. *Cardiovasc Res*. Oxford University Press; 2014;101:434–43.
294. Kanda T, Nishida A, Takahashi K, Hidaka K, Imaeda H, Inatomi O, et al. Interleukin(IL)-36 α and IL-36 γ Induce Proinflammatory Mediators from Human Colonic Subepithelial Myofibroblasts. *Front Med*. 2015;2:69.
295. Wynn TA, Vannella KM. Macrophages in Tissue Repair, Regeneration, and Fibrosis. *Immunity*. NIH Public Access; 2016;44:450–62.
296. Dvorak HF. Tumors: wounds that do not heal-redux. *Cancer Immunol Res*. NIH Public Access; 2015;3:1–11.
297. Rybinski B, Franco-Barraza J, Cukierman E. The wound healing, chronic fibrosis, and cancer progression triad. *Physiol Genomics*. American Physiological Society; 2014;46:223–44.
298. Cirri P, Chiarugi P. Cancer associated fibroblasts: the dark side of the coin. *Am J Cancer Res*. e-Century Publishing Corporation; 2011;1:482–97.
299. Kendall RT, Feghali-Bostwick CA. Fibroblasts in fibrosis: novel roles and mediators. *Front Pharmacol*. 2014;5:123.
300. Yeung TM, Buskens C, Wang LM, Mortensen NJ, Bodmer WF. Myofibroblast activation in colorectal cancer lymph node metastases. *Br J Cancer*. Nature Publishing Group; 2013;108:2106–15.
301. Wang Z-S, Cong Z-J, Luo Y, Mu Y-F, Qin S-L, Zhong M, et al. Decreased expression of interleukin-36 α predicts poor prognosis in colorectal cancer patients. *Int J Clin Exp Pathol*. e-Century Publishing Corporation; 2014;7:8077–81.
302. Barksby HE, Nile CJ, Jaedicke KM, Taylor JJ, Preshaw PM. Differential expression of immunoregulatory genes in monocytes in response to

- Porphyromonas gingivalis and Escherichia coli lipopolysaccharide. Clin Exp Immunol. Wiley-Blackwell; 2009;156:479–87.
303. Smith JJ, Deane NG, Wu F, Merchant NB, Zhang B, Jiang A, et al. Experimentally derived metastasis gene expression profile predicts recurrence and death in patients with colon cancer. Gastroenterology. NIH Public Access; 2010;138:958–68.
304. Mizuno H, Kitada K, Nakai K, Sarai A. PrognScan: a new database for meta-analysis of the prognostic value of genes. BMC Med Genomics. BioMed Central; 2009;2:18.
305. Sharda DR, Yu S, Ray M, Squadrito ML, De Palma M, Wynn TA, et al. Regulation of macrophage arginase expression and tumor growth by the Ron receptor tyrosine kinase. J Immunol. NIH Public Access; 2011;187:2181–92.
306. Wink DA, Hines HB, Cheng RYS, Switzer CH, Flores-Santana W, Vitek MP, et al. Nitric oxide and redox mechanisms in the immune response. J Leukoc Biol. The Society for Leukocyte Biology; 2011;89:873–91.
307. Lu G, Zhang R, Geng S, Peng L, Jayaraman P, Chen C, et al. Myeloid cell-derived inducible nitric oxide synthase suppresses M1 macrophage polarization. Nat Commun. Nature Publishing Group; 2015;6:6676.
308. Ekmekcioglu S, Grimm EA, Roszik J. Targeting iNOS to increase efficacy of immunotherapies. Hum Vaccin Immunother. Taylor & Francis; 2017;13:1105–8.
309. Van den Bossche J, Baardman J, Otto NA, van der Velden S, Neele AE, van den Berg SM, et al. Mitochondrial Dysfunction Prevents Repolarization of Inflammatory Macrophages. Cell Rep. Elsevier; 2016;17:684–96.
310. Afonina IS, Müller C, Martin SJ, Beyaert R. Proteolytic Processing of Interleukin-1 Family Cytokines: Variations on a Common Theme. Immunity. 2015;42:991–1004.

311. Thompson ED, Enriquez HL, Fu Y-X, Engelhard VH. Tumor masses support naive T cell infiltration, activation, and differentiation into effectors. *J Exp Med*. Rockefeller University Press; 2010;207:1791–804.
312. Henry CM, Sullivan GP, Clancy DM, Afonina IS, Kulms D, Martin SJ. Neutrophil-Derived Proteases Escalate Inflammation through Activation of IL-36 Family Cytokines. *Cell Rep*. 2016;14:708–22.
313. Schrama D, Straten P, Fischer WH, McLellan AD, Bröcker E-B, Reisfeld RA, et al. Targeting of Lymphotoxin- α to the Tumor Elicits an Efficient Immune Response Associated with Induction of Peripheral Lymphoid-like Tissue. *Immunity*. Elsevier; 2001;14:111–21.
314. Yu P, Fu Y-X. Targeting tumors with LIGHT to generate metastasis-clearing immunity. *Cytokine Growth Factor Rev*. 19:285–94.
315. Jiang W, Chen R, Kong X, Long F, Shi Y. Immunization with adenovirus LIGHT-engineered dendritic cells induces potent T cell responses and therapeutic immunity in HBV transgenic mice. *Vaccine*. 2014;32:4565–70.
316. Wengner AM, Höpken UE, Petrow PK, Hartmann S, Schurigt U, Bräuer R, et al. CXCR5- and CCR7-dependent lymphoid neogenesis in a murine model of chronic antigen-induced arthritis. *Arthritis Rheum*. 2007;56:3271–83.
317. Winter S, Loddenkemper C, Aebischer A, Räbel K, Hoffmann K, Meyer TF, et al. The chemokine receptor CXCR5 is pivotal for ectopic mucosa-associated lymphoid tissue neogenesis in chronic *Helicobacter pylori*-induced inflammation. *J Mol Med (Berl)*. Springer; 2010;88:1169–80.
318. Litsiou E, Semitekolou M, Galani IE, Morianos I, Tsoutsas A, Kara P, et al. CXCL13 Production in B Cells via Toll-like Receptor/Lymphotoxin Receptor Signaling Is Involved in Lymphoid Neogenesis in Chronic Obstructive Pulmonary Disease. *Am J Respir Crit Care Med*. 2013;187:1194–202.

319. Hsu RYC, Chan CHF, Spicer JD, Rousseau MC, Giannias B, Rousseau S, et al. LPS-induced TLR4 signaling in human colorectal cancer cells increases beta1 integrin-mediated cell adhesion and liver metastasis. *Cancer Res. American Association for Cancer Research*; 2011;71:1989–98.
320. Zhu G, Huang Q, Huang Y, Zheng W, Hua J, Yang S, et al. Lipopolysaccharide increases the release of VEGF-C that enhances cell motility and promotes lymphangiogenesis and lymphatic metastasis through the TLR4- NF- κ B/JNK pathways in colorectal cancer. *Oncotarget. Impact Journals, LLC*; 2016;7:73711–24.
321. Qi X-W, Xia S-H, Yin Y, Jin L-F, Pu Y, Hua D, et al. Expression features of CXCR5 and its ligand, CXCL13 associated with poor prognosis of advanced colorectal cancer. *Eur Rev Med Pharmacol Sci*. 2014;18:1916–24.
322. Mahmoudi M, Farokhzad OC. Cancer immunotherapy: Wound-bound checkpoint blockade. *Nat Biomed Eng. Nature Publishing Group*; 2017;1:31.
323. Alsaab HO, Sau S, Alzhrani R, Tatiparti K, Bhise K, Kashaw SK, et al. PD-1 and PD-L1 Checkpoint Signaling Inhibition for Cancer Immunotherapy: Mechanism, Combinations, and Clinical Outcome. *Front Pharmacol. Frontiers Media SA*; 2017;8:561.
324. Le DT, Uram JN, Wang H, Bartlett BR, Kemberling H, Eyring AD, et al. PD-1 Blockade in Tumors with Mismatch-Repair Deficiency. *N Engl J Med. NIH Public Access*; 2015;372:2509–20.
325. Passardi A, Canale M, Valgiusti M, Ulivi P. Immune Checkpoints as a Target for Colorectal Cancer Treatment. *Int J Mol Sci. Multidisciplinary Digital Publishing Institute (MDPI)*; 2017;18.
326. Singh PP, Sharma PK, Krishnan G, Lockhart AC. Immune checkpoints and immunotherapy for colorectal cancer. *Gastroenterol Rep. Oxford University Press*;

2015;3:gov053.

327. El Osta B, Hu F, Sadek R, Chintalapally R, Tang S-C. Not all immune-checkpoint inhibitors are created equal: Meta-analysis and systematic review of immune-related adverse events in cancer trials. *Crit Rev Oncol Hematol*. Elsevier; 2017;119:1–12.
328. Chung KY, Gore I, Fong L, Venook A, Beck SB, Dorazio P, et al. Phase II Study of the Anti-Cytotoxic T-Lymphocyte–Associated Antigen 4 Monoclonal Antibody, Tremelimumab, in Patients With Refractory Metastatic Colorectal Cancer. *J Clin Oncol*. 2010;28:3485–90.
329. Topalian SL, Hodi FS, Brahmer JR, Gettinger SN, Smith DC, McDermott DF, et al. Safety, Activity, and Immune Correlates of Anti–PD-1 Antibody in Cancer. *N Engl J Med*. 2012;366:2443–54.
330. Gresnigt MS, Rösler B, Jacobs CWM, Becker KL, Joosten LAB, van der Meer JWM, et al. The IL-36 receptor pathway regulates *Aspergillus fumigatus*-induced Th1 and Th17 responses. *Eur J Immunol*. 2013;43:416–26.
331. Kovach MA, Singer B, Martinez-Colon G, Newstead MW, Zeng X, Mancuso P, et al. IL-36 γ is a crucial proximal component of protective type-1-mediated lung mucosal immunity in Gram-positive and -negative bacterial pneumonia. *Mucosal Immunol*. Nature Publishing Group; 2017;10:1320–34.
332. Chustz RT, Nagarkar DR, Poposki JA, Favoreto S, Avila PC, Schleimer RP, et al. Regulation and Function of the IL-1 Family Cytokine IL-1F9 in Human Bronchial Epithelial Cells. *Am J Respir Cell Mol Biol*. American Thoracic Society; 2011;45:145–53.
333. Palamara F, Meindl S, Holcman M, Lührs P, Stingl G, Sibilina M. Identification and characterization of pDC-like cells in normal mouse skin and melanomas treated with imiquimod. *J Immunol*. 2004;173:3051–61.

334. Drobits B, Holcman M, Amberg N, Swiecki M, Grundtner R, Hammer M, et al. Imiquimod clears tumors in mice independent of adaptive immunity by converting pDCs into tumor-killing effector cells. *J Clin Invest. American Society for Clinical Investigation*; 2012;122:575–85.
335. Koizumi S, Masuko K, Wakita D, Tanaka S, Mitamura R, Kato Y, et al. Extracts of *Larix Leptolepis* effectively augments the generation of tumor antigen-specific cytotoxic T lymphocytes via activation of dendritic cells in TLR-2 and TLR-4-dependent manner. *Cell Immunol. Academic Press*; 2012;276:153–61.
336. Plowman J, Narayanan VL, Dykes D, Szarvasi E, Briet P, Yoder OC, et al. Flavone acetic acid: a novel agent with preclinical antitumor activity against colon adenocarcinoma 38 in mice. *Cancer Treat Rep.* 1986;70:631–5.
337. Corrales L, Glickman LH, McWhirter SM, Kanne DB, Sivick KE, Katibah GE, et al. Direct Activation of STING in the Tumor Microenvironment Leads to Potent and Systemic Tumor Regression and Immunity. *Cell Rep. NIH Public Access*; 2015;11:1018–30.
338. Andzinski L, Spanier J, Kasnitz N, Kröger A, Jin L, Brinkmann MM, et al. Growing tumors induce a local STING dependent Type I IFN response in dendritic cells. *Int J cancer.* 2016;139:1350–7.
339. Li K, Qu S, Chen X, Wu Q, Shi M. Promising Targets for Cancer Immunotherapy: TLRs, RLRs, and STING-Mediated Innate Immune Pathways. *Int J Mol Sci. Multidisciplinary Digital Publishing Institute (MDPI)*; 2017;18.
340. Kaczanowska S, Joseph AM, Davila E. TLR agonists: our best frenemy in cancer immunotherapy. *J Leukoc Biol. The Society for Leukocyte Biology*; 2013;93:847–63.
341. Kuroda K, Okumura K, Isogai H, Isogai E. The Human Cathelicidin Antimicrobial Peptide LL-37 and Mimics are Potential Anticancer Drugs. *Front Oncol. Frontiers*

- Media SA; 2015;5:144.
342. Cheng M, Ho S, Yoo JH, Tran DH-Y, Bakirtzi K, Su B, et al. Cathelicidin suppresses colon cancer development by inhibition of cancer associated fibroblasts. *Clin Exp Gastroenterol*. Dove Press; 2015;8:13–29.
 343. Li D, Liu W, Wang X, Wu J, Quan W, Yao Y, et al. Cathelicidin, an antimicrobial peptide produced by macrophages, promotes colon cancer by activating the Wnt/ β -catenin pathway. *Oncotarget*. Impact Journals, LLC; 2015;6:2939–50.
 344. Amaria RN. Intratumoral Injections of LL37 for Melanoma - Full Text View - ClinicalTrials.gov [Internet]. ClinicalTrials.gov. [cited 2018 Feb 19]. Available from: <https://clinicaltrials.gov/ct2/show/NCT02225366>
 345. Deslouches B, Di YP. Antimicrobial peptides with selective antitumor mechanisms: prospect for anticancer applications. *Oncotarget*. Impact Journals, LLC; 2017;8:46635–51.
 346. Gad E, Rastetter L, Slota M, Koehnlein M, Treuting PM, Dang Y, et al. Natural history of tumor growth and immune modulation in common spontaneous murine mammary tumor models. *Breast Cancer Res Treat*. NIH Public Access; 2014;148:501–10.
 347. Wing K, Onishi Y, Prieto-Martin P, Yamaguchi T, Miyara M, Fehervari Z, et al. CTLA-4 Control over Foxp3+ Regulatory T Cell Function. *Science* (80-). 2008;322:271–5.
 348. Finn OJ, Gantt KR, Lepisto AJ, Pejawar-Gaddy S, Xue J, Beatty PL. Importance of MUC1 and spontaneous mouse tumor models for understanding the immunobiology of human adenocarcinomas. *Immunol Res*. Humana Press Inc; 2011;50:261–8.
 349. Alishekevitz D, Bril R, Loven D, Miller V, Voloshin T, Gingis-Velistki S, et al. Differential therapeutic effects of anti-VEGF-A antibody in different tumor models:

implications for choosing appropriate tumor models for drug testing. *Mol Cancer Ther.* American Association for Cancer Research; 2014;13:202–13.